High-Performance/High-Strength Lightweight Concrete for Bridge Girders and Decks

DETAILS

81 pages | 8.5 x 11 | PAPERBACK

ISBN 978-0-309-25888-3 | DOI 10.17226/22638

AUTHORS

Cousins, Tommy; Roberts-Wollmann, Carin; and Brown, Michael C.

NATIONAL COOPERATIVE HIGHWAY RESEARCH PROGRAM

NCHRP REPORT 733

High-Performance/High-Strength Lightweight Concrete for Bridge Girders and Decks

Tommy Cousins and Carin Roberts-Wollmann
THE CHARLES E. VIA, JR., DEPARTMENT OF CIVIL AND ENVIRONMENTAL ENGINEERING
VIRGINIA POLYTECHNIC INSTITUTE AND STATE UNIVERSITY
Blacksburg, VA

Michael C. Brown
VIRGINIA CENTER FOR TRANSPORTATION INNOVATION AND RESEARCH
Charlottesville, VA

Subscriber Categories
Bridges and Other Structures • Materials

Research sponsored by the American Association of State Highway and Transportation Officials
in cooperation with the Federal Highway Administration

TRANSPORTATION RESEARCH BOARD

WASHINGTON, D.C.
2013
www.TRB.org

NATIONAL COOPERATIVE HIGHWAY RESEARCH PROGRAM

Systematic, well-designed research provides the most effective approach to the solution of many problems facing highway administrators and engineers. Often, highway problems are of local interest and can best be studied by highway departments individually or in cooperation with their state universities and others. However, the accelerating growth of highway transportation develops increasingly complex problems of wide interest to highway authorities. These problems are best studied through a coordinated program of cooperative research.

In recognition of these needs, the highway administrators of the American Association of State Highway and Transportation Officials initiated in 1962 an objective national highway research program employing modern scientific techniques. This program is supported on a continuing basis by funds from participating member states of the Association and it receives the full cooperation and support of the Federal Highway Administration, United States Department of Transportation.

The Transportation Research Board of the National Academies was requested by the Association to administer the research program because of the Board's recognized objectivity and understanding of modern research practices. The Board is uniquely suited for this purpose as it maintains an extensive committee structure from which authorities on any highway transportation subject may be drawn; it possesses avenues of communications and cooperation with federal, state and local governmental agencies, universities, and industry; its relationship to the National Research Council is an insurance of objectivity; it maintains a full-time research correlation staff of specialists in highway transportation matters to bring the findings of research directly to those who are in a position to use them.

The program is developed on the basis of research needs identified by chief administrators of the highway and transportation departments and by committees of AASHTO. Each year, specific areas of research needs to be included in the program are proposed to the National Research Council and the Board by the American Association of State Highway and Transportation Officials. Research projects to fulfill these needs are defined by the Board, and qualified research agencies are selected from those that have submitted proposals. Administration and surveillance of research contracts are the responsibilities of the National Research Council and the Transportation Research Board.

The needs for highway research are many, and the National Cooperative Highway Research Program can make significant contributions to the solution of highway transportation problems of mutual concern to many responsible groups. The program, however, is intended to complement rather than to substitute for or duplicate other highway research programs.

NCHRP REPORT 733

Project 18-15
ISSN 0077-5614
ISBN 978-0-309-25888-3
Library of Congress Control Number 2013930599

COPYRIGHT INFORMATION

NOTICE

The project that is the subject of this report was a part of the National Cooperative Highway Research Program, conducted by the Transportation Research Board with the approval of the Governing Board of the National Research Council.

The members of the technical panel selected to monitor this project and to review this report were chosen for their special competencies and with regard for appropriate balance. The report was reviewed by the technical panel and accepted for publication according to procedures established and overseen by the Transportation Research Board and approved by the Governing Board of the National Research Council.

The opinions and conclusions expressed or implied in this report are those of the researchers who performed the research and are not necessarily those of the Transportation Research Board, the National Research Council, or the program sponsors.

The Transportation Research Board of the National Academies, the National Research Council, and the sponsors of the National Cooperative Highway Research Program do not endorse products or manufacturers. Trade or manufacturers' names appear herein solely because they are considered essential to the object of the report.

Published reports of the

NATIONAL COOPERATIVE HIGHWAY RESEARCH PROGRAM

are available from:

Transportation Research Board
Business Office
500 Fifth Street, NW
Washington, DC 20001

and can be ordered through the Internet at:

http://www.national-academies.org/trb/bookstore

Printed in the United States of America

THE NATIONAL ACADEMIES

Advisers to the Nation on Science, Engineering, and Medicine

The **National Academy of Sciences** is a private, nonprofit, self-perpetuating society of distinguished scholars engaged in scientific and engineering research, dedicated to the furtherance of science and technology and to their use for the general welfare. On the authority of the charter granted to it by the Congress in 1863, the Academy has a mandate that requires it to advise the federal government on scientific and technical matters. Dr. Ralph J. Cicerone is president of the National Academy of Sciences.

The **National Academy of Engineering** was established in 1964, under the charter of the National Academy of Sciences, as a parallel organization of outstanding engineers. It is autonomous in its administration and in the selection of its members, sharing with the National Academy of Sciences the responsibility for advising the federal government. The National Academy of Engineering also sponsors engineering programs aimed at meeting national needs, encourages education and research, and recognizes the superior achievements of engineers. Dr. Charles M. Vest is president of the National Academy of Engineering.

The **Institute of Medicine** was established in 1970 by the National Academy of Sciences to secure the services of eminent members of appropriate professions in the examination of policy matters pertaining to the health of the public. The Institute acts under the responsibility given to the National Academy of Sciences by its congressional charter to be an adviser to the federal government and, on its own initiative, to identify issues of medical care, research, and education. Dr. Harvey V. Fineberg is president of the Institute of Medicine.

The **National Research Council** was organized by the National Academy of Sciences in 1916 to associate the broad community of science and technology with the Academy's purposes of furthering knowledge and advising the federal government. Functioning in accordance with general policies determined by the Academy, the Council has become the principal operating agency of both the National Academy of Sciences and the National Academy of Engineering in providing services to the government, the public, and the scientific and engineering communities. The Council is administered jointly by both Academies and the Institute of Medicine. Dr. Ralph J. Cicerone and Dr. Charles M. Vest are chair and vice chair, respectively, of the National Research Council.

The **Transportation Research Board** is one of six major divisions of the National Research Council. The mission of the Transportation Research Board is to provide leadership in transportation innovation and progress through research and information exchange, conducted within a setting that is objective, interdisciplinary, and multimodal. The Board's varied activities annually engage about 7,000 engineers, scientists, and other transportation researchers and practitioners from the public and private sectors and academia, all of whom contribute their expertise in the public interest. The program is supported by state transportation departments, federal agencies including the component administrations of the U.S. Department of Transportation, and other organizations and individuals interested in the development of transportation. **www.TRB.org**

www.national-academies.org

COOPERATIVE RESEARCH PROGRAMS

CRP STAFF FOR NCHRP REPORT 733

Christopher W. Jenks, *Director, Cooperative Research Programs*
Crawford F. Jencks, *Deputy Director, Cooperative Research Programs*
Amir N. Hanna, *Senior Program Officer*
Andrea Harrell, *Senior Program Assistant*
Eileen P. Delaney, *Director of Publications*
Hilary Freer, *Senior Editor*

NCHRP PROJECT 18-15 PANEL
Field of Materials and Construction—Area of Concrete Materials

Bijan Khaleghi, *Washington State DOT, Tumwater, WA* (Chair)
David Hohmann, *HDR Engineering, Inc., Austin, TX* (formerly with Texas DOT)
Hossein Ghara, *Louisiana DOTD, Baton Rouge, LA*
Jose A. Lopez, *Plainsboro, NJ* (formerly with New Jersey DOT)
Ric Maggenti, *California DOT, Sacramento, CA*
Vicki R. Stewart, *Maryland State Highway Administration, Hanover, MD*
Maher K. Tadros, *University of Nebraska–Lincoln, Omaha, NE*
Benjamin A. Graybeal, *FHWA Liaison*
Frederick Hejl, *TRB Liaison*

AUTHOR ACKNOWLEDGMENTS

The research reported herein was performed under NCHRP Project 18-15 by Virginia Tech (VT), the Virginia Center for Transportation Innovation and Research (VCTIR), and PE Structural Consultants, Inc.

At VT, the principal investigator was Tommy Cousins and the co-principal investigator was Carin Roberts-Wollmann. Major contributions to the project were made by Ben Cross, Bernie Kassner, Jana Scott, and Jon Marston. The hard work of Chinmay Damle, Brett Farmer, and Dennis Huffman is also gratefully acknowledged.

At VCTIR, the research was performed under the direction of Michael Brown, with significant contributions from Brenton Stone. At PE Structural Consultants, Inc., the design examples and parametric studies were performed by Nestor Rubiano, under the direction of Lisa Powell. The assistance of all these individuals is gratefully acknowledged.

FOREWORD

By Amir N. Hanna
Staff Officer
Transportation Research Board

This report presents proposed changes to the AASHTO LRFD bridge design and construction specifications to address the use of lightweight concrete in bridge girders and decks. These modified specifications will provide highway agencies with the information necessary to develop comparable designs of lightweight and normal weight concrete bridge elements for use in evaluating alternatives and selecting the alternative that will yield economic benefits. The material contained in the report should be of immediate interest to state bridge engineers and others involved in the design and construction of concrete bridges.

Use of high-strength prestressed concrete girders and high-performance bridge decks has become accepted practice by many state highway agencies because of the associated technical and economic benefits. These girders and decks are generally manufactured with concrete made with natural normal weight aggregates. Use of manufactured lightweight coarse aggregate, such as expanded shale, slate, and clay, to produce lightweight concrete offers the benefit of reducing the weight of the superstructure, leading to reductions in the size of girders, substructure, and foundations. These size and weight reductions facilitate shipping, handling, and construction or replacement of bridge elements and thus result in economic benefits.

Recent advances in high-performance/high-strength lightweight concrete have had limited application in bridge construction because of the lack of design and construction guidelines and concerns about material properties and their impact on performance. Thus research was needed to (1) address the factors that significantly influence the design, constructibility, and performance of high-strength prestressed concrete bridge girders and high-performance bridge decks and (2) propose appropriate changes to the AASHTO LRFD bridge design and construction specifications to adequately address the use of lightweight concrete for these applications.

Under NCHRP Project 18-15, "High-Performance/High-Strength Lightweight Concrete for Bridge Girders and Decks," Virginia Polytechnic Institute and State University (Virginia Tech) conducted a review of the use of lightweight concrete in bridge decks and girders and executed an experimental investigation to evaluate the performance of specimens and bridge beams made with lightweight concrete mixtures. Based on the findings of the literature review and the experimental investigation, the research proposed changes to the AASHTO LRFD bridge design and construction specifications, primarily to the equations for estimating modulus of elasticity, modulus of rupture, and creep. The research also presented examples that considered proposed changes to illustrate the change in prestressing steel requirements of typical bridge girders if lightweight concrete is used

instead of normal weight concrete. These modified specifications will provide highway agencies with the information necessary to develop designs of lightweight concrete bridge elements that are comparable to those made with normal weight concrete to provide the basis for an equitable comparison.

The attachments contained in the research agency's final report provide elaborations and detail on several aspects of the research. Attachments A and B provide proposed changes to AASHTO LRFD bridge design and bridge construction specifications, respectively; these are included in the report. Attachments C through R are not published herein but are available by searching for *NCHRP Report 733* on the TRB website.

CONTENTS

Note: Many of the photographs, figures, and tables in this report have been converted from color to grayscale for printing. The electronic version of the report (posted on the Web at www.trb.org) retains the color versions.

SUMMARY

High-Performance/High-Strength Lightweight Concrete for Bridge Girders and Decks

Background

Use of high-strength prestressed concrete girders and high-performance bridge decks has become accepted practice by many state highway agencies because of their technical and economic benefits. These girders and decks are generally constructed with concrete made with natural normal weight aggregates. Use of manufactured lightweight coarse aggregates (e.g., expanded shale, slate, and clay) to produce lightweight concrete offers the benefit of reducing the weight of the superstructure, leading to reductions in the size of girders, substructure, and foundations. These size and weight reductions facilitate shipping, handling, and construction or replacement of bridge elements and result in economic benefits.

Recent advances in high-performance/high-strength lightweight concrete have had limited application in bridge construction because of the lack of design and construction guidelines and concerns about material properties and their impact on performance. Research is needed to address the factors that significantly influence the design, constructability, and performance of high-strength prestressed concrete bridge girders and high-performance bridge decks and to recommend changes to the AASHTO LRFD bridge specifications. These modified specifications will provide highway agencies with better guidance for considering lightweight concrete mixtures that are expected to yield economic benefits.

Project Scope

This research focused on developing recommended changes to the *AASHTO LRFD Bridge Design Specifications* (2010) and the *AASHTO LRFD Bridge Construction Specifications* (2010) relevant to high-strength lightweight concrete girders and high-performance lightweight concrete decks.

The research (and resulting specifications and recommendations) dealt with mixtures made with normal weight fine aggregates and manufactured lightweight shale, clay, or slate coarse aggregates to produce concrete with equilibrium density, as determined according to ASTM C567, of not more than 125 lb/ft^3. To accomplish these objectives the research included work to

- Develop mix designs and material properties for lightweight concrete used in bridge decks and precast, prestressed bridge elements;
- Evaluate key design parameters for lightweight concrete;
- Propose relevant changes to AASHTO LRFD Specifications; and
- Perform design examples illustrating the effect of the proposed changes on design practice.

Overview of the Project

The research performed in this project began with an extensive literature review and practitioner survey conducted as Phase I of the project. Results of the literature review and practitioner survey are provided in Attachments C and D, respectively (available by searching for *NCHRP Report 733* on the TRB website). The literature review and practitioner survey gave the researchers insight into the areas of investigation needed to achieve the project objectives and provided the basis and justification for the resulting Phase II work plan. The results of the project are recommended changes to the AASHTO LRFD Bridge Design Specifications and Construction Specifications, provided in Attachments A and B.

The Phase II work plan (provided in Attachment E available by searching for *NCHRP Report 733* on the TRB website) included both material property characterization and structural performance testing. During the material property characterization portion of this project a selection of lightweight aggregate sources was made, representing regional variations and a range of aggregate qualities, to identify a finite set of aggregates to be used for further investigation under this study. These aggregate sources were used to develop mixtures exhibiting a range of compressive and tensile properties. A typical normal weight mixture was selected for comparison purposes. Compressive, splitting tensile, and modulus of elasticity tests were conducted on all lightweight concrete mixtures used in this project. Based on the results of these tests, several mix designs were selected for use during the structural testing portion of this project. In addition, while structural testing was occurring, time-dependent material properties (e.g., creep and shrinkage) as well as other material properties (e.g., coefficient of thermal expansion and permeability) of representative lightweight concrete mix designs were investigated.

The structural testing portion of the project included the following:

- Push-off specimens (non-prestressed) to investigate interface shear strength in lightweight concrete bridge decks and girders;
- Laboratory-cast prestressed beams to investigate prestress loss, transfer length, development length, deflections, and camber; and
- Full-size prestressed girders to investigate shear strength, prestress losses, camber, and deflections.

Specimens containing normal weight concrete were fabricated and served as control specimens.

Comparative deck and girder designs were performed to investigate the changes in structural design that resulted from the use of lightweight prestressed concrete girders with lightweight concrete decks instead of normal weight prestressed concrete girders with a normal weight concrete deck.

Research Findings

The major findings of this research are summarized below. These findings are applicable only to the materials used in this project.

- Lightweight concrete with a compressive strength of 7000 psi and a unit weight less than 125 lb/ft^3 can be produced with a 0.30 w/cm and 800 lb of cementitious material with expanded shale and slate aggregates. Concrete mixtures containing slate aggregate consistently produced higher compressive strength concretes than mixtures made with other lightweight aggregates.
- The AASHTO LRFD equation for modulus of elasticity (with $K_1 = 1.0$) is appropriate for lightweight aggregates. Predictions of modulus can be improved by calibrating the K_1 value for each aggregate type.

- On average, the modulus of rupture of the lightweight concrete ranged from $0.26\sqrt{f'_c}$ to $0.36\sqrt{f'_c}$, with an average of $0.31\sqrt{f'_c}$.
- $\sqrt{f'_c}$ is more appropriate for use in shear strength calculations for sand lightweight concrete than $0.85\sqrt{f'_c}$ which is required in AASHTO LRFD Section 5.8.2.2.
- Based on a reliability analysis of interface and beam shear, a phi factor of 0.85 is appropriate for shear design of sand lightweight concrete.
- The AASHTO equations and the Ramirez and Russell equation for transfer length and development length provide a reasonable upper bound to the measured transfer lengths in the lightweight and normal weight girders.
- The current AASHTO refined method for calculating prestress losses is appropriate for lightweight girders with lightweight decks.
- The AASHTO model for creep and shrinkage results in good estimates of prestress loss and is appropriate for use with lightweight prestressed concrete girders.
- The *PCI Bridge Design Manual* improved multiplier method, using the AASHTO creep and shrinkage models, provides a good estimate of camber at the time of erection.

CHAPTER 1

Introduction

1.1 Background

Use of high-strength prestressed concrete girders and high-performance bridge decks has become accepted practice by many state highway agencies because of their technical and economic benefits. These girders and decks are generally constructed with concrete made with natural normal weight aggregates. Use of manufactured lightweight coarse aggregates (e.g., expanded shale, slate, and clay) to produce lightweight concrete offers the benefit of reducing the weight of the superstructure, leading to reductions in the size of girders, substructure, and foundations. These size and weight reductions facilitate shipping, handling, and construction or replacement of bridge elements and result in economic benefits.

Recent advances in high-performance/high-strength lightweight concrete have had limited application in bridge construction because of the lack of design and construction guidelines and concerns about material properties and their impact on performance. Research was needed to address the factors that significantly influence the design, constructability, and performance of high-strength prestressed concrete bridge girders and high-performance bridge decks and to recommend changes to the AASHTO LRFD bridge specifications. These modified specifications will provide highway agencies with better guidance for considering lightweight concrete mixtures that are expected to yield economic benefits.

1.2 Project Objectives and Scope

This research focused on developing recommended changes to the *AASHTO LRFD Bridge Design Specifications* (2010) and the *AASHTO LRFD Bridge Construction Specifications* (2010) relevant to high-strength lightweight concrete girders and high-performance lightweight concrete decks.

This research dealt with mixtures made with normal weight fine aggregates and manufactured lightweight shale, clay or slate coarse aggregates to produce concrete with equilibrium density, as determined according to ASTM C567, of not more than 125 lb/ft^3. To accomplish these objectives, the research included work to

- Develop mix designs and material properties for lightweight concrete used in bridge decks and precast, prestressed bridge elements;
- Identify and evaluate key design parameters for lightweight concrete;
- Propose relevant changes to the *AASHTO LRFD Bridge Design Specifications* and *AASHTO LRFD Bridge Construction Specifications;* and
- Perform design examples to investigate the effect of the proposed changes on design practice.

1.3 Research Plan and Methodology

The following tasks were performed to achieve the project objectives:

1. Review of relevant design standards and recent research results on the use of lightweight concrete in bridges.
2. Synthesis of survey results from state departments of transportation concerning use of lightweight concrete in bridge decks and girders.
3. Development and execution of an experimental investigation which included the proportioning of lightweight concrete mixtures and the manufacture and testing of lab-cast beams, full-scale beams, and interface shear test specimens.
4. Development of proposed changes to the *AASHTO LRFD Bridge Design Specifications* and the *AASHTO LRFD Bridge Construction Specifications.*

5. Preparation of design examples showing the effect of proposed design specification changes on typical superstructure designs.
6. Preparation of a report that documents the entire research.

1.4 Organization of the Report

This chapter presents the background, objectives, methodology, and scope of the project. Chapter 2 summarizes the findings of the research, including the material testing and structural testing portions of the project. Chapter 3 provides background for the research program and the details of the testing program. Chapter 4 presents a review of the interpretation and appraisal of the project results. Chapter 5 provides the project conclusions and suggested future research. Attachments A and B give the suggested changes to the *AASHTO LRFD Bridge Design Specifications* and the *AASHTO LRFD Bridge Construction Specifications.* Attachments C, D, and E contain a detailed literature review, survey results, and a literature summary and the approved work plan, respectively. Attachments F through M provide details of the experimental program that were not able to be included in the body of this report. Attachments N through Q present design examples of bridges containing lightweight concrete and details of the parametric study. Attachment R is a detailed reference list. Attachments C through R are not included herein but are available by searching for *NCHRP Report 733* on the TRB website.

CHAPTER 2

Findings

The research began with an extensive literature review and practitioner survey, both of which are provided in Attachment C (available by searching for *NCHRP Report 733* on the TRB website). Based on the literature review, practitioner survey, and review of the *AASHTO LRFD Bridge Design Specifications* and the *AASHTO LRFD Bridge Construction Specifications,* those aspects of the specifications that could be improved to better reflect the behavior of lightweight concrete were identified. It was found that the areas of highest importance were shear strength of composite lightweight prestressed concrete girders, estimation of prestress loss and camber in bridge girders, bond of prestressing strand to lightweight concrete, and numerous material properties (strength, modulus of elasticity, creep, shrinkage, and durability).

The work plan included both material property characterization and structural performance tests designed to investigate these areas of highest importance. Specific findings derived from both the material characterization and structural performance testing portions of this project are provided in this section. The resulting proposed changes to the AASHTO specifications are presented in Attachments A and B.

2.1 Materials Testing

The mix design and material property portion of the project consisted of two phases. The first phase focused on lightweight aggregate selection and developing mix designs for concrete used in bridge decks and girders. Ninety-five concrete batches were mixed in the laboratory to evaluate the relative performance of six aggregate sources across a range of mixture designs. Targeted variables in the screening mixture design matrix included aggregate source, w/cm (0.30 or 0.40), supplementary cementitious materials, and total cementitious content.

The second phase involved the determination of the material properties of the developed mix designs when used on a production basis. Based on findings from the laboratory screening tests, mixtures were identified for further large-scale testing in laboratory and lab-cast beams, full-size girders, and deck segments. Two lightweight aggregates were selected for use in the large-scale test specimens. These aggregates, when used in laboratory mixtures, yielded test results consistent with what is needed for structural concretes. Three categories of lightweight mixtures were selected, representing moderate and high-strength lightweight girder mixtures and a lightweight deck mixture.

The lightweight concrete mixtures were required to have a unit weight less than 125 lb/ft^3. To account for variability in concrete properties, all mixtures were designed for a target fresh unit weight of 122 lb/ft^3. The measured unit weight ranged from 119 to 125 lb/ft^3.

The compressive strength of concrete mixtures containing certain lightweight aggregates was consistently higher than those made with other lightweight aggregates. The binder proportions that provided the best combination of workability and strength incorporated either slag cement or silica fume in addition to portland cement. Mixtures containing slag cement were typically very workable and easily provided the desired air content. Lightweight concrete with a compressive strength of 7000 psi and a unit weight of less than 125 lb/ft^3 was produced with a 0.30 w/cm and 800 lb of cementitious material.

The *AASHTO LRFD Bridge Design Specifications* Section 5.4.2.4 (2010) provides the following equation to predict the modulus of elasticity based on compressive strength, unit weight of concrete, and aggregate source used as follows:

$$E_c = 33{,}000 K_1 w_c^{1.5} \sqrt{f'_c}$$

where

K_1 = correction factor for source of aggregate
w_c = unit weight of concrete (kcf)
f'_c = specified compressive strength of concrete (ksi)

A statistical analysis of the modulus of elasticity test values obtained from the laboratory and production mixtures was

performed in order to determine the appropriate K_1 factor to be used. The analysis showed that using a value of $K_1 = 1$ in the AASHTO equation for modulus of elasticity gave good correlation with the test results for lightweight concrete.

The relationship between splitting tensile strength f_{ct} and $\sqrt{f'_c}$ was used to evaluate the effects of lightweight aggregates on splitting tensile strength of concrete. This was done by determining the factor "a", where $f_{ct} = a\sqrt{f'_c}$, for the lightweight mixes tested in this study. The value for factor a ranged from about 0.23 to 0.27, with an overall average of 0.25 for these lightweight mixtures, well above the value of 0.21 inferred from the AASHTO specifications. This indicated the need to consider modifying Section 5.8.2.2 of the AASHTO specifications.

The measured values of flexural strength were compared to the predictions from AASHTO specifications. For sand lightweight concrete, AASHTO specifications (Section 5.4.2.6) require using $f_r = 0.20\sqrt{f'_c}$, where f_r and f'_c are expressed in ksi, for calculating modulus of rupture. For normal weight concrete, factors before the radical include 0.20 for cracking moment when calculating V_{ci}, and 0.24 for calculating deflections. Comparison of the predicted results for flexural strength with the measured results at 28 days showed the factor for sand lightweight concrete significantly underestimates flexural strength.

The concrete creep test results were compared with the AASHTO, ACI 209, and CEB-FIP Model Code 1990 (CEB MC90) models. For the concrete mixtures tested, creep coefficients for normal weight and lightweight girders were best predicted by the AASHTO model. Therefore, use of the AASHTO creep coefficient calculation method is recommended for estimating prestress losses and deflections of lightweight concrete girders. The lightweight high performance concrete (LWHPC) deck mixtures exhibited considerable variation in creep coefficients, which were best predicted by the ACI 209 model. However, because the creep behavior of the deck is secondary in importance to the girder creep characteristics, continued use of the AASHTO creep coefficient for calculation of the deck properties is appropriate.

2.2 Interface Shear Strength

Precast girders with cast-in-place decks is a common type of bridge construction. Developing composite action between the two components is a key requirement of this type of design, and providing adequate horizontal shear strength at the interface of these components is necessary for developing this composite action. Tests were performed to examine the interface or horizontal shear strength of lightweight concrete. The current *AASHTO LRFD Bridge Design Specifications* (5th Edition) design equation for interface shear strength of cast-in-place concrete decks on precast concrete girders suggests more variability of lightweight concrete's behavior in shear than of normal weight concrete. To reflect this difference, a resistance factor of 0.7 is used for lightweight concrete and a resistance factor of 0.9 is used for normal weight concrete.

Push-off tests were conducted to compare the interface shear strength of lightweight concrete to that of normal weight concrete. These tests investigated (1) the ratio of the area of interface shear reinforcement to the area of concrete at the interface of the bridge deck and bridge girder and (2) combinations of deck and girder concretes. Four levels of this shear reinforcement were investigated: no horizontal shear reinforcement, the minimum allowed, the maximum allowed, and an intermediate amount. The combinations of deck and girder concrete were a lightweight deck cast on a lightweight girder, a lightweight deck cast on a normal weight girder, and a normal weight deck cast on a normal weight girder. These test variables resulted in 12 configurations of push-off tests, all of which were repeated three times to provide information on the variability of test behavior. Details of the testing program are provided later in this report.

The following observations are made based on the interface shear tests:

- The current AASHTO LRFD design equation (with a strength reduction factor of 0.9) underestimated interface horizontal shear strength of all of the lightweight deck-lightweight girder specimens, 8 of 9 of the normal weight-lightweight specimens, and 8 of 9 normal weight-normal weight specimens. A strength reduction factor of 0.8 is more appropriate for predicting interface shear strength of these specimens.
- On average, design calculations were more conservative in predicting the strength of the lightweight concrete than the strength of specimens containing normal weight concrete.
- The normal weight girder with lightweight deck exhibited behavior similar to that of the lightweight girder with lightweight deck. The interface shear strength of girder/deck combinations with lightweight concrete was greater than that of normal weight concrete deck on a normal weight concrete girder.
- The average post-crack interface strength for normal weight/normal weight specimens was greater than for lightweight specimens when interface shear reinforcement was provided. Specimens without interface shear reinforcement had slightly higher post-crack interface strengths when lightweight concrete was used.
- As the amount of shear reinforcement at the interface increased, the ratio of measured horizontal shear strength to LRFD calculated strength decreased.
- Resistance factors calculated from the reliability analysis performed on test data indicated that the same resistance factor used for normal weight concrete could be used for lightweight concrete. The reliability index for lightweight

concrete interface shear strength tests was higher than that for normal weight concrete tests, when analyzed for the same resistance factor.

2.3 Laboratory Beam Tests

Laboratory test specimens were T-shaped beams and contained either three 0.5-in.- or three 0.6-in.-diameter prestressing strands. A total of 12 beams were made (10 with lightweight concrete and 2 with normal weight concrete) which resulted in 24 transfer length and development length tests. In addition, the prestress loss and camber of each beam were monitored over time.

Direct pullout tests on strand specimens were performed on each strand size to determine strand bond quality. All tested samples for both sizes met the National Association of Strand Producers (NASP) requirements for strand bond with measured slip values far less than expected at the required load values. Large Block Pullout Tests were also performed on strand samples following the procedures recommended by Logan (1997). All strand samples exceeded the minimum pullout load requirements proposed by Logan.

The measured transfer lengths for all lightweight and normal weight beams were less than the current AASHTO LRFD specifications (Section 5.11.4) and the proposed specification changes by Ramirez and Russell (2008). Based on this data and the data from Meyer (2002), both the current AASHTO LRFD specification of 60-strand diameters and the proposed changes to the AASHTO specification by Ramirez and Russell provide conservative predictions of transfer lengths of high-strength lightweight concrete (HSLWC) beams. The measured development lengths for the lightweight concrete beams were slightly longer than measured for the normal weight beams. However, all measured development lengths were substantially less than those calculated using the AASHTO Specifications (Eq. 5.11.4.2-1) as well as those calculated using the proposed Ramirez and Russell equation (Ramirez and Russell (2008)). This data confirms the findings of earlier studies that the AASHTO LRFD equation for development length provides a conservative estimate for HSLWC.

2.4 Shear Tests

Six full-scale prestressed girders with cast-in-place composite decks were tested to investigate shear strength of lightweight prestressed concrete girders. The *AASHTO LRFD Bridge Design Specifications* include two reductions to calculated shear strength of lightweight concrete prestressed girders. The first is a 0.85 modifier for the $\sqrt{f'_c}$ term used in calculating concrete shear strength (given in Section 5.8.2.2). The second is the use of a resistance factor (ϕ) for shear design of lightweight concrete girder of 0.7 (compared to 0.9 for normal weight concrete girder). Based on the test results from the six girders and full-size girder test results found in the literature, the following conclusions were made:

- The AASHTO modification factor (λ_v) applied to $\sqrt{f'_c}$ term in shear strength calculations is not needed for sand lightweight concrete prestressed concrete girders. This conclusion is primarily based on the results of full-size girder tests; it is also supported by the finding from the material portion of this study that the tensile strength of lightweight concrete was similar in magnitude to that of normal weight concrete.
- In Section 5.5.4.2, the *AASHTO LRFD Bridge Design Specifications* require that a ϕ of 0.7 be used for calculation of the shear strength of lightweight prestressed concrete girders as compared with 0.9 for normal weight prestressed concrete girders. Based on analysis of all available full-size girder test results, the ϕ required for use with lightweight prestressed concrete girders is 0.85.

2.5 Time-Dependent Behavior of Lab-Cast and Full-Scale Beams

Two aspects of time-dependent behavior were studied: prestress losses and deflection. Each plant-cast girder and lab-cast girder had a vibrating wire gage installed at midspan at the level of the centroid of the prestressing force. This gage monitored changes in strain in the concrete at the centroid of the strand from just prior to release of prestress to the time of testing of the girders. In addition, each beam was equipped with a taut-wire deflection measurement system to measure beam deflection at the quarter points and midspan. The initial displacement reading was made just prior to release of prestress, and readings were taken regularly from release to testing of each girder.

Measurements of strain changes, as well as the initial camber and changes in camber with time, were compared to the calculated prestress loss and camber changes obtained from several methods. The improved multiplier method (*PCI Bridge Design Manual,* (1997)) and a general method using the age adjusted effective modulus (AAEM) were used for camber calculations. The AASHTO refined method (Section 5.9.5.4 in AASHTO LRFD) and the AAEM method were used for prestress loss calculations. Three creep and shrinkage models, AASHTO (Section 5.4.2.3 in AASHTO LRFD), ACI 209 (1997), and CEB MC90 (1990), were used with the camber and prestress loss calculations.

Based on comparisons of calculated values and measured values, the following conclusions can be drawn regarding prestress losses and camber growth in lightweight concrete girders:

- The AASHTO refined method for prestress loss calculation using the AASHTO creep and shrinkage model overestimates the measured losses.
- The ACI 209 and CEB MC90 models for creep and shrinkage used with the AASHTO refined method overestimate prestress loss more than the AASHTO creep and shrinkage models.
- Initial cambers and elastic shortening can be estimated using the AASHTO equation for modulus of elasticity with a measured compressive strength.
- The PCI improved multiplier method, used with the AASHTO creep and shrinkage model, provides reasonable estimates of camber at the time of erection, but not of camber growth after the composite deck is placed.

CHAPTER 3

Background and Research Approach

3.1 Mix Designs and Material Properties

Research Approach

The mix design and material property portion of the project consisted of two phases. The first phase focused on selecting lightweight aggregate and developing concrete mix designs for use in bridge decks and girders. The second phase involved the determination of the material properties of the mix designs selected for use on a production basis. A description of this work is given below and is followed by discussions of the materials used in the concrete mixtures, concrete mixing procedures, and fresh and hardened concrete test procedures. Further details of the mix design and material properties investigation can be found in Attachment F (available by searching for *NCHRP Report 733* on the TRB website).

Laboratory Material and Mixtures Screening Tests

To facilitate the selection of aggregate, manufacturers of structural-grade lightweight aggregate were contacted and test data, typical mixture designs, and other information were acquired from each of the production facilities. Structural grade aggregates are those used in ready-mix or precast, prestressed concrete applications. Aggregate used primarily in concrete masonry units (CMUs) was not considered to be structural aggregate. A database of material properties (including elastic modulus, unit weight, specific gravity, absorption rates, and angularity of the aggregate) was compiled for lightweight aggregate sources in the United States.

Based on data received, the highest documented compressive strength for each concrete mixture and the corresponding unit weight together with the highest aggregate absorption recorded in laboratory tests were determined for each aggregate source. Several aggregate sources were chosen to provide geographic distribution, to include at least one source from each of the three material types (clay [CL], shale [SH], and slate [SL]), and to include sources believed to be capable of achieving the strength requirements for this research. Six candidate aggregates were selected for testing in this project:

- CL1 - expanded clay source one
- CL2 - expanded clay source two
- SH1 - expanded shale source one
- SH2 - expanded shale source two
- SH3 - expanded shale source three
- SL1 - expanded slate source one

Concrete mixtures using each of these six aggregates were developed. Mixture proportions were designed for (1) water-cementitious material ratios (*w/cm*) of 0.30, representing high-strength, low-permeability beam mixtures; (2) *w/cm* of 0.40, representing moderate-strength and moderate-permeability beam mixtures; and (3) good quality concrete deck mixtures. Mineral admixtures used included fly ash (FA), slag, and silica fume (SF), which were used at typical rates to produce high-performance concrete mixtures. Screening tests were executed on these concrete mixtures to determine basic material properties. Testing considered ¾ in. and ½ in. nominal coarse aggregate sizes, depending on availability. Table 1 presents the cementitious materials used in making concrete batches with aggregate from each source.

Specimens from each screening batch were subjected to the tests listed in Table 2. Based on the results of these tests, mixtures for use in structural testing were identified.

The selected mixture designs for deck concrete had a target compressive strength (f'_c) of 4 ksi. The mixtures selected for girder concrete included one typical of present practice (f'_c = 8 ksi) with two different aggregates and one having a higher strength than typically used in bridges (f'_c = 10 ksi). The maximum design strength that appears achievable on a production basis was 10 ksi. A typical normal weight high-performance concrete (NWHPC) mixture was used to cast control specimens

Table 1. Cementitious materials for screening test batches.

Mixture Description		Number of Batches from Each Coarse Aggregate Type
w/cm	Binder	
0.3	OPC	2
	OPC+20%FA	2
	OPC+40% SLAG	2
	OPC+7%SF	2
0.4	OPC	2
	OPC+20%FA	2
	OPC+40% SLAG	2

for structural test comparisons. Table 3 lists the types of concrete mixes selected for use in the structural testing portion of this project. Based on the screening test results, two lightweight aggregates were selected for further use. These two aggregates were the shale aggregate from source three (SH3) and the slate aggregate source from source one (SL1).

Production Material Property Verification Tests

During casting of the beams and interface shear and full-size test specimens, samples of the concrete were obtained for material property tests. For these samples, either a comprehensive test regime or a basic test regime was conducted. For the comprehensive test regime, in addition to the material properties performed in the screening phase, tests were performed to characterize time-dependent parameters that affect prestress loss (e.g., shrinkage) and bulk diffusion characteristics that influence durability. During fabrication at the precast plant, companion specimens were obtained from the concrete used in the precast girders. Additionally, specimens were obtained from the ready-mix concrete used in the lab-cast beams, interface shear specimens, and decks. The test matrix is presented in Table 4. The basic test regime typically included fresh concrete tests (slump, air content, and unit weight) as well as compressive strength and modulus of elasticity.

Table 2. Number of samples for material screening tests.

Material Property	AASHTO Test Method	Number of Samples			
		Age (days)			
		7	28	56	90
Compressive Strength /Modulus of Elasticity	T 22	2	3	3	2
Modulus of Rupture	T 97	-	3	-	-
Split Tensile Strength	T 198	2	3	3	2
Shrinkage	T 160	3	-	-	-
Permeability / Absorption	T 277	-	2	2	-

Table 3. Concrete mixtures for structural testing.

Mix Designation*	Aggregate Source	Specimens	Bridge Use
NWHPC 1 (8 ksi)	normal weight aggregate	Lab cast, full size, interface shear	girders
NWHPC 2 (4ksi)	normal weight aggregate	Interface shear	deck
LWHPC 1 (8 ksi)	SL1	Lab cast, full size, interface shear	girders
LWHPC 2 (8 ksi)	SH3	Lab cast	girders
LWHPC 3 (10 ksi)	SL1	Lab cast & full size	girders
LWHPC 4 (4 ksi)	SL1	Full size & interface shear	deck

*Target f'_c is shown in parentheses.

Table 4. Material property tests for full-scale production.

Property	AASHTO Test Method	Number of Specimens				
		Age (days)				
		1	7	28	56	90
Compressive Strength / Modulus of Elasticity	T 22	-	2	3	3	2
Modulus of Rupture	T 97	-	-	3	-	-
Split Tensile Strength	T 198	-	2	3	3	2
Shrinkage	T 160	3	-	-	-	-
Permeability / Absorption	T 277	-	-	2	2	-
Freeze-thaw	T 161 Proc. A	-	-	2	-	-

Table 5. Creep tests for full-scale specimen production.

Mix Designs	Use	Number of Tests			
		First Test Group	Second Test Group	Third Test Group	Fourth Test Group
NWHPC1	Girder	1	1	-	1
LWHPC 1		-	1	-	-
LWHPC 2		1	-	-	-
LWHPC 3		1	1	-	-
LWHPC 4	Deck	-	-	3	2

Creep characteristics were measured for a number of concrete mix designs used during full-scale specimen production. Table 5 presents the number of creep tests performed on each test group. Each test group consisted of three sets of three concrete cylinders and one control cylinder.

Materials

The following materials were used for preparing the different concrete mixtures used in the tests.

Coarse Aggregate. Lightweight aggregates were chosen to represent a broad sample set from across the United States. Raw materials used to manufacture these expanded lightweight aggregates included shale, clay, and slate products. Six lightweight aggregates were selected which included three expanded shale (SH1, SH2, and SH3), two expanded clay (CL1 and CL2), and one expanded slate (SL1) (see Figure 1).

After receiving the lightweight aggregates from the manufacturers, a series of tests were conducted to confirm the physical properties reported by the manufacturer of each aggregate. The tests conducted included gradation, specific gravity, and absorption. A gradation of ½ in. × No. 4 was required for this study, and deviations were recorded. If the nominal maximum aggregate size (NMAS) is taken as the first sieve which retains 5–15% of the material in a standard gradation test, then samples from CL2 and SH2 were closer to a ⅜-inch NMAS. SL1 had the most retained on the ½-inch sieve at 30%.

The specific gravity and absorption tests were conducted according to ASTM C127, *Standard Test Method for Density, Relative Density (Specific Gravity) and Absorption of Coarse Aggregate.* Although the test is specified only for normal weight aggregate, it was chosen because no standard exists for specifically testing lightweight aggregate. Table 6 provides the results of specific gravity and absorption tests for the six aggregates.

Figure 1. Lightweight aggregates (from left to right): CL1, SH1, SH2, CL2, SH3, and SL1.

Fine Aggregate. Fine aggregate used throughout this research was obtained from a local ready-mixed concrete supplier. The source of the fine aggregate is an area known as Curles Neck, a natural deposit along the James River near Richmond, VA.

Cement. Laboratory concrete was made using a Type I/II portland cement conforming to AASHTO M 85 (*Standard Specification for Portland Cement*).

Slag Cement. The slag cement used for this project conformed to the requirements of ASTM C 989, *Standard Specification for Slag Cement for Use in Concrete and Mortars.*

Fly Ash. Class F fly ash conforming to the requirements of ASTM C618, *Standard Specification for Coal Fly Ash and Raw or Calcined Natural Pozzolan for Use in Concrete,* was used in this project because of its pozzolanic reactivity with portland cement, as well as a relatively low calcium oxide (CaO) content.

Silica Fume. Silica fume conforming to the requirements of ASTM C1240, *Standard Specification for Silica Fume Used in Cementitious Mixtures* was used.

Admixtures. Air-entraining admixture (AEA) and high-range water-reducing admixture (HRWR) were used.

Mix Designs and Mixing Procedures

Several concrete mixtures were designed to investigate use of different lightweight aggregates for producing concrete mixtures appropriate for bridge girders (mixtures with a 0.30 w/cm ratio) and for decks (mixtures with 0.40 w/cm ratio).

In developing the mixture designs, compressive strength and unit weight took precedence over other material properties such as tensile strength, modulus, shrinkage, and perme-

Table 6. Specific gravity and absorption.

Property	Aggregate Designation					
	CL1	CL2	SH1	SH2	SH3	SL1
Oven Dry Weight (g)	1850	2000	2240	2140	3040	2950
SSD Weight (g)	2120	2310	2560	2310	3500	3410
Weight in Water (g)	906	420	988	476	1510	1260
SG (Oven Dry)	1.51	1.06	1.43	1.17	1.53	1.37
SG (SSD)	1.74	1.22	1.63	1.26	1.76	1.59
SG (Apparent)	1.97	1.27	1.79	1.29	1.99	1.74
Absorption, %	15.1	15.4	14.3	7.9	15.1	15.4
Manufacturer SG (SSD)	1.75	1.25	1.73	1.20	1.55	1.52

ability. One goal of the research is to recommend changes to the *AASHTO LRFD Bridge Design Specifications* and the *AASHTO LRFD Bridge Construction Specifications* relevant to high-strength lightweight concrete girders and high-performance lightweight concrete decks. To address this goal, the research involved developing mix designs of lightweight concrete with design compressive strengths of 8 and 10 ksi for girders and 4 ksi for decks. The limiting factor on fresh concrete properties was that unit weight be no greater than 125 lb/ft^3.

The lightweight coarse aggregate was subjected to a 24-hour saturation soak and allowed to drain for an additional 24 hours to place the aggregate in a saturated surface-dry (SSD) condition, per standard industry practice. The CL1 aggregate, which contained a large quantity of fine material, required longer than 24 hours to drain. The stockpile of fine aggregate was somewhat moist, but a 500-g sample was oven dried and tested to determine the moisture state for each day of mixing and adjust the amount of mixing water to maintain the design w/cm ratio.

Test Results

Concrete batches were mixed in the laboratory to evaluate the performance of the six aggregate sources for a range of mixture designs. Based on results of the screening tests, mixtures were identified for use in large-scale testing in laboratory and lab-cast beams, full-size girders, and deck segments. Three lightweight mixtures represented moderate- and high-strength lightweight girder mixtures and a lightweight deck mixture. In addition, two lightweight aggregates (SH3 and SL1) were selected for use in the large-scale test specimens. These aggregates, when used in laboratory mixtures, yielded the properties needed for structural concretes. A mixture using normal weight aggregate was also tested for comparison with the lightweight mixtures. Cylinders and prisms were cast from these production mixtures to characterize the materials used in the structural test specimens. Table 7 lists the structural test specimens as well as concrete type, casting location, and test regime (comprehensive and basic test regimes are labeled C and B, respectively). Table 8 provides

Table 7. Concrete mixtures for structural test specimens.

Designation	Location	Specimen Type	Bridge Use	Test Regime
NWHPC1	Lab	2 Lab cast beams	Girders	C
LWHPC1	Lab	2 Lab cast beams	Girders	C
LWHPC3	Lab	4 Lab cast beams	Girders	C
NWHPC1	Lab	2 Lab cast beams	Girders	C
LWHPC2	Lab	2 Lab cast beams	Girders	C
LWHPC1	Lab	Interface shear	Girders	B
LWHPC1	Plant	2 AASHTO II	Girders	C
LWHPC1	Plant	1 PCBT-45	Girders	C
LWHPC3	Plant	2 PCBT-45	Girders	C
LWHPC4	Lab	CIP Deck	Deck	C
LWHPC4	Lab	CIP Deck	Deck	C
LWHPC4	Lab	Interface shear	Deck	B
LWHPC4	Lab	Interface shear	Deck	B
NWHPC2	Lab	Interface shear	Deck	B
LWHPC4	Lab	CIP Deck	Deck	C
LWHPC4	Lab	CIP Deck	Deck	C
LWHPC4	Lab	CIP Deck	Deck	B
NWHPC1	Plant	1 PCBT-45	Girders	B
LWHPC4	Lab	CIP Deck	Deck	B

Table 8. Mix designs for production concrete.

Ingredients*	Concrete Mix Designations (Aggregate Type) & Use								
	NWHPC1 (NW)		NWHPC 2 (NW)	LWHPC 1 (SL1)		LWHPC 2 (SH3)	LWHPC 3 (SL1)		LWHPC 4 (SL1)
	One PCBT-45 girder	Lab cast beams & Interface shear specimens	Interface shear	AASHTO II girders & one PCBT-45 girder	Lab cast beams & Interface shear	Lab cast beams	Lab cast beams	Two PCBT-45 girders	Interface shear specimens & cast-in-place decks
Cement	720	652	560	480	740	480	540	495	535
Fly ash	180		140		60			90	140
Microsilica		53							
Slag				320		320	360	315	
Sand	1,035	1,229	1,085	1,368	1,343	1,297	1,253	1,318	1,305
NW stone	1,683	1,700	1,746						
LW stone				920	910	956	874	920	875
Water	275	247	283	232	240	242	268	246	304

*All quantities are in pounds.
NW= Normal weight
LW= Lightweight

the mix designs used in the lab-cast beams, full-size girders, and deck segments.

Material Properties

Equilibrium Unit Weight. Testing for equilibrium unit weight was conducted according to ASTM C567, *Standard Test Method for Determining Density of Structural Lightweight Concrete,* of all laboratory mixtures. The design fresh unit weight for all tests was 122 lb/ft^3. Measured unit weight ranged between 119 and 125 lb/ft^3.

Compressive Strength. Identifying a binary lightweight concrete mixture that yielded a high compressive strength proved to be difficult. Table 9 lists the measured average 28-day compressive strengths for lightweight mixtures with different aggregates and combinations of binder proportions. All test cylinders were stored and tested according to the AASHTO standard test requirements and capped using sulfur compound. The table shows results for mix designs using 0.40, 0.30, and 0.25 w/cm ratios. All mixtures with 100% ordinary portland cement (OPC) and a 0.40 w/cm ratio performed similarly, regardless of the lightweight aggregate used. The

Table 9. Average compressive strengths of HPLWC laboratory mixtures.

w/cm	TCM* (lb/yd^3)	Agg. Source	OPC (ksi)	OPC + 20% FA (ksi)	OPC + 40% Slag (ksi)	OPC + 7% SF (ksi)
0.40	752	CL1	5.54	4.61	4.58	
		CL2	6.17	5.46	6.00	
		SH1	6.26	5.48	6.18	
		SH2	6.10	5.32	6.18	
		SH3	5.83	5.82	5.93	
		SL1	7.18	6.24	7.03	
0.30	800	CL1	6.21	6.16	6.63	6.27
		CL2	7.37	6.92	7.58	7.43
		SH1	7.50	7.24	7.48	7.31
		SH2	7.00	6.59	7.33	7.12
		SH3	8.45	7.90	8.55	8.90
		SL1	9.00	8.50	9.77	9.35
	850	SL1	8.74		9.38	9.43
	900	SL1		8.61	9.83	
0.25		SL1			9.87	

*TCM = total cementitious materials (sum of OPC, FA, Slag, and SF).

compressive strengths ranged from 5 to 6 ksi. The strength of the other mixtures with a 0.40 w/cm ratio also ranged from 5 to 6 ksi range, but with greater variation. For each combination of binder proportions, concrete made with SL1 lightweight aggregate provided higher strength than comparable mixtures containing other aggregates.

Concrete with SL1 and SH3 lightweight aggregates and a 0.30 w/cm ratio consistently provided higher compressive strength. None of the lightweight concrete mixtures provided the expected strength of 10 ksi. The mixture containing 40% slag cement and 7% silica fume exhibited the highest compressive strengths. The mixture with SL1 and 40% slag cement had compressive strength exceeding 9.5 ksi at 28 days, meeting the 8.5 ksi design strength requirement.

Increase in the total cementitious material from 800 lb to 850 lb only slightly increased the maximum compressive strength of one of the three mixtures using lightweight slate aggregate (SL1). Further, there was a smaller strength increase using 900 lb of total cementitious material. Considering the harshness of the mix, wherein workability was dramatically reduced, and the small strength gain, this mixture would not make a good choice for use in the field.

Based on the compressive strength test results, the SH3 and SL1 lightweight aggregates were chosen for use in the structural concrete mixtures.

Modulus of Elasticity. Approximately 80% and 50% of the cylinders tested for compressive and splitting tensile strength, respectively, were previously tested for modulus of elasticity. *AASHTO LRFD Bridge Design Specifications* (Section 5.4.2.4) provide the following equation to predict modulus of elasticity based on compressive strength and unit weight of concrete:

$$E_c = 33{,}000 K_1 w_c^{1.5} \sqrt{f'_c}$$

where

K_1 = correction factor for source of aggregate (taken as 1.0 unless determined by physical test, and as approved)
w_c = unit weight of concrete (kcf)
f'_c = specified compressive strength of concrete (ksi)

Modulus of elasticity values for SH3 and SL1 lightweight aggregate concretes ranged from 4,000 to 5,000 ksi. One concrete mixture exceeded 5,000 ksi: a SL1 mixture contained 40% slag cement and 60% portland cement for a total cementitious material content of 850 lb. However, the modulus of elasticity for all SH3 mixtures with a w/cm ratio of 0.30 and 50 lb/yd^3 less cementitious material was nearly 5,000 ksi.

Figure 2 shows a comparison of the measured results to predicted modulus of elasticity based on the equation provided in AASHTO LRFD specifications with $K_1 = 1.0$.

As noted above, the AASHTO equation for modulus of elasticity includes a factor to adjust for aggregate type, such as

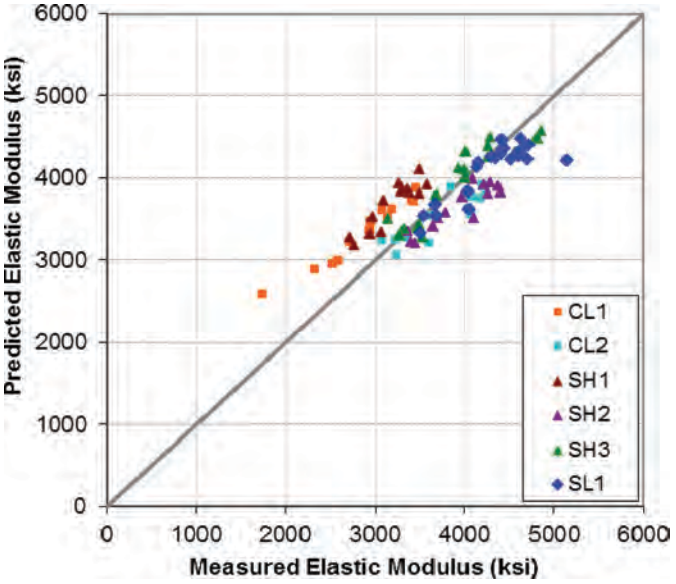

Figure 2. Measured modulus of elasticity versus AASHTO prediction.

lightweight aggregate. This factor, K_1, can be calibrated from a series of tests for a particular source aggregate; it was determined for each lightweight aggregate source by least-squares fit of the predictive equation to the measured values. Table 10 lists the K_1 factor determined for each aggregate source based on laboratory tests. Figure 3 shows the estimated modulus values versus the measured values using the K_1 listed in Table 10. Note that a least-squares fit across all lightweight aggregate types resulted in a K_1 value of 1.00.

The accuracy of the modulus of elasticity prediction models for the production mixtures was investigated. A scatter plot was constructed with the experimental results and the associated values predicted by the AASHTO equation with K_1 values of 1.0. As depicted in Figure 4, the AASHTO equation provided reasonable predictions for lightweight concrete deck mixtures.

Splitting Tensile Strength. Although AASHTO specifications do not provide an equation for splitting tensile strength

Table 10. Modulus of elasticity factors for lightweight aggregates.

Lightweight Aggregate Source	K_1 factor
CL1	0.87
CL2	1.06
SH1	0.87
SH2	1.08
SH3	1.00
SL1	1.06
All Lightweight	1.00

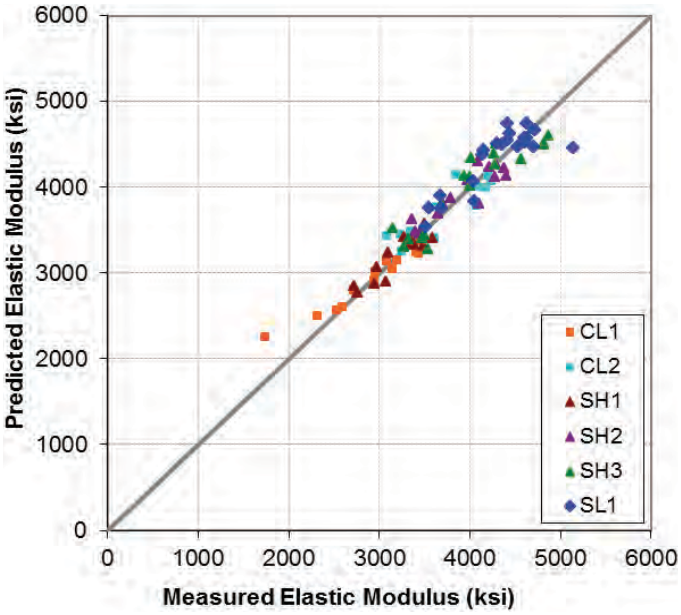

Figure 3. Measured modulus of elasticity versus AASHTO prediction using K_1 from Table 10.

of concrete (f_{ct}), it can be determined from information given in Article 5.8.2.2. This article requires that $\sqrt{f'_c}$ be replaced with $4.7\,f_{ct}$ in shear design calculations given in Articles 5.8.2 and 5.8.3 when f_{ct} is specified. In addition, $0.85\sqrt{f'_c}$ should be substituted for the $\sqrt{f'_c}$ term when f_{ct} is not specified. The factor 0.85 is required to be used for sand lightweight concrete. The first provision (f_{ct} specified) indicates a relationship between compressive strength and splitting tensile strength of lightweight concretes (without regard to fine aggregate type), capped at $\sqrt{f'_c}$, consistent with the relationship assumed for

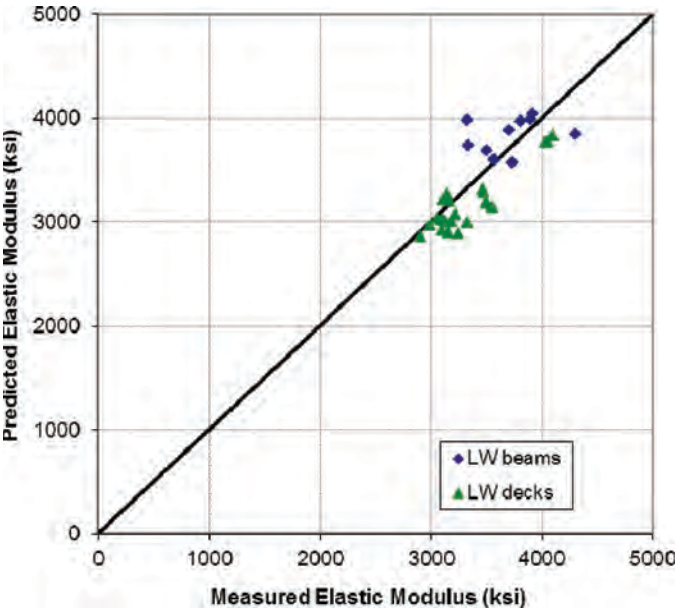

Figure 4. Measured versus predicted modulus of elasticity for production mixtures.

normal weight concrete. The second provision (f_{ct} not specified), gives a discount factor for lightweight concrete, with adjustment for fine aggregate type. Using $\sqrt{f'_c}$ as the upper bound for splitting tensile strength similar to that of normal weight in the first expression, the expression was considered as an equality and the terms rearranged to yield the following equation for f_{ct} as a function of f'_c:

$$f_{ct} = \sqrt{f'_c}/4.7$$

The relationship between splitting tensile strength and $\sqrt{f'_c}$ was determined by introducing the factor "a", where $f_{ct} = a\sqrt{f'_c}$. Figure 5 shows average values of factor a for a range of mixtures, all with total cementitious material (TCM) contents ranging from 752 to 900 lb/yd^3. The values of a were slightly higher for 0.40 w/cm mixtures than for the 0.30 w/cm mixtures. The average a values for the lightweight mixtures ranged from about 0.23 to 0.27, with an overall average of 0.25, which is higher than the value of 0.21 derived from Article 5.8.2.2, suggesting the consideration for modifying Section 5.8.2.2 of the AASHTO specifications.

Modulus of Rupture. For every concrete mixture, flexural strength specimens were cast and tested at 28 days of age according to AASHTO T 97, *Standard Test Method for Flexural Strength of Concrete (Using Simple Beam with Third-Point Loading)*, to determine modulus of rupture (f_r).

The measured values of modulus of rupture of lightweight concrete were compared to those predicted by the AASHTO equation relating flexural strength to compressive strength. According to AASHTO Section 5.4.2.6, for sand lightweight concrete, $f_r = 0.20\sqrt{f'_c}$, where f_r and f'_c are expressed in ksi. For normal weight concrete, the factors given in AASHTO Section 5.4.2.6 to be used before the radical are 0.20 for estimating cracking moment and calculating V_{ci} and 0.24 for calculating deflections. A graph of measured results from this research and those predicted for lightweight concrete is given in Figure 6. Comparison of the predicted results for flexural strength with the measured results at 28 days showed the default factor of 0.20 significantly underestimates the flexural strength for sand lightweight.

A statistical analysis of the data was used to determine the 95% prediction interval shown in Figure 6. The lower bound of the interval is approximately $0.26\sqrt{f'_c}$, which is larger than the current AASHTO equation $\left(0.20\sqrt{f'_c}\right)$.

Modulus of rupture for the production mixtures were compared to predictions using the current AASHTO equation $\left(0.20\sqrt{f'_c}\right)$ as well as $0.26\sqrt{f'_c}$. Figure 7 shows that modulus of rupture of production mixtures was significantly underpredicted by the current AASHTO equation, as was seen with the laboratory mixtures. The sample size used for this comparison was very small. However, adjusted predictions using

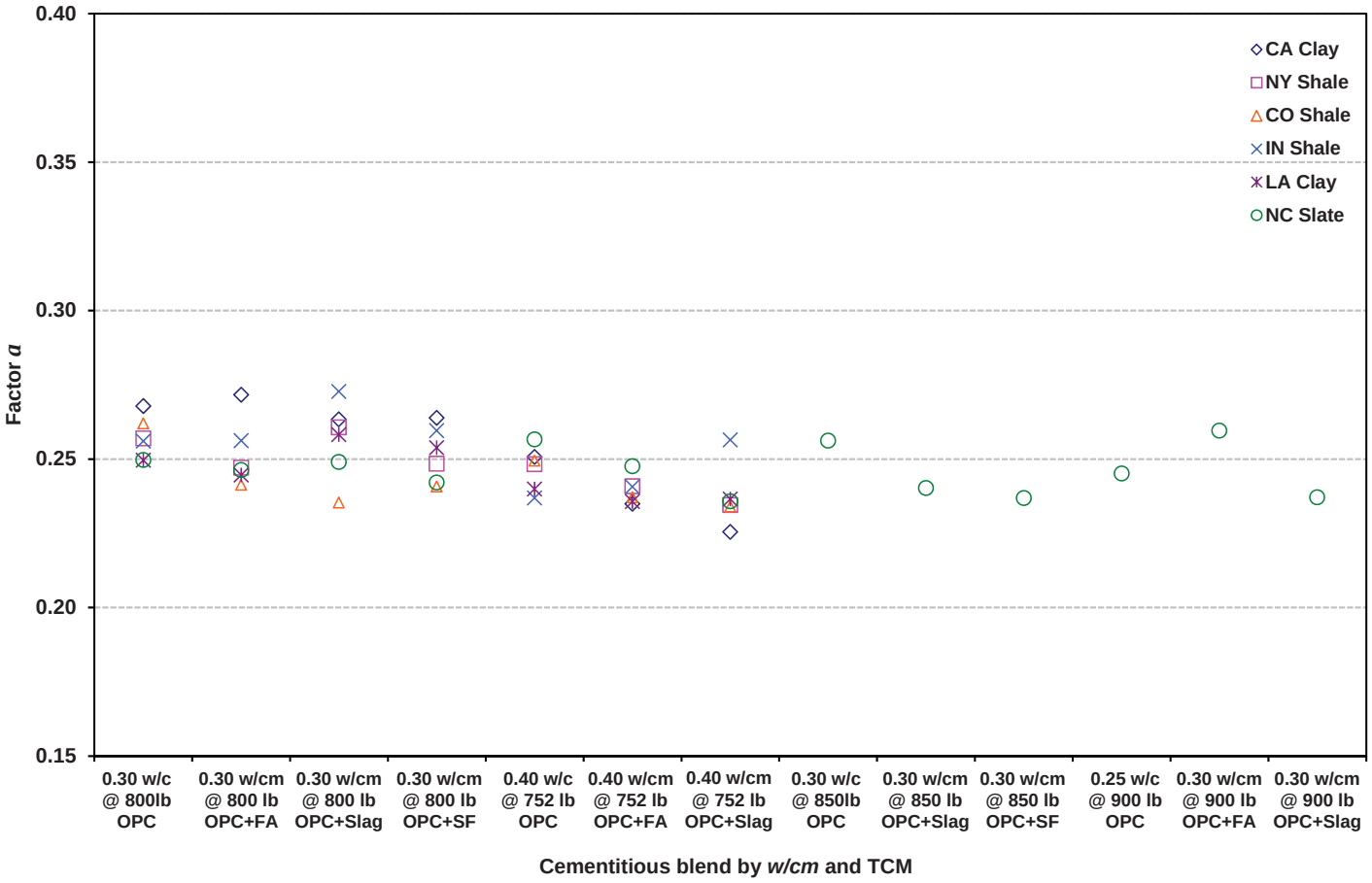

Figure 5. Factor a (where $f_{ct} = a\sqrt{f'_c}$) at 28 days.

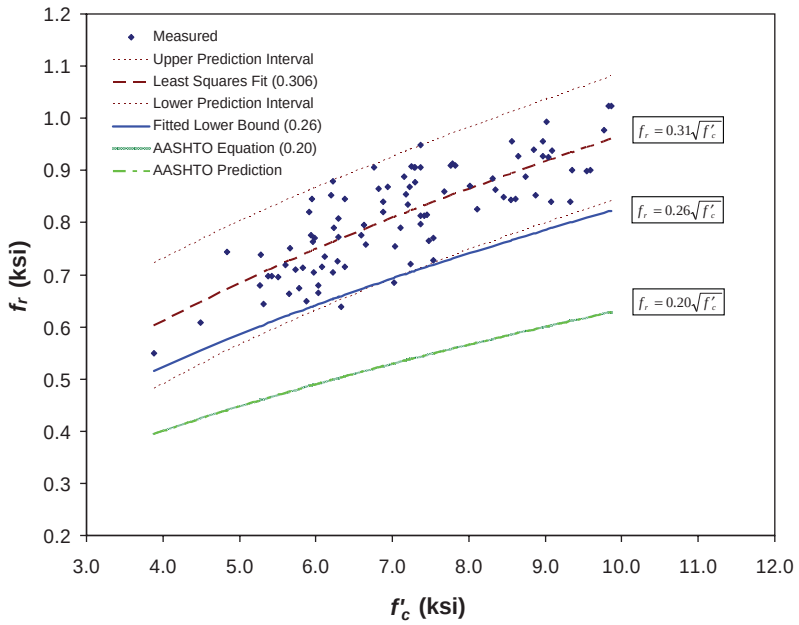

Figure 6. Flexural strength versus compressive strength at 28 days of age.

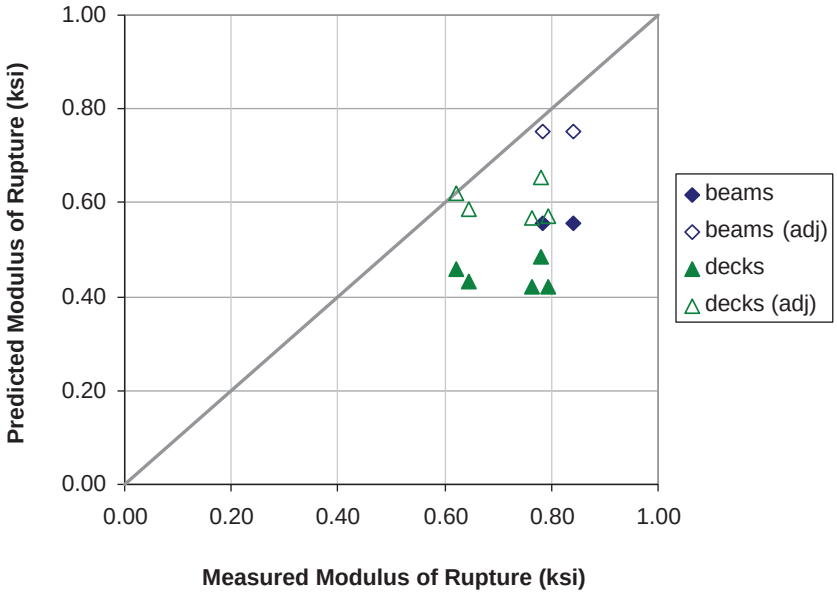

Figure 7. Measured versus predicted modulus of rupture for production mixtures.

$0.26\sqrt{f'_c}$ resulted in a closer yet conservative prediction of modulus of rupture.

Permeability. Rapid chloride ion permeability tests were conducted on the top 2 in. of a 4 in.-diameter cylinder at both 28 and 56 days from casting. Two specimens from each mixture were tested, and their values were averaged and assigned a permeability rating according to AASHTO T 277, *Standard Test Method for Electrical Indication of Concrete's Ability to Resist Chloride Ion Penetration.* The rating system is shown in Table 11.

The use of any of the supplementary cementitious materials (fly ash, silica fume, slag cement) substantially improved the lightweight concrete's ability to resist the ingress of chloride ions. Additionally, the measured air content of the mixtures seemed to be no indication of a more- or less-permeable material. Therefore, use of supplementary cementitious materials is appropriate for situations requiring a low-permeability concrete, such as bridge decks in regions receiving deicing treatments in winter months or bridge piers in harsh environments.

Table 11. Chloride ion penetrability based on charge passed (AASHTO T 277).

Charge Passed (coulombs)	Chloride Ion Penetrability
> 4,000	High
2,000 - 4,000	Moderate
1,000 - 2,000	Low
100 - 1,000	Very Low
< 100	Negligible

A representative sample of permeability test results for mixtures containing the SL1 aggregate is shown in Figure 8. Concrete made with cement and no supplementary cementitious materials consistently gave the highest permeability values based on charge passed. Permeability values for lightweight concrete containing portland cement only and SL1 aggregate ranged from 2200 and 2800 coulombs. Considering all aggregate types, the only mixtures to rate "Moderate" or "High" were mixtures with 100% portland cement binder. The permeability of concretes containing a cement replacement (either silica fume, fly ash, or slag) were much lower than for mixtures with 100% portland cement. The permeability of lightweight mixtures with some supplementary cementitious material was less than 1000 coulombs, with the lowest values obtained for mixtures containing silica fume.

Freezing and Thawing Resistance. Concrete exposed to a combination of saturating moisture and cycles of freezing and thawing in service may be susceptible to damage. The concrete mixtures used for full-scale girders and decks were subjected to rapid freezing and thawing in water in accordance with AASHTO T 161, Procedure A, except that a 5% NaCl solution was applied instead of tap water to simulate conditions of exposure common with bridge decks subject to snowfall, deicing, and subsequent freezing. As shown in Table 12, girder mixtures exhibited high resistance to freezing and thawing. The deck mixtures showed variable (but in some cases low) mass loss. Poor performance of a few deck mixtures is attributed primarily to the low air content in the mixtures. However, better performances were obtained for the girder mixtures.

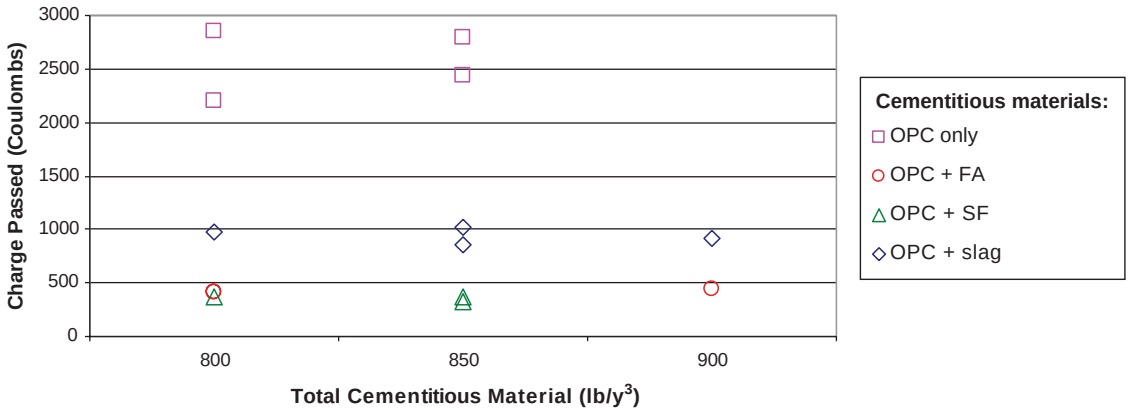

Figure 8. Permeability of concrete containing SL1 slag aggregate.

Shrinkage. Shrinkage testing was performed in accordance with ASTM C157. The amount of shrinkage was measured on two prisms with a steel stud cast into each end to serve as a gage point for length change measurements. Immediately after removing from the molds, the specimens were stored in a moist curing room for 28 days.

The measured shrinkage values for the production concrete mixtures were compared to those obtained from three prediction models: the AASHTO LRFD model contained in the *AASHTO LRFD Bridge Design Specifications* (Section 5.4.2.3), ACI 209, and CEB MC90. None of these models accounted for supplementary cementitious materials (SCMs) or type of aggregate (i.e., lightweight or normal weight) used.

Scatter plots were assembled to evaluate the applicability of the three models for lightweight concrete. Plotted points are for measured and predicted values at a given age, ranging from 1 to 448 days. Figure 9 shows measured versus predicted values using the AASHTO method for all the production mixtures, which were classified as normal weight girder mixtures, lightweight girder mixtures (w/cm = 0.30), or lightweight deck mixtures (w/cm = 0.40). The AASHTO model under-predicted the shrinkage strain in most lightweight deck mixtures, slightly over-predicted shrinkage in LWHPC girder mixtures, and closely predicted shrinkage of the normal weight girder mixtures.

Figure 10 generally shows that the ACI 209 model over-predicted the shrinkage strain for the lightweight girder mixtures, slightly under-predicted the shrinkage for the normal weight girders, and reasonably predicted shrinkage strains of lightweight deck mixtures.

As shown in Figure 11, the CEB MC90 model typically under-predicted shrinkage, particularly for the lightweight

Table 12. Rapid freezing and thawing durability results.

Mixture Designation	Aggregate	Weight Loss	Durability Factor	Surface Rating (0 to 5)	Unit Weight (lb/ft^3)	Air Content (%)
LWHPC 1 (8ksi girder)	SL1	0.24%	100	0.6	-	5.8
		1.87%	100	0.7	-	4.8
		0.29%	100	0.4	115.3	7.5
LWHPC 2 (8ksi girder)	SH3	0.41%	100	0.6	118	8.0
LWHPC 3 (10ksi girder)	SL1	0.47%	100	0.7	121.9	4.0
LWHPC 4 (4ksi deck)	SL1	4.70%	100	1.1	120	4.5
		22.72%	52	2.7	123.4	3.5
		12.50%	100	1.3	121.6	3.3
		25.47%	100	2.7	121.6	2.5
		59.77%	0	4.9	122	2.5
NWHPC 1 (8ksi girder)	NW	0.14%	83	0.3	145	4.0
		0.07%	100	0.1	-	-

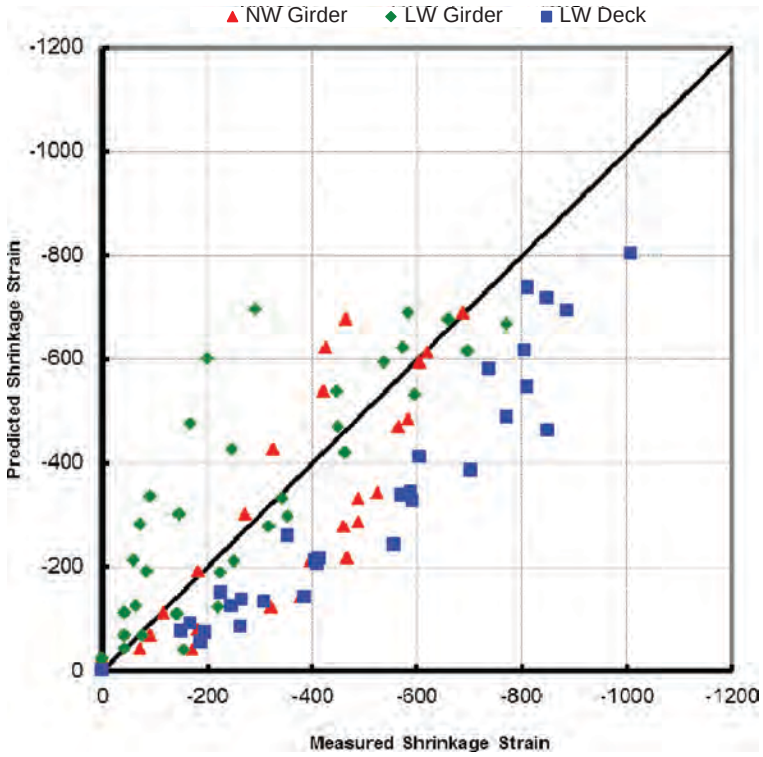

Figure 9. Measured versus predicted shrinkage strain (AASHTO model).

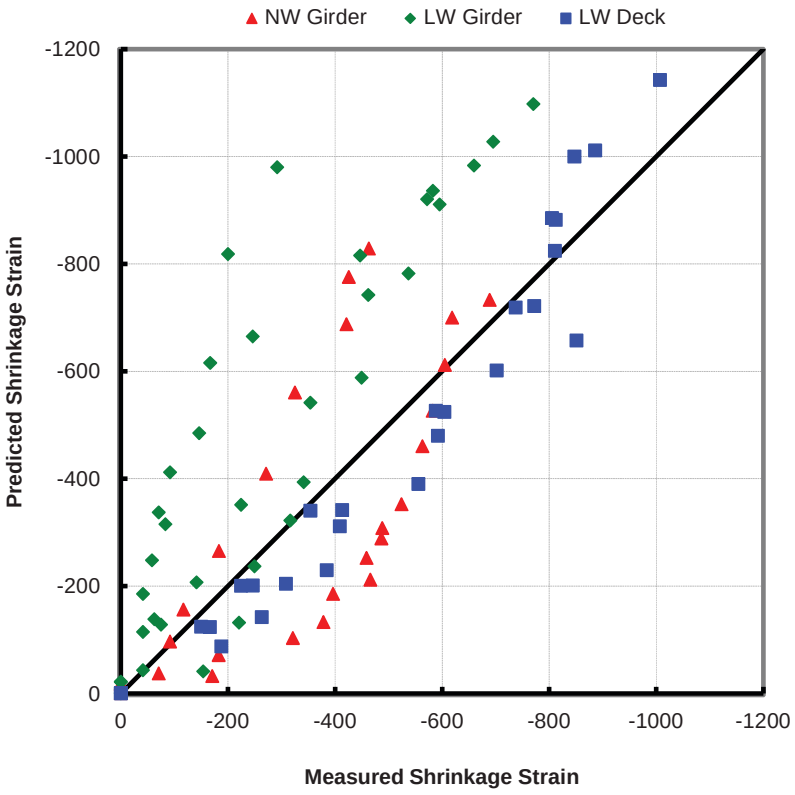

Figure 10. Measured versus predicted shrinkage strain (ACI 209 model).

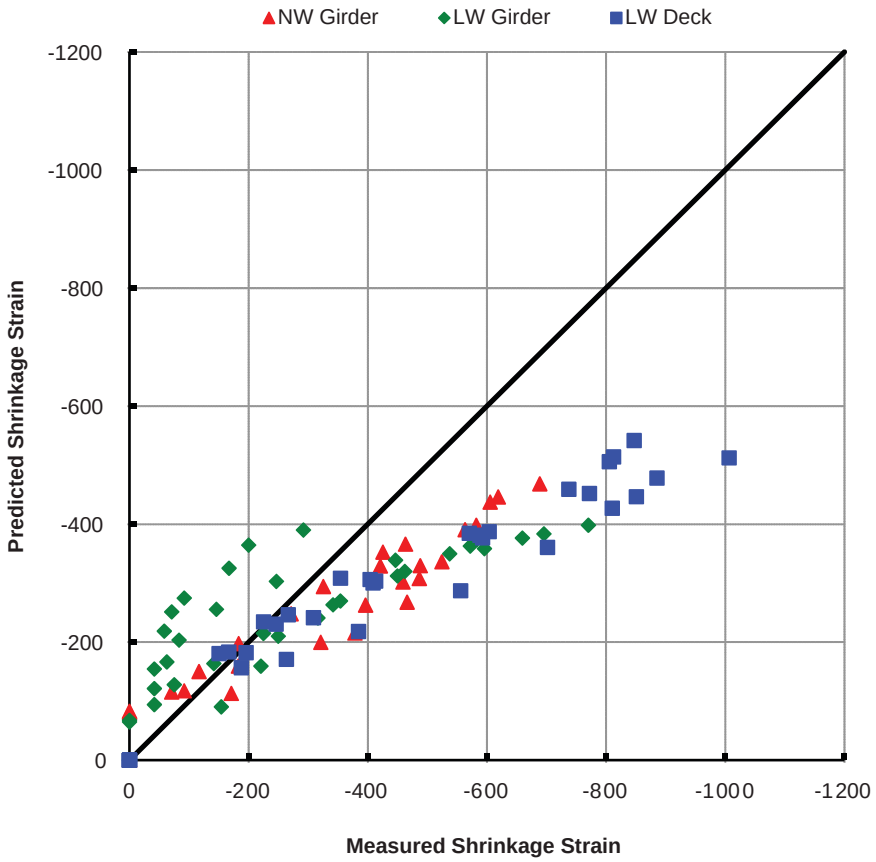

Figure 11. Measured versus predicted shrinkage strain (CEB MC90 model).

deck and normal weight girder mixtures. At early ages, the CEB MC90 model generally over-predicted shrinkage for lightweight girder mixtures but accurately predicted shrinkage for lightweight deck mixtures.

In general, the AASHTO models reasonably predicted shrinkage in lightweight girder mixtures. At later ages, the AASHTO model was the closest predictor of shrinkage for lightweight girder mixtures. For the three normal weight mixtures tested, no single model consistently predicted the shrinkage strain over the full range of testing ages, although the AASHTO model provided the best estimate. Based on these comparisons, use of the AASHTO model for predicting shrinkage of lightweight concrete is justified.

Creep. Concrete materials used in full-scale girders or decks were tested to determine their creep characteristics in accordance with ASTM C512/C512M-10, Standard Test Method for Creep of Concrete in Compression. Specimens from girder mixtures were loaded at 24 hours after steam curing, and specimen deck mixtures were loaded after 28 days of moist curing. Unsealed specimens were loaded in sets of three in hybrid hydraulic/spring-loaded frames to approximately 20% of ultimate compressive strength, well within the range of elastic behavior. Creep frames were placed in a chamber maintained at 73 ± 3°F and 50 ± 4% relative humidity. The observed values from creep testing were grouped by mixture class (NW Girder, LW Girder, or LW Deck) and plotted versus predicted values as a function of time from one of the applicable models. Plotted values represent creep at ages 1 day through the end of testing. A comparison of predicted to measured creep strains for the AASHTO, ACI 209, and CEB MC90 models are presented in Figures 12 through 14, respectively. These figures show that creep coefficients for normal weight and lightweight girders overall can be best predicted by the AASHTO model. The lightweight (LWHPC) deck mixtures exhibited considerable variation in creep coefficients that were best predicted by the ACI 209 model. However, creep behavior of the deck is secondary in importance to the girder creep.

Summary

Based on these tests, the following conclusions were made:

- The SH3 lightweight aggregate and the SL1 lightweight aggregate were selected for use in the large-scale test specimens. When used in laboratory mixtures, these aggregates

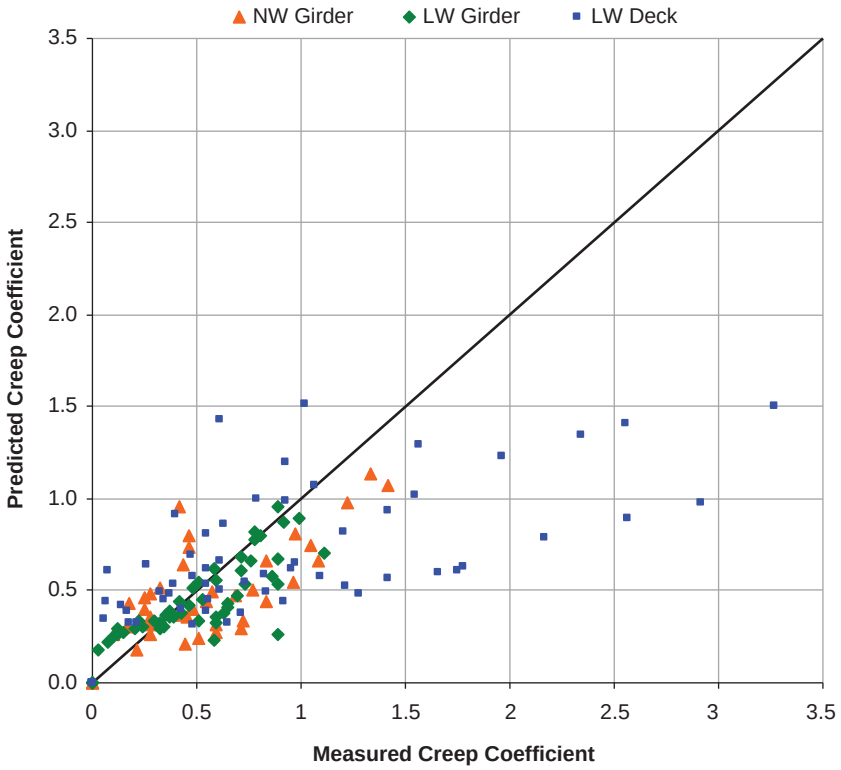

Figure 12. Measured versus predicted creep coefficients (AASHTO model).

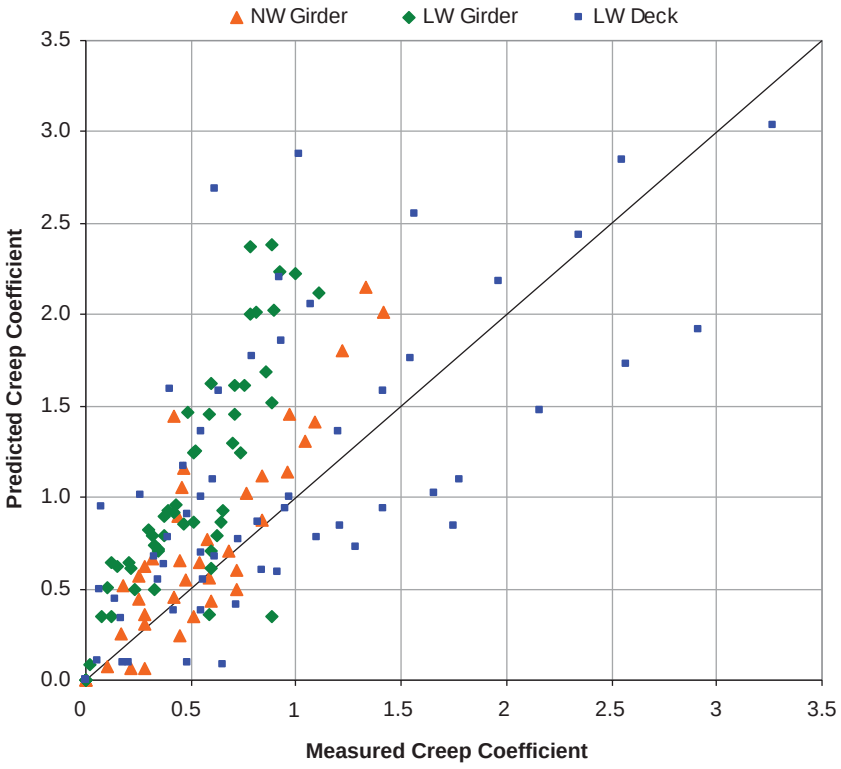

Figure 13. Measured versus predicted creep coefficients (ACI 209 model).

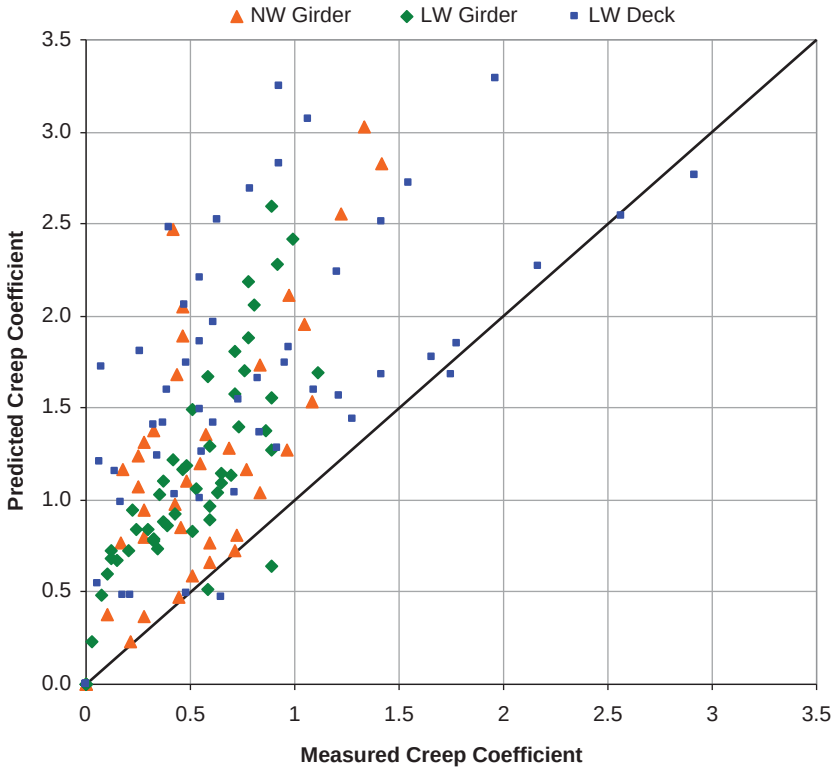

Figure 14. Measured versus predicted creep coefficients (CEB MC90 model).

yielded test results consistent with what is needed for structural concretes.

- Lightweight concrete with a compressive strength of 7000 psi and a unit weight less than 125 lb/ft^3 can be produced with a 0.30 w/cm and 800 lb of cementitious material with expanded shales and slates. The slate (SL1) mixture consistently produced the highest strength concretes.
- The AASHTO LRFD equation for modulus of elasticity with $K_1 = 1.0$ is appropriate for lightweight aggregates. Predictions can be improved by calibrating the K_1 value for each aggregate type.
- The average splitting tensile strength of lightweight concrete mixtures exceeded $\sqrt{f'_c}/4.7$ or $0.21\sqrt{f_c}$.
- The average modulus of rupture of the lightweight concrete can be expressed as $0.31\sqrt{f'_c}$, with a lower bound of $0.26\sqrt{f'_c}$.
- The use of supplementary cementitious materials resulted in low-permeability lightweight concrete. The best permeability results were achieved by using silica fume as a supplementary cementitious material.
- The AASHTO model for shrinkage reasonably predicted the shrinkage of lightweight concrete.
- The AASHTO model for creep reasonably predicted the creep coefficients of the lightweight girder mixtures. The creep coefficients of the deck concrete mixtures were reasonably predicted by the ACI 209 model.

3.2 Interface Shear Strength

Review of *AASHTO LRFD Bridge Design Specifications* (5th Edition)

The design procedure described in Section 5.8.4 of *AASHTO LRFD Bridge Design Specifications* was examined. The design for horizontal shear (as found in the specifications) is based on the following equations:

$$V_{ri} \geq V_{ui}$$

$$V_{ri} = \phi V_{ni}$$

where

V_{ri} = factored interface shear resistance
V_{ui} = factored interface shear due to applicable load combinations
V_{ni} = nominal interface shear resistance
ϕ = resistance factor for shear with
$\phi = 0.90$ for normal weight concrete
$\phi = 0.70$ for lightweight concrete

The nominal shear resistance of the interface plane is calculated as follows:

$$V_{ni} = cA_{cv} + \mu\left(A_{vf}f_y + P_c\right) \le \text{minimum of } K_1 f'_c A_{cv} \text{ or } K_2 A_{cv}$$

where

A_{cv} = area of concrete engaged in interface shear transfer
c = cohesion factor
μ = friction factor
A_{vf} = area of shear reinforcement crossing shear plane within the area A_{cv}
f_y = yield stress of reinforcement (not to exceed 60 ksi)
P_c = permanent net compressive force normal to the shear plane
f'_c = 28-day compressive strength of weaker concrete
K_1 = fraction of concrete strength available to resist interface shear
K_2 = limiting interface shear resistance

The equation is based on experimental data from normal weight concrete with strengths ranging from 2.5 to 16.5 ksi and lightweight concrete with compressive strengths ranging from 2.0 to 6.0 ksi. The yield strength of the shear reinforcing steel is limited to 60 ksi because experimental data showed that the equation over-estimates the horizontal shear strength of the interface for a higher steel yield strength.

The second term in the equation, μ, stems from a shear friction model. The net clamping force is the sum of the tension in the reinforcing steel, $A_{vf}f_y$, and the normal force, P_c, that applies compression to the interface. Multiplying the net clamping force by a friction coefficient term transforms the clamping force to a shear force at the interface. The first term of the equation, cA_{cv}, represents the shear strength provided by cohesion and aggregate interlock at the interface. This modification was made because the experimental data showed that cohesion and aggregate interlock affect interface shear strength.

Values of c, μ, K_1, and K_2 depend on surface preparation and the type of concrete (lightweight or normal weight). The term $K_1 f'_c A_{cv}$ gives the force required to prevent shearing or crushing of aggregate along the shear plane while the term $K_2 A_{cv}$ accounts for the lack of test data above the K_2 values.

Section 5.8.4.3 of *AASHTO LRFD Bridge Design Specifications* stipulates the following values for a cast-in-place slab on a clean concrete girder, free of laitance with the surface intentionally roughened to an amplitude of 0.25 in.:

- $c = 0.28$ ksi
- $\mu = 1.0$
- $K_1 = 0.3$
- $K_2 = 1.8$ ksi for normal weight concrete
- $K_2 = 1.3$ ksi for lightweight concrete

Test Specimens

To investigate the horizontal shear strength of lightweight concrete at the interface of a precast girder and cast-in-place concrete deck, 36 push-off tests were performed. The test arrangement allowed application of the horizontal force directly to the interface of the deck and girder. The typical push-off test specimen is illustrated in Figure 15.

Specimen Fabrication

Twelve different specimen configurations were tested. These configurations included three combinations of slab and girder concrete with four amounts of horizontal shear reinforcement as shown in Table 13. Each of the twelve configurations was repeated three times to provide multiple test results to examine the variability in horizontal shear strength of lightweight and normal weight concrete.

The three combinations of slab and girder concrete were as follows:

- Normal weight girder with a normal weight deck
- Normal weight girder with a lightweight deck
- Lightweight girder with a lightweight deck

The four amounts of horizontal shear reinforcement tested were as follows:

- No reinforcement: $\rho\ (A_{vf}/A_{cv}) = 0.000$
- Minimum horizontal shear reinforcement: $\rho\ (A_{vf}/A_{cv}) = 0.001$
- Maximum horizontal shear reinforcement: $\rho\ (A_{vf}/A_{cv}) = 0.012$
- Intermediate horizontal shear reinforcement: $\rho\ (A_{vf}/A_{cv}) = 0.005$

Thirty-six tests were performed with three tests for each combination of variables. The proportions for the girder and the deck concrete mixtures are listed in Table 8.

The minimum and maximum ratios of interface shear reinforcement are those identified in the *AASHTO LRFD Bridge Design Specifications.* Specimens with the minimum amount of shear reinforcement had one No. 4 stirrup placed at the center of the interface. For the maximum amount of shear reinforcement, five No. 6 stirrups were used. The specimens with the intermediate amount of horizontal shear reinforcement contained three No. 5 stirrups.

The bottom half of the specimen was cast first, mimicking a precast girder. The surface of the girder was raked to an amplitude of 0.25 in. to improve bond with the cast-in-place deck concrete. The slump of the concrete used in the bottom half of the specimen was 4 to 6 in. Once all of the 36 girder specimens were cast, the deck specimens were then cast directly on the girders, simulating typical construction of a precast concrete girder with a cast-in-place deck.

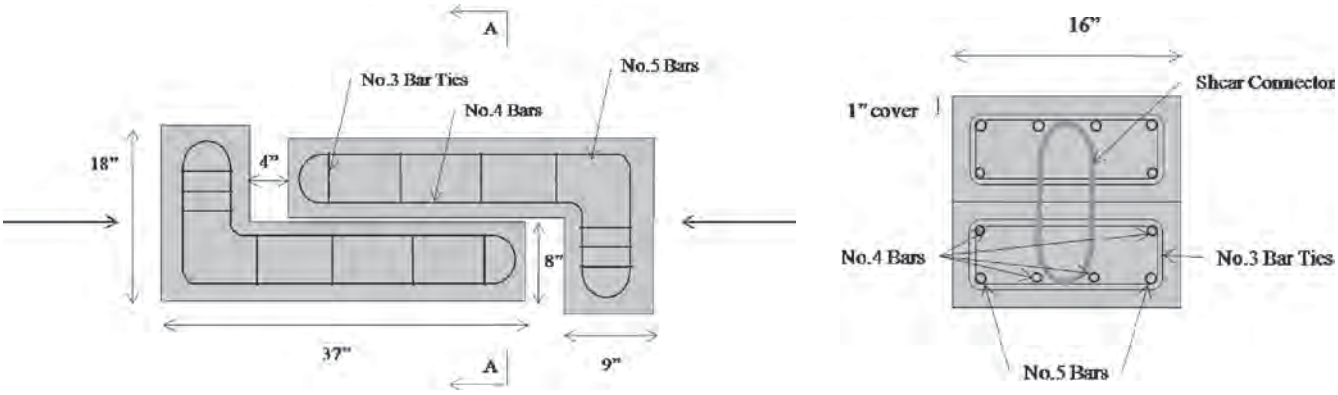

Figure 15. Push-off test specimen.

Test Setup

Figure 16 shows a typical test setup. The testing frame consisted of two steel bulkheads bolted to the floor. A 200-ton actuator was bolted to one of the bulkheads and used to apply a horizontal load to the specimen. The other bulkhead was used as an abutment to prevent the deck side from moving the test specimen, and the specimen was supported on four steel rollers.

A normal force of 2.5 kips was placed on top of the specimen to represent the dead weight on this section of a girder. This dead weight was estimated for an 8.5-in.-thick deck and 10-ft-girder spacing and was provided by two concrete blocks held together by a steel frame that rested on top of the test specimen.

A load cell was horizontally aligned at the height of the girder and deck interface. The load cell was placed in front of the actuator and bore against an 8-in.-by-8-in. steel plate which rested flat against the back of the girder side of the specimen. The center of the steel plate was also aligned with the center of the load cell at the height of the interface. An 8-in.-by-8-in. steel plate was welded to the abutment on the deck side and also aligned with the center of the girder and deck interface.

Table 13. Test matrix for push-off specimens.

Girder Concrete*	Deck Concrete*	$\rho_{iv} = A_{vf}/A_{cv}$
NWHPC1 (8 ksi)	NWHPC2 (4 ksi)	0
		0.001
		0.005
		0.012
NWHPC1 (8 ksi)	LWHPC4 (4 ksi)	0
		0.001
		0.005
		0.012
LWHPC1 (8 ksi)	LWHPC4 (4 ksi)	0
		0.001
		0.005
		0.012

*Design f'_c is shown in parentheses

Instrumentation. A load cell was used to monitor the applied horizontal shear load. Two 2-in. linear variable differential transformers (LVDTs) were used to measure the slip of the girder side relative to the deck side.

Strain gages were placed on the horizontal shear stirrups to measure the strain in the stirrups while the horizontal load was being applied. One strain gage was placed on each leg of the shear stirrup, on the side of the stirrup that would exhibit tension during the test. Two strain gages were used for specimens with one No. 4 bar. Four strain gages were used for the specimens with three No. 5 and five No. 6 bars: two gages were placed on the first shear stirrup and two gages on the last stirrup.

Testing Procedure. Each specimen was centered in the test frame and placed on the four steel rollers. The center of the specimen was lined up with the center of the actuator and abutment. The load cell was then centered between the actuator and the girder end of the specimen. The normal force blocks were placed on top of the specimen and centered above the area of the interface. The testing instruments were then zeroed and the horizontal load was applied.

The horizontal force was slowly applied in 20-kip increments. The specimen was examined at each increment to note any cracks that might have occurred. Loading continued until peak load was reached and the specimen cracked along the interface, signifying the bond breaking between

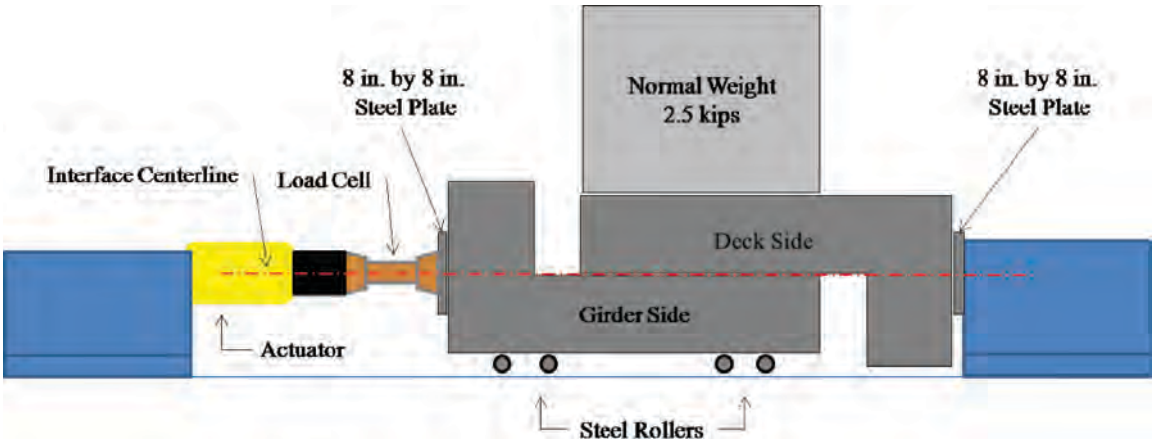

Figure 16. Push-off test setup.

the specimens. The horizontal force continued to be applied until about an inch of slip occurred between the deck and girder.

Test Results

All push-off specimens behaved similarly at the beginning of testing. The load increased steadily with little slip between the two specimens until the bond failure load was reached. The bond failure load was defined as the load at which the cohesion at the interface was broken. The load in the actuator then decreased and leveled off at different loads, depending on the amount of shear reinforcement provided at the interface. Specimens without shear reinforcement maintained a small amount of resistance once the bond at the interface was broken. Figure 17 presents the designation used for each test and a key to decipher what each part of the label represents.

Table 14 presents the results of the push-off tests. The percent yield strain in the reinforcement (ε_y) was taken as the recorded strain in the reinforcement at peak load divided by a yield strain of 0.00207 for reinforcing steel with a reported

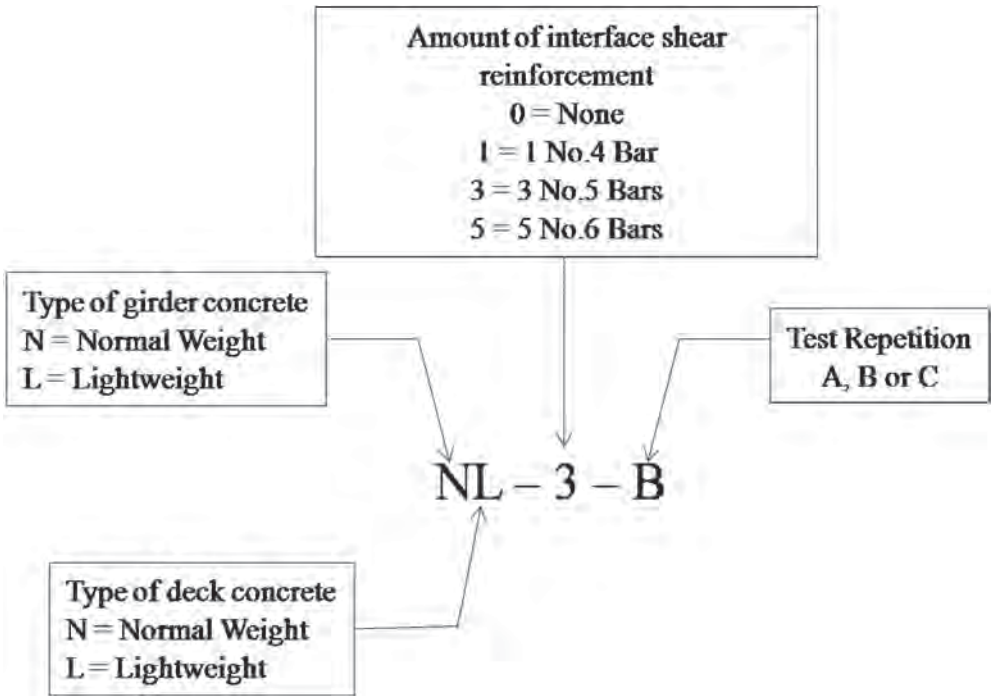

Figure 17. Specimen designation.

yield stress of 60 ksi and elastic modulus of 29,000 ksi. The recorded strain in the reinforcement was not pure axial strain but also incorporated bending. Specimens with one reinforcing bar had two strain gages, and the percent yield strain reported in the table is an average of the two gages. Specimens with three reinforcing bars (LL-3, NN-3, and NL-3 in Table 14) had a total of four strain gages. The upper value is the average of the two front strain gages (on the left in Figure 16) and the lower value is the average of the two back strain gages (on the right in Figure 16). Other information in the table includes

A_{cv} = area of concrete at the interface
A_{vf} = total area of reinforcement crossing the interface
f_y = reported yield stress of reinforcement
P_c = permanent net compressive force normal to the shear plane
ε_y = percent of yield strain in the reinforcement measured at peak load

The results of the heavily reinforced specimens ($\rho_{iv} = 0.012$) are not reported. Because of the very large area of steel crossing the interface, the failure of the specimen occurred

Table 14. Results of push-off tests.

Specimen Designation	A_{cv} (in^2)	A_{vf} (in^2)	f_y (ksi)	P_c (kips)	f'_c deck (ksi)	f'_c girder (ksi)	ε_y (%)	Peak Load (kips)
LL-0-A	384	0	60	2.54	6.25	11.1		132
LL-0-B	384	0	60	2.54	6.25	11.1		140
LL-0-C	384	0	60	2.54	6.25	11.1		178
NN-0-A	384	0	60	2.54	6.15	7.78		153
NN-0-B	384	0	60	2.54	6.15	7.78		160
NN-0-C	384	0	60	2.54	6.15	7.78		156
NL-0-A	384	0	60	2.54	6.25	7.78		186
NL-0-B	384	0	60	2.54	6.25	7.78		131
NL-0-C	384	0	60	2.54	6.25	7.78		197
LL-1-A	384	0.4	60	2.54	6.25	11.1	71	422
LL-1-B	384	0.4	60	2.54	6.25	11.1	134	147
LL-1-C	384	0.4	60	2.54	6.25	11.1	121	188
NN-1-A	384	0.4	60	2.54	6.15	7.78	7	123
NN-1-B	384	0.4	60	2.54	6.15	7.78	5	141
NN-1-C	384	0.4	60	2.54	6.15	7.78	5	173
NL-1-A	384	0.4	60	2.54	6.25	7.78	205	169
NL-1-B	384	0.4	60	2.54	6.25	7.78	*	175
NL-1-C	384	0.4	60	2.54	6.25	7.78	10	183
LL-3-A	384	1.84	60	2.54	5.73	11.1	66 32	201
LL-3-B	384	1.84	60	2.54	5.73	11.1	95 32	223
LL-3-C	384	1.84	60	2.54	5.73	11.1	73 35	230
NN-3-A	384	1.84	60	2.54	6.15	7.78	* 12	195
NN-3-B	384	1.84	60	2.54	6.15	7.78	41 23	218
NN-3-C	384	1.84	60	2.54	6.15	7.78	* *	229
NL-3-A	384	1.84	60	2.54	5.73	7.78	68 25	242
NL-3-B	384	1.84	60	2.54	5.73	7.78	12 13	238
NL-3-C	384	1.84	60	2.54	5.73	7.78	88 82	183

*Strain gage damaged; no data available.

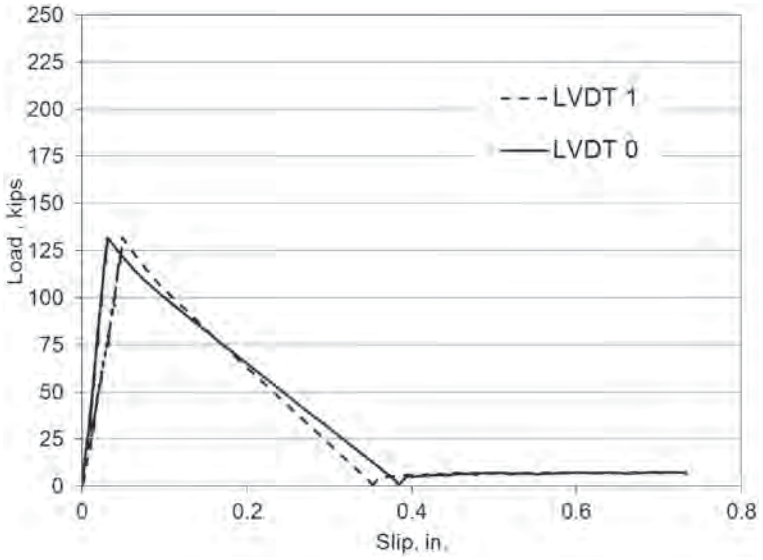

Figure 18. Typical load versus slip behavior for specimens without shear reinforcement.

in the vertical leg of the deck side specimen and not at the interface.

Typical Load Slip Behavior. All of the specimens exhibited similar pre-crack behavior in which little or no slip occurred as the load continuously increased until the bond between the concrete at the interface failed. The load that caused the interface crack was always the peak load. Once the interface bond failed, post-peak behavior varied with the amount of reinforcing steel across the interface. Figures 18 through 20 present typical load slip plots for specimens with no reinforcing, with one No. 4 stirrup, and with three No. 5 stirrups, respectively. In all cases, the load dropped considerably after the interface crack occurred. For the specimen with three No. 5 stirrups, the first drop in load was due to the interface crack, and the second drop was due to rupture of two of the bars. All specimens maintained a smaller load after considerable slip. The post-peak strength increased with increasing reinforcement across the interface.

Failure Surfaces. The failure surface varied with the type of concrete constituting the specimens but generally was in

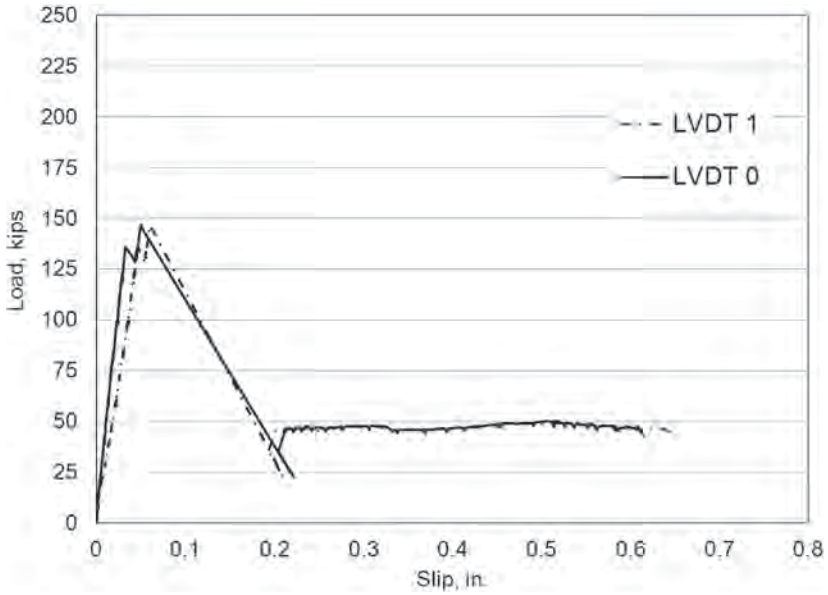

Figure 19. Typical load versus slip behavior for specimens with one No. 4 stirrup.

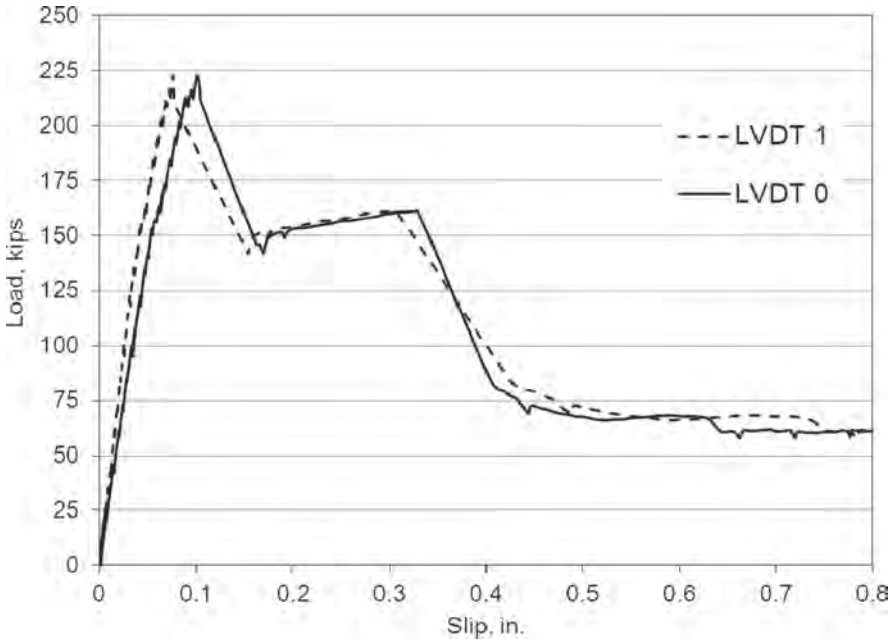

Figure 20. Typical load versus slip behavior for specimens with three No. 5 stirrups.

or around the deck/girder interface. Figure 21 shows cracking in the interface region for the three concrete combinations of deck concrete (on the top) and girder concrete (on the bottom). The NW-NW crack was generally along the interface and relatively straight. The LW-NW failure surface was along the interface in some locations and through the lightweight concrete in others. The LW-LW failure surface was typically entirely through the deck-side concrete.

Data Analysis

Detailed information about each interface shear test, including load versus deflection plots, are provided in Attachment G.

Comparison of Results to AASHTO LRFD. The current AASHTO LRFD (2010) requirements for nominal shear resistance at the interface of a precast concrete girder with a cast-in-place concrete deck are given in Section 5.8.4. Values for the cohesion factor (c) and friction factor (μ) are dependent on surface preparation and how the composite system is constructed. AASHTO specifies for a cast-in-place concrete slab on a clean concrete surface raked to an amplitude of 0.25 in.

A summary of the calculated and experimental horizontal shear resistance is provided in Table 15. The experimental strength divided by the calculated nominal strength is called the bias. A bias of 1.0 indicates the calculated value to be the same as the experimental value. As the value of the bias increases above 1.0, the level of conservativeness of the equation also increases. The coefficient of variation of the test data was also used to measure the dispersion of data. A lower coefficient of variation indicates a lower ratio of the standard deviation to the mean of the data.

The bias was generally larger for the specimens with lightweight concrete (1.26 for LW-LW and 1.29 for LW-NW) than for normal weight (1.16). This is probably due to the lightweight aggregate absorption properties which enhance bond across the shear interface. However, there was greater scatter in the results with lightweight concrete as evidenced by the higher coefficient of variation (0.235 for LW-LW and 0.233 for LW-NW) than for normal weight (0.195). Also the bias decreased with increasing reinforcement.

Test data for horizontal shear strength and those predicted by the AASHTO equation are presented in Figure 22. Data (for three NN specimens and one NL and LL specimen each) fell below those from the equation. The figure also shows the data using equations with reduction factors (ϕ) of 0.9 and 0.7, which are the currently specified factors for shear for normal weight and lightweight concrete, respectively. With a ϕ factor of 0.9, two specimens have strengths lower than predicted (one NN and one NL). A ϕ factor of 0.7 provides much lower values than obtained from the tests for all specimens.

Reliability Analysis. A reliability analysis was performed to examine the current resistance factor (ϕ) used in AASHTO LRFD specifications for interface shear resistance in lightweight concrete. For this analysis, the shear resistance was considered a random variable and the uncertainty of the resistance estimate was separated into three categories: (1) a material factor that encompasses the uncertainty introduced due to variability in the materials used; (2) a fabrication factor representing

Normal weight – Normal weight

Normal weight – Lightweight

Lightweight-Lightweight

Figure 21. Side view of typical failure cracks.

variability in the fabrication of the specimens; and (3) a professional factor representing the uncertainty of the theoretical model by representing variability of the ratio of tested values to calculated values. The material and fabrication factors were taken from previous work (Nowak (1999) and Nowak and Rakoczy (2010)), but the professional factor was extracted from test data. The mean horizontal shear resistance could then be taken as the product of the nominal resistance multiplied by these three factors.

The current equation in the AASHTO LRFD specifications (2010) was used to calculate horizontal shear resistance at the interface. The professional factors, bias (λ_P) and coefficient of variation (CoV_P) were calculated from the test results for each concrete combination listed in Table 14.

The material and fabrication factors, λ_F, λ_M, CoV_F, and CoV_M were presented in previous research. Nowak and Szerszen (2003) provide information on the fabrication factors for cast-in-place and plant-cast concrete. For horizontal shear strength, the width of the top flange and the area of the reinforcing steel are of greatest importance. A fabrication bias of $\lambda_F = 1.0$ and a coefficient of variation $CoV_F = 0.01$ were selected. Nowak and Rakoczy (2010) presented compressive

Table 15. Calculated horizontal shear resistance.

Specimen Designation	LRFD Calculated V_{ni} (kips)	Maximum Test Load (kips)	Mean Test Load (kips)	Bias V_{test}/V_{ni}	Mean Bias	Overall Bias	CoV	Overall CoV
LL-0-A	110	132	150	1.20	1.36	1.26	0.163	0.235
LL-0-B		140		1.28				
LL-0-C		178		1.61				
LL-1-A	134	242	192	1.81	1.43		0.249	
LL-1-B		147		1.10				
LL-1-C		188		1.40				
LL-3-A	221	201	218	0.91	0.99		0.070	
LL-3-B		223		1.01				
LL-3-C		230		1.04				
NN-0-A	110	153	156	1.39	1.42	1.16	0.023	0.195
NN-0-B		160		1.46				
NN-0-C		156		1.41				
NN-1-A	134	123	146	0.92	1.09		0.172	
NN-1-B		141		1.06				
NN-1-C		173		1.29				
NN-3-A	221	195	214	0.885	0.97		0.080	
NN-3-B		218		0.99				
NN-3-C		229		1.04				
NL-0-A	110	186	172	1.69	1.56	1.29	0.206	0.233
NL-0-B		131		1.19				
NL-0-C		197		1.79				
NL-1-A	134	169	176	1.26	1.31		0.040	
NL-1-B		175		1.30				
NL-1-C		183		1.37				
NL-3-A	221	242	221	1.10	1.00		0.148	
NL-3-B		238		1.08				
NL-3-C		183		0.83				

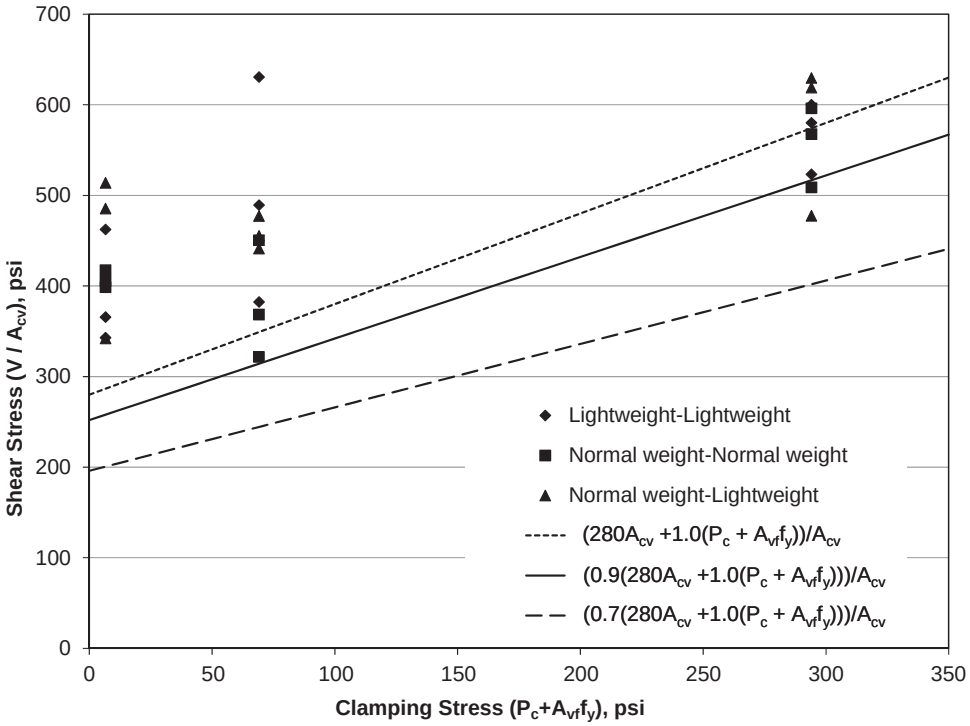

Figure 22. Shear stress using AASHTO equation with different Φ factors compared to test results.

strength data from over 8000 samples of lightweight and normal weight concrete and determined the bias and coefficient of variation for a wide range of concrete strengths. For typical deck concrete (4 ksi compressive strength), the factors for lightweight concrete are $\lambda_M = 1.338$ and $CoV_M = 0.123$, and for normal weight the factors are $\lambda_M = 1.213$ and $CoV_M = 0.155$.

The information gathered from tests and the literature was used to calculate a resistance bias and coefficient of variation for lightweight/lightweight, normal weight/normal weight, and normal weight/lightweight combinations; a summary is given in Table 16.

The limit state load combination for horizontal shear resistance at the interface of a bridge deck and bridge girder was considered to be the Strength I load combination. Using the information in Section 5.8.4.1 of the *AASHTO LRFD Bridge Design Specifications* and appropriate load factors, the horizontal shear resistance can be determined as follows:

$$V_{nh} \geq \left[1.25\ DC + 1.5\ DW + 1.75\ (LL + IM)\right] / \Phi$$

where

DC = dead load from weight of structural and nonstructural components
DW = dead load from the weight of the wearing surface
LL + IM = live load and impact load from moving vehicles on the bridge

Statistical parameters given by Nowak (1999) including a bias factor of 1.05 for both types of dead loads and 1.28 for the live load, and coefficients of variation of 0.1, 0.25, and 0.18 for DC, DW, and LL, respectively, were used. To analyze the limit state, different ratios of dead load to total load were considered. The mean load and standard deviation for each ratio was calculated using the load parameters.

A reliability index (β) could then be calculated for each girder/deck concrete combination. Reliability indices describe a probability of failure (P_F) as a function of the limit state function, the resistances, and the loads. The probability of failure is the probability that the resistance factor multiplied by the calculated resistance is less than the factored loads. A higher reliability index signifies a lower probability of failure (a $\beta = 3.09$ corresponds to a probability of failure of one in one thousand, and $\beta = 3.71$ corresponds to a probability of failure of one in ten thousand). Using the statistical parameters calculated for resistance and the statistical parameters for the load combination, a reliability index could be calculated using the following equation (Nowak and Szerszen, 2003):

$$\beta = \left(\mu_R + \mu_Q\right) / \left(\sigma_R^2 + \sigma_Q^2\right)^{1/2}$$

where

μ_R = mean of the resistance
μ_Q = mean of the load combination
σ_R = standard deviation of the resistance
σ_Q = standard deviation of the load combination

Reliability indices were calculated for an assumed resistance factor and multiple loading possibilities. The average β was then taken for multiple combinations of load variations. Figure 23 shows β for normal weight and lightweight concrete. Note that for a given resistance factor, the lightweight-lightweight and normal weight-lightweight concrete combinations provide a higher reliability index than for the normal weight-normal weight concrete combination. The equations used in the analysis are further explained in Attachment G.

Based on review of the results of nine tests for each concrete combination, the lightweight resistance factors should be greater than 0.7 and thus closer to that for normal weight concrete. The tests also showed that although the coefficient of variation for lightweight was higher than for normal weight, the bias was also higher. The data from Nowak and Rakoczy (2010) also indicated that the bias of normal weight concrete compressive strength was lower than for lightweight concrete, and the coefficient of variation was larger. The combination of these factors suggests that an increased resistance factor for sections containing lightweight concrete is appropriate. Because there is no distinction between interface and beam shear resistance factors provided in the AASHTO LRFD specifications, changes to the shear resistance factors given in these specifications seem appropriate; recommendations will be given later in this report.

Table 16. Bias and coefficients of variation.

Concrete Combination	λ_F	λ_M	λ_P	λ_R	CoV_F	CoV_M	CoV_P	CoV_R
LL	1.00	1.338	1.26	1.69	0.01	0.123	0.25	0.28
NN	1.00	1.213	1.15	1.40	0.01	0.155	0.20	0.26
NL	1.00	1.338	1.29	1.73	0.01	0.123	0.23	0.26

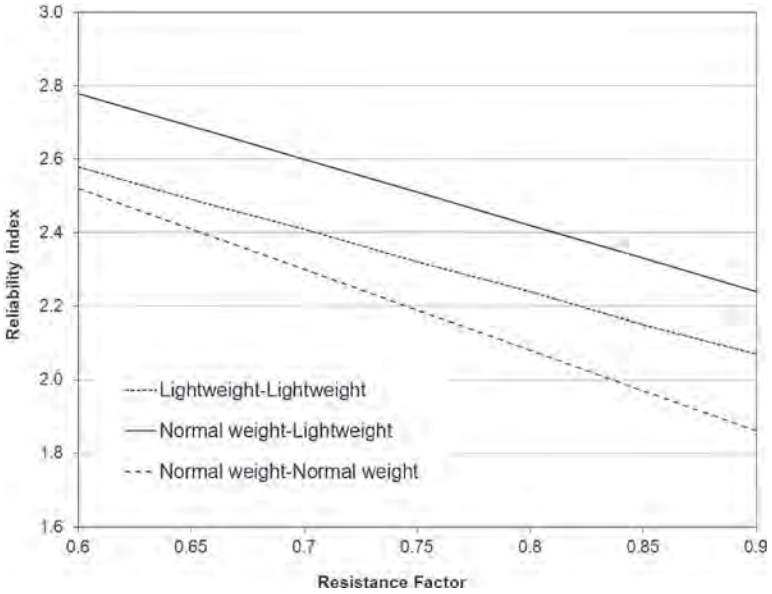

Figure 23. Reliability indices versus resistance factors.

Summary

The interface shear tests revealed the following:

- The bias of the measured shear strengths to the nominal shear strength computed with the AASHTO equation for a concrete deck placed on the top flange of a girder which has been intentionally roughened was 1.16 for N-N, 1.29 for L-N, and 1.26 for L-L.
- The AASHTO LRFD equation for interface shear design is less conservative with increasing reinforcement ratios, which indicates the friction coefficient may be too high.
- Based on a reliability analysis, lightweight concrete should have a higher strength reduction factor for interface shear than currently stipulated in specifications. Because AASHTO equations do not differentiate between different kinds of shear in reinforced concrete, changes to the shear strength reduction factors given in AASHTO need to be considered.

3.3 Laboratory Beam Test Results and Analysis

Test beam specimens contained either 0.5 in. or 0.6 in. prestressing strands and had one of two T-shaped cross-sections, depending on the diameter of the prestressing strand being used. The cross-sections are shown in Figures 24 and 25 and section properties are listed in Table 17. The cross-sectional design provides (1) for large compressive stresses at the level of the prestressing strands and at the beam ends after release to allow easy measurement of transfer lengths and (2) for large tensile stresses in the prestressing strands at flexural failure.

The beams were designed for stresses approximately equal to the allowable stress limits given in the AASHTO LRFD specifications. As per AASHTO LRFD Article 5.11.4.2, the development length of prestressing strand depends on the tensile stress in the steel. The beams were designed for a tensile strain between 0.04 in./in. and 0.05 in./in. at flexural failure. This was accomplished by using the wide T-flanges, which result in a small neutral axis depth at flexural failure when compared to the overall depth of the beams, indicating large tensile strains in the steel. This also ensured that the beams would fail in a ductile manner.

All beams were 24 feet in length. Concrete mix types and strand size used is given in Table 18 with mixture proportions given in Table 8. Overall, there were eight beams containing 0.5 in. strands and four beams containing 0.6 in. strands. Normal weight concrete beams were included to allow for comparison of results to those found for the lightweight concrete beams.

Each beam specimen contained three straight, Grade 270, low-relaxation, fully bonded, pretensioned strands. These strands were spaced 2 inches on center and located at a distance of 2 inches on center from the bottom surface. The two outer strands were located at a distance of 2 inches on center from the vertical bulb surfaces. All strands contained an oily surface residue which was allowed to remain during fabrication so as to create a realistic worst-case scenario for prestress transfer and development length purposes. The strand was stored indoors to prevent corrosion. As shown in Figure 25, reinforcing steel was provided to meet anchorage requirements at transfer and shear requirements during flexural testing. All mild steel used in the beams was Grade 60. With this arrangement, a flexural or bond failure would occur prior to a shear failure.

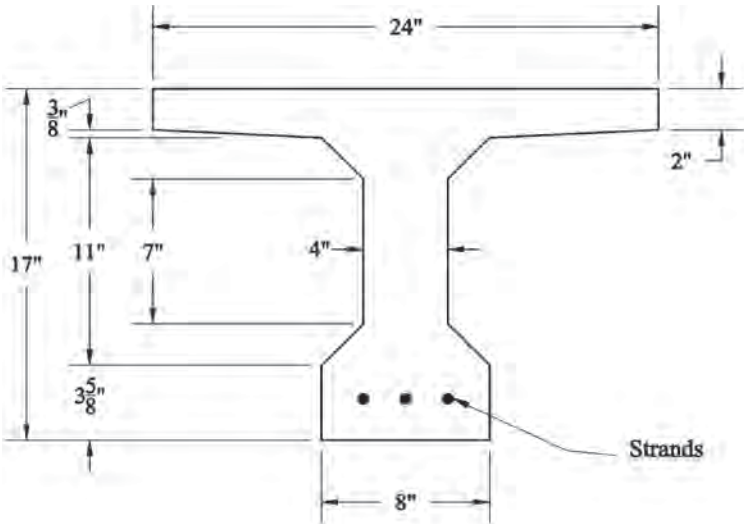

a) Beams containing 0.5-in.-diameter strands.

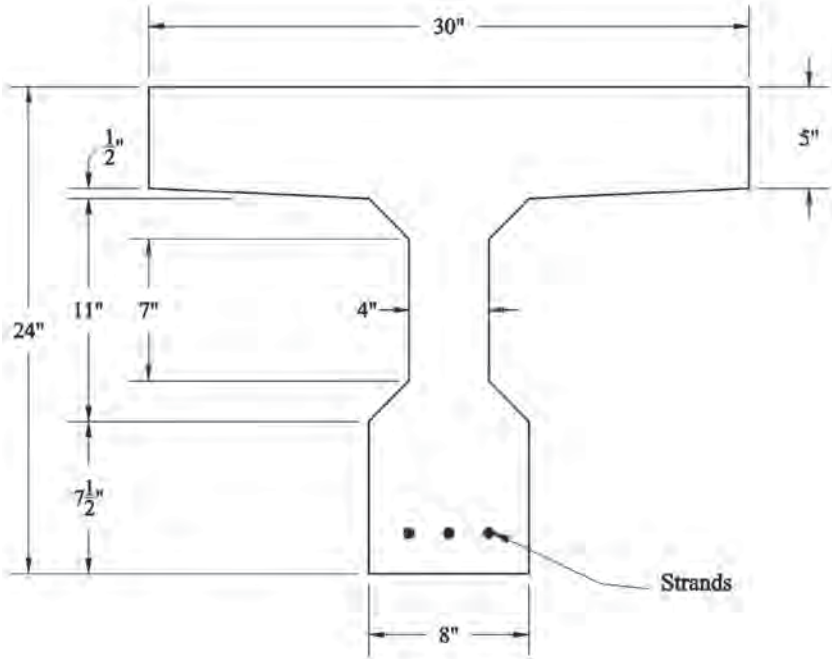

b) Beams containing 0.6-in.-diameter strands.

Figure 24. Beam cross-sectionals.

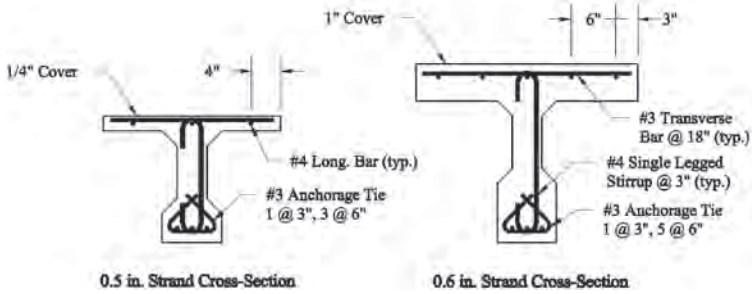

Figure 25. Reinforcement details.

Table 17. Beam cross-section properties.

Property	Beams containing 0.5-in.–dia. strands	Beams containing 0.6-in.–dia. strands
A_g (in^2)	135	273
I_g (in^4)	4537	15320
y_b (in)	10.3	15.9
y_t (in)	6.73	8.13
e_g (in)	8.27	13.9
S_b (in^3)	442	965
S_t (in^3)	672	1884

The scheme used to identify the laboratory beams is illustrated in Figure 26. The "Abutment" identifier specifies the closest adjacent abutment during casting. The live end of a beam refers to the end in which the strands were flame cut, while the dead end refers to that opposite the live end (closest to an abutment during casting). The beam side refers to the left or right side of the beam as seen when looking toward the beam dead end from the beam live end. The scheme can be used to identify a particular beam or a particular beam end by dropping the end components. For example, 1.LW1.5A refers to a single beam, while 1.LW1.5A.B refers to the dead end of that beam, and 1.LW1.5A.BL refers to the left-side of the dead end of that beam.

Concrete and Strand Material Properties

Tests were conducted on the concrete mixes and prestressing steel, but no material property tests were carried out on the mild reinforcing steel used. For analysis purposes, the mild reinforcing steel was assumed to have a modulus of elasticity of 29,000 ksi and a yield stress of 60 ksi. Test results for fresh concrete properties as well as compressive strength, modulus of elasticity, splitting tensile strength, and modulus of rupture are shown in Table 19.

The 28-day compressive strengths for the LWHPC1, LWHPC2, and NWHPC1 mixes were less than the design f'_c of 8 ksi; however, the compressive strength for these mixes exceeded 8 ksi at 90 days. For the LWHPC3 mix, the design strength, f'_c of 10 ksi, was not obtained even after 90 days. This highlights the difficulty in achieving high compressive strengths of concrete containing lightweight aggregates in the field.

Strand tension tests were performed on samples of the prestressing strand in accordance with ASTM A416. Six tests were performed for the 0.5 in. strand and four tension tests for the 0.6 in. strand. Average test results for modulus of elasticity (E_{ps}), yield stress (f_{py}), and ultimate stress (f_{pu}) were 27,500 ksi, 240 ksi, and 278 ksi, respectively.

Also, direct pullout tests were performed on NASP Bond specimens to examine strand bond capability. All tested samples for both strand sizes met the NASP requirements with measured slip values far less than expected at the required load values. Large Block Pullout Tests were also performed on strand samples according to procedures recommended by Logan (1997). More details of the NASP testing of strand samples are provided in Attachment H. Pullout blocks were fabricated using the NW1 concrete mix, and six 0.5 in. strand samples and four 0.6 in. strand samples were tested. All strand samples exceeded the minimum pullout load requirements proposed by Logan.

Transfer Length

The compressive strains at different locations along the beam length were measured at transfer and at 28 days after transfer using a digital DEMEC strain gage; a sample strain profile is shown in Figure 27. The measured strains on each side of the beam are shown in the figure along with the average strain. The profile has been drawn assuming zero strains at the end of the beams.

Transfer lengths were determined from strain profiles using a graphical procedure known as the 95% Average Maximum Strain (AMS) method (Russell and Burns (1993)). The AMS method is the average concrete surface strain between the transfer lengths. The method was conceived as a way to prevent arbitrary interpretation of strain profile data when determining transfer lengths. Table 20 provides the measured transfer lengths for all beams. AMS significantly increased over time due to creep and shrinkage of the concrete.

Article 5.11.4.1 of the AASHTO LRFD specifications requires that the transfer length of pretensioned concrete components be taken as 60 times the strand diameter. Ramirez and

Table 18. Summary of beam specimens.

Pour Number	Number of Beams	Concrete Type	Strand Size (in)
1	2	LWHPC1	0.5
	2	NWHPC1	0.5
2	2	LWHPC3	0.5
	2	LWHPC3	0.6
3	2	LWHPC2	0.5
	2	NWHPC1	0.6

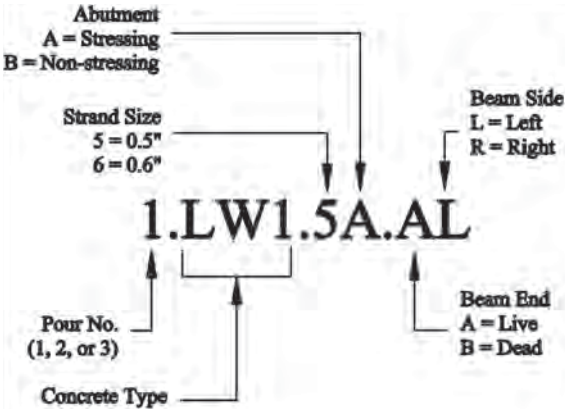

Figure 26. Beam identification diagram.

Russell (2008) have recently proposed changes to the AASHTO specifications based on research conducted in NCHRP Project 12-60 (2008) that showed a correlation between bond quality and the square root of the concrete strength. The proposed equation for transfer length, l_t, is

$$l_t = \left(120/\sqrt{f'_{ci}}\right) d_b \geq 40 d_b$$

where f'_{ci} is the concrete strength at transfer and d_b is the strand diameter. Figure 28 compares the transfer length measured at transfer from this research with AASHTO requirements and the proposed equation by Ramirez and Russell. In all cases the two methods provide an upper bound estimate of the transfer length in lightweight concrete beams.

Table 19. Concrete material property test results.

Concrete	Property	Time after Casting				
		Fresh	7 days	28 days	56 days	90 days
NWHPC1	Slump (in)	5.5				
	Air (%)	5.0				
	Wt.(lb/ft3)	146				
	f'_c (ksi)		6.16	7.39		8.20
	E_c (ksi)		4790	5720		5200
	f_t (ksi)		0.650	0.770		0.825
	f_r (ksi)			1.02 (2)		
LWHPC1	Slump (in.)	6.75				
	Air (ksi)	4.75				
	Wt. (ksi)	120				
	f'_c (ksi)		7.10	8.39		8.59
	E_c (ksi)		3660	4120		3680
	f_t (ksi)		0.610	0.715		0.760
	f_r (ksi)			0.780		
LWHPC3	Slump (in.)	10.0				
	Air (ksi)	8.0				
	Wt. (ksi)	115				
	f'_c (ksi)	5.02	7.74	8.07	8.31	
	E_c (ksi)	2920	3560	3580	3630	
	f_t (ksi)	0.520	0.680	0.670	0.745	
	f_r (ksi)		0.785			
NWHPC1	Slump (in.)	6.0				
	Air (ksi)	4.5				
	Wt. (ksi)	147				
	f'_c (ksi)	6.20	7.97	8.54	8.43	8.29
	E_c (ksi)	4570	5520	5290	5470	4360
	f_t (ksi)	0.670	0.735	0.820	0.780	0.796
	f_r (ksi)		0.885			
LWHPC2	Slump (in.)	6.25				
	Air (ksi)	8.0				
	Wt. (ksi)	119				
	f'_c (ksi)	5.89	7.73	8.32	8.17	8.95
	E_c (ksi)	3060	3420	3540	3740	3240 (2)
	f_t (ksi)	0.620	0.665	0.715	0.660	0.766 (2)
	f_r (ksi)		0.840			

Note: (2) denotes a 2 specimen average.

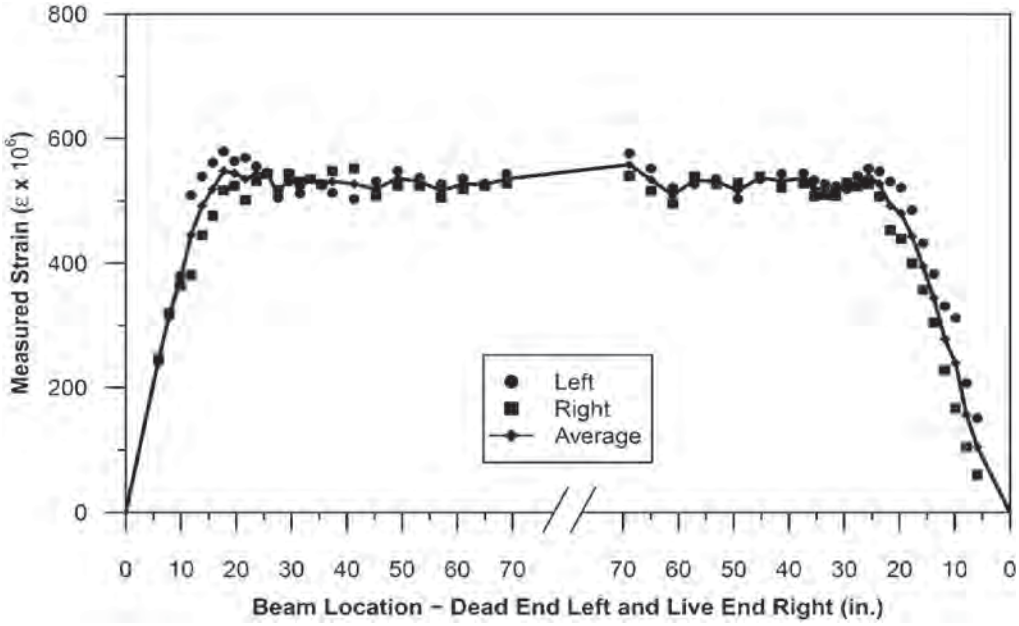

Figure 27. Sample strain profile (2.LW3.5A at transfer).

Table 20. Measured transfer lengths.

Beam ID	Time	Transfer Length (in.)		AMS (με)
		Dead End	Live End	
1.NW1.5A	Transfer	11.5	18.5	453
	28 Days	14.0	18.0	812
1.NW1.5B	Transfer	12.0	20.0	457
	28 Days	14.5	21.0	800
1.LW1.5A	Transfer	12.0	20.5	502
	28 Days	11.5	20.0	727
1.LW1.5B	Transfer	12.0	21.0	503
	28 days	12.0	19.0	733
2.LW3.5A	Transfer	14.5	22.5	530
	14 Days	14.0	23.0	667
	28 Days	14.0	22.5	784
2.LW3.5B	Transfer	14.5	21.0	537
	14 Days	15.0	21.0	666
	28 Days	16.5	21.5	797
2.LW3.6A	Transfer	14.0	25.0	562
	14 Days	15.5	23.5	687
	28 Days	15.5	23.0	805
2.LW3.6B	Transfer	16.0	23.5	551
	14 Days	16.5	25.0	683
	28 Days	16.0	24.5	790
3.NW1.6A	Transfer	11.0	17.0	435
	14 Days	12.0	18.0	543
	28 Days	12.0	18.5	641
3.NW1.6B	Transfer	12.0	17.0	417
	14 Days	11.5	16.5	522
	28 Days	12.0	16.5	610
3.LW2.5A	Transfer	15.5	24.5	579
	14 Days	15.0	21.5	665
	28 Days	15.0	21.5	743
3.LW2.5B	Transfer	15.0	22.5	565
	14 Days	14.5	23.5	679
	28 Days	14.0	21.5	754

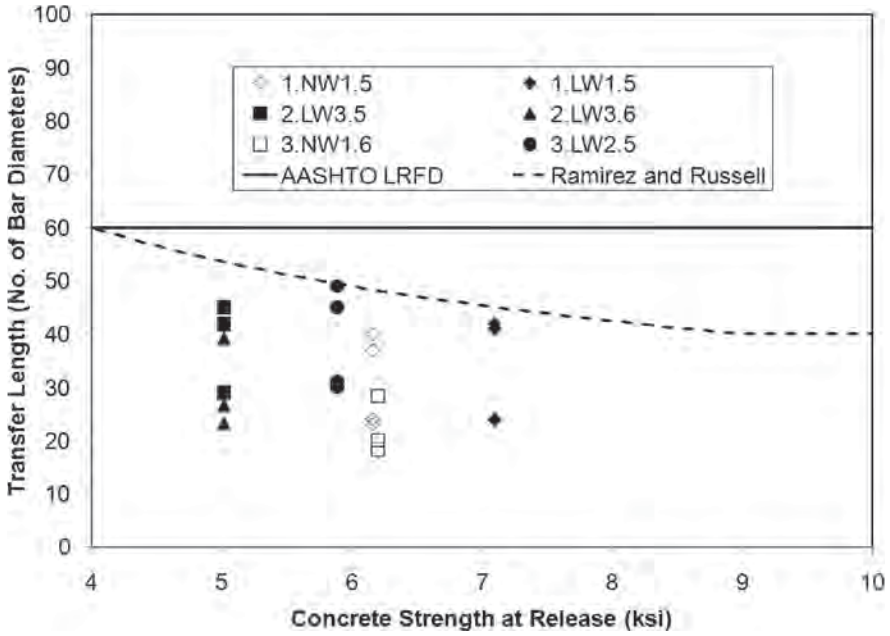

Figure 28. Summary of transfer length results.

Figure 29 compares these two calculation methods with the results from other research on lightweight concrete (Kolozs 2000; Meyer 2002; Nassar 2002; Zena 1996). All transfer lengths shown that are greater than either of the calculated values were measured on specimens containing strand with no test for bond quality. The research by Ramirez and Russell (2008) states that the difference in bond quality of strands produced by different manufacturers can be significant. Meyer conducted tests on strand quality using the large block pullout test suggested by Logan (1997). In addition, very scattered data was obtained from small rectangular cross-sections (Zena 1996).

Regardless, comparison of the test results found in the literature with those from this research lead to the conclusion that these methods provide a reasonable upper bound for the transfer length of lightweight concrete strengths. When compared to the test for strand bond (based on the NASP test procedure) as proposed by Ramirez and Russell,

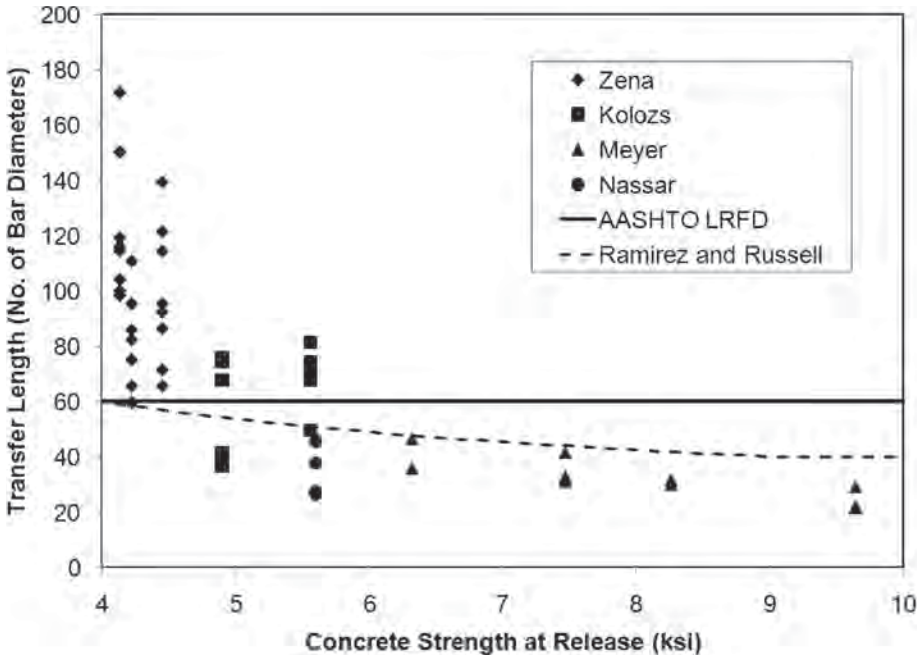

Figure 29. Summary of reported HSLWC transfer length data.

the current specification provides conservative estimates of transfer length for HSLWC members.

Development Length

Development length of prestressing strand is the embedment length required to ensure a flexural failure mode. Article 5.11.4.2 of the AASHTO LRFD Specifications provides the following equation for the development length, l_d, of prestressed components:

$$l_d \geq \kappa\left(f_{ps} - \left(2/3\right)f_{pe}\right)d_b$$

where

f_{ps} = average stress in prestressing steel at nominal resistance (ksi)
f_{pe} = effective stress in the prestressing steel considering losses (ksi)
d_b = the nominal strand diameter (in.)
κ = 1.6 for pretensioned members with depth > 24 in., 1.0 otherwise

Ramirez and Russell (2008) proposed that the expression for development length be changed to

$$l_d = \left[\left(120/\sqrt{f'_d}\right) + \left(225/f'_c\right)\right]d_b \geq 100d_b$$

Development length was determined by testing each end of each beam in flexure using the test setup shown in Figure 30. An iterative test procedure was used with both flexural and bond failures resulting, and a range for development length was subsequently determined. Test results are shown in Table 21.

The last column in Table 21 gives the observed type of failure. Following are brief descriptions of each failure type: (1) Flexure—The beam failed in a flexural mode at a load greater than the AASHTO-predicted nominal moment capacity with no measured strand end slip greater than 0.01 in. (there were two types of flexural failure: concrete compression and strand rupture); (2) Bond Slip—The AASHTO moment capacity was not reached and at least one of the prestressing strands had an end slip greater than 0.01 in.; and (3) Hybrid—The AASHTO moment capacity was reached and at least one strand had an end slip greater than 0.1 in.

Measured flexural bond length intervals and calculated development length intervals from flexural tests are shown in Table 22. The development length interval was conservatively calculated by adding the longest measured transfer length for a particular beam pair in question to the longest flexural bond length resulting in a bond failure (called Lower in Table 22) and the shortest flexural bond length, resulting in a flexural failure (called Upper in Table 22). Also shown are the development lengths calculated using the equations provided. For the AASHTO calculation, the effective prestress was calculated at the day of testing. It appears from the table that the lightweight concrete beams have slightly longer development lengths than normal weight beams. However, all development length upper bounds were substantially less than those calculated using the AASHTO Specifications as well as those calculated using the proposed Ramirez and Russell equation. In considering these results, it should also be recognized that the flexural test loading case is a worst-case scenario, as in general the loading results in a situation where the maximum moments occur at approximately the same location as the maximum shears. Despite this fact, many of the beams had to be loaded at extremely short flexural bond lengths to obtain bond slip failures.

Summary

The following observations can be made from the lab-cast beam tests:

- The AASHTO transfer length requirement (found in Section 5.11.4.1) and the Ramirez and Russell (2008) equation for transfer length both provide a reasonable upper bound to the measured transfer lengths of lightweight and normal weight girders.
- The AASHTO 5.11.4.2-1 equation and the Ramirez and Russell (2008) equation for development length both

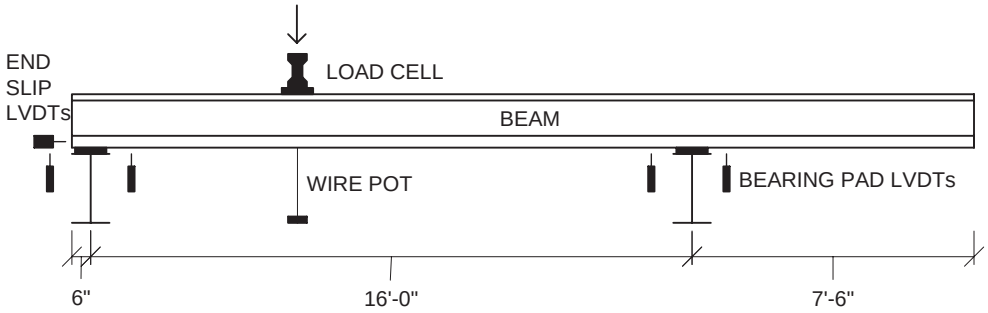

Figure 30. Development length test setup.

Table 21. Results of development length tests.

Beam Designation	End	Shear Span (in.)	Embedment Length (in.)	Transfer Length (in.)	Flex. Bond Length (in.)	Failure Mode
1.NW1.5A	Dead	54	62	11.5	50.5	Flexure - Concrete Crushing
	Live	54	62	18.5	43.5	Flexure - Concrete Crushing
1.NW1.5B	Dead	42	51	12.0	39.0	Flexure - Concrete Crushing
	Live	42	51	20.0	31.0	Flexure - Concrete Crushing
1.LW1.5B	Dead	54	62	12.0	50.0	Flexure - Concrete Crushing
	Live	54	62	21.0	41.0	Flexure - Concrete Crushing
1.LW1.5A	Live	42	51	20.5	30.5	Flexure - Concrete Crushing
	Dead	30	40	12.0	28.0	Hybrid
2.LW3.5B	Dead	42	51	14.5	36.5	Flexure - Concrete Crushing
	Live	42	51	21.0	30.0	Bond Slip
2.LW3.5A	Dead	36	45	14.5	30.5	Bond Slip
	Live	48	56	22.5	33.5	Flexure - Concrete Crushing
3.LW2.5A	Dead	42	51	15.5	35.5	Flexure - Concrete Crushing
	Live	42	51	24.5	26.5	Flexure - Concrete Crushing
3.LW2.5B	Dead	24	34	15.0	19.0	Bond Slip
	Live	36	45	22.5	22.5	Bond Slip
3.NW1.6B	Live	72	79	17.0	62.0	Flexure - Concrete Crushing
	Dead	48	56	12.0	44.0	Flexure - Strand Rupture
3.NW1.6A	Live	48	56	17.0	39.0	Hybrid
	Dead	36	45	11.0	34.0	Bond Slip
2.LW3.6B	Live	72	79	23.5	55.5	Flexure - Concrete Crushing
	Dead	48	56	16.0	40.0	Bond Slip
2.LW3.6A	Dead	54	62	14.0	48.0	Flexure - Concrete Crushing
	Live	60	68	25.0	43.0	Flexure - Concrete Crushing

provide a reasonable upper bound to the measured development lengths of lightweight and normal weight girders.

3.4 Shear Performance of Full-Scale Beams

Work Plan

The investigators reviewed available literature to (1) identify tests that had been conducted on shear strength of lightweight concrete beams and (2) develop a test program. Consideration was given to shear span-to-depth (a/d_v) ratios, mild steel reinforcement, unit weight, and compressive strength.

The testing program, presented in Figure 31, included full-scale prestressed girders with cast-in-place composite decks. All cast-in-place decks were made with lightweight concrete. One end of each beam was tested with a short shear span and the other a longer shear span. The results of these tests provided information on the differences in concrete contribution to shear strength between lightweight and normal weight concrete. Specimens T2.8.Typ and T2.8.Min were

Table 22. Development length intervals.

Designation	Longest Measured Transfer Length (in.)	Measured Flexural Bond Length Range (in.)		Development Interval (in.)		Calculated Development Length (in.)	
		Lower	Upper	Lower	Upper	AASHTO	Ramirez & Russell
1.NW1.5	20		31.0		51	77	64
1.LW1.5	21		28.0		49	79	61
2.LW3.5	22.5	30.5	33.5	53	56	83	66
3.LW3.5	24.5	22.5	26.5	47	51	80	62
3.NW1.6	17	34.0	39.0	51	56	94	76
2.LW3.6	25	40.0	43.0	65	68	100	79

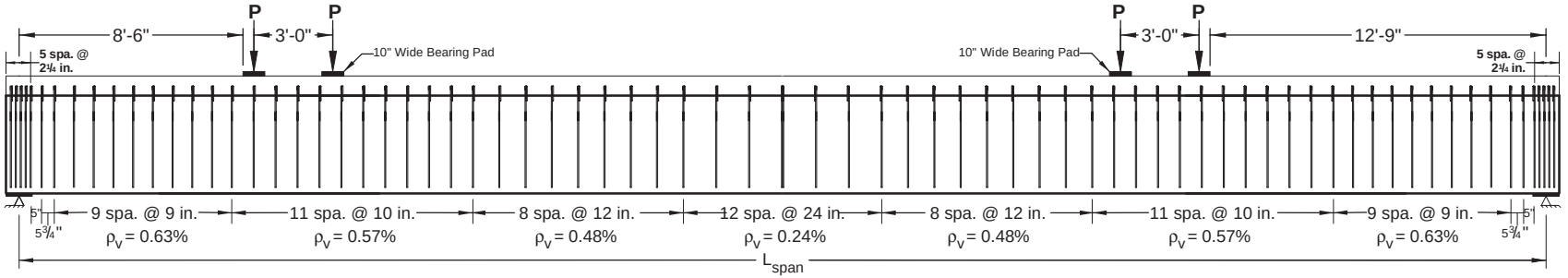

BT.8.Typ

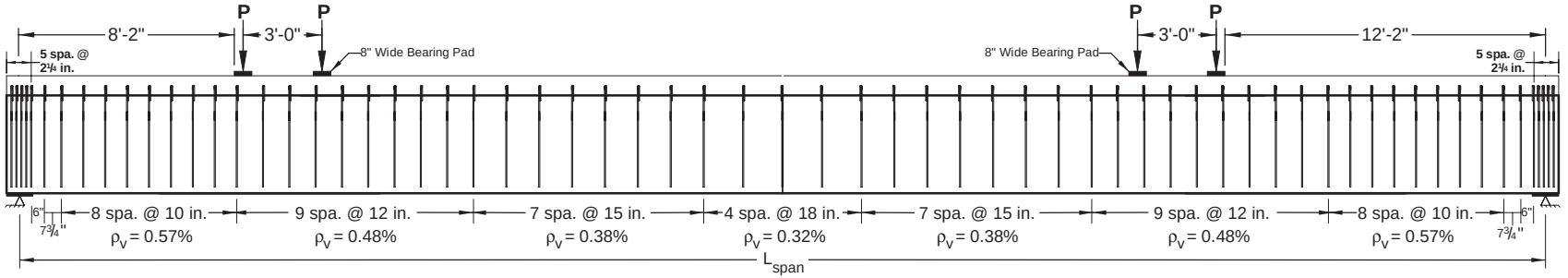

BT.10.Typ

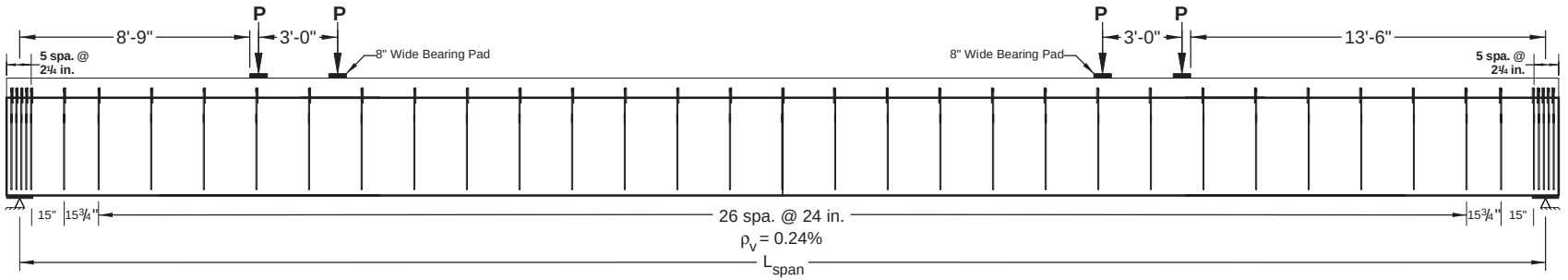

BT.10.Min

Figure 31. Loading parameters and stirrup spacing for large-scale girder testing.

(continued on next page)

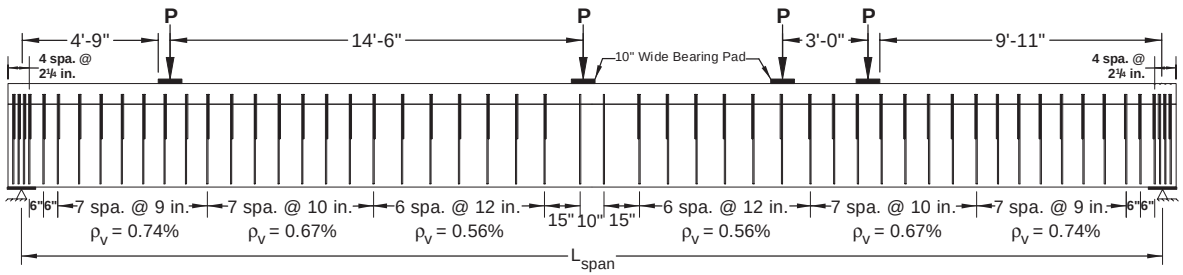

T2.8.Typ

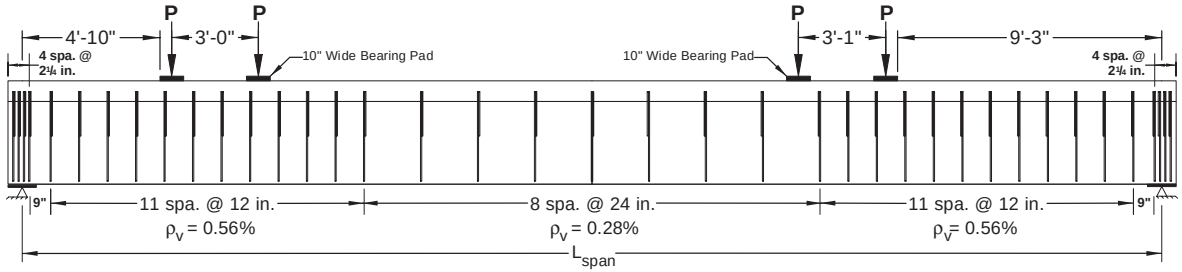

T2.8.Min

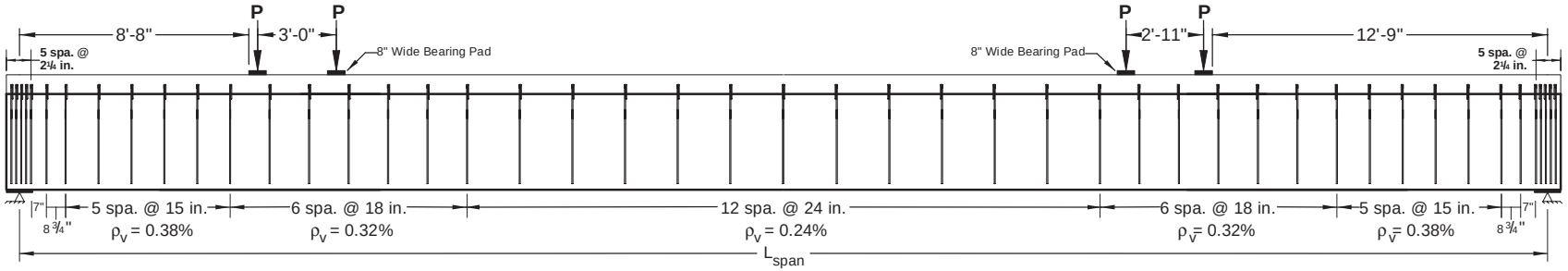

BT.8N.Typ

Figure 31. (Continued).

Table 23. Design geometric and measured girder material properties.

Test ID	Concrete Type	L (ft)	a/d_v	Air Content (%)	Slump (in.)	w_c (lb/ft3)	f'_c (ksi)	E_c (ksi)
T2.8.Typ.1	LWHPC1	40.0	1.5	4.75	9.5	117	8.9	3610
T2.8.Typ.2		35.1	3.1	4.75	9.5	117	8.9	3610
T2.8.Min.1		40.0	1.5	4.75	9.5	117	8.9	3610
T2.8.Min.2		34.8	2.9	4.75	9.5	117	9.0	3610
BT.8.Typ.1		58.0	2.0	4.75	-	121	9.1	3650
BT.8.Typ.2		49.5	3.1	4.75	-	121	9.1	3660
BT.8N.Typ.1	NWHPC1	57.9	2.1	4.0	8	145	8.5	4820
BT.8N.Typ.2		49.0	3.0	5.0	7.75	145	8.6	4580
BT.10.Typ.1	LWHPC3	57.9	2.0	5.0	10.75	120	8.9	3910
BT.10.Typ.2		49.4	2.9	4.0	-	124	9.9	4060
BT.10.Min.1		58.0	2.1	4.0	-	124	9.7	4040
BT.10.Min.2		49.5	3.0	3.5	-	126	10.3	4140

both AASHTO Type II beams whereas the other four girders were the bulb tee shapes. The designation "Typ" identifies test specimen with a typical amount of shear reinforcement, and the designation "Min" refers to test specimens with the AASHTO LRFD minimum amount of shear reinforcement. The typical amount of reinforcement was determined for the two girder sizes by designing typical interior girders with a transverse girder spacing of 8 feet for each. The AASHTO Type II girder had a span length of 60 feet and the PCBT-45 girder had a span length of 85 feet. The minimum amount of reinforcement was determined as per AASHTO LRFD requirements.

Full-Scale Girder Testing

Material and Section Properties. The primary purpose of the full-scale girder tests was to compare shear strengths as calculated using the AASHTO LRFD Specifications to those obtained from the tests. Six girders were tested, with two tests conducted on each. Type and strength of concrete, the amount of shear reinforcement, and a/d_v (where a is measured from the center of bearing) were investigated in these tests. The compressive strength and modulus of elasticity were measured at the time of testing. Major properties for each of the twelve tests are listed in Table 23.

Each test specimen was assigned a four-term designation. The first term indicated the girder size, either an AASHTO Type II beam (T2) or a PCBT-45 girder (BT), where the section properties are shown in Table 24 and basic geometries are shown in Figure 32. Detailed girder properties for these two classes of girders are provided in Attachment J. The second term gave the design compressive strength of the girder (either 8 ksi or 10 ksi). The third term described the amount of shear reinforcement (Typ for typical reinforcement or Min for minimum reinforcement, as prescribed by the AASHTO LRFD specifications). The last term indicated which end of the girder was being tested. All beams were constructed with lightweight concrete except for BT.8N.Typ, which was built with normal weight concrete (identified by the letter N).

All six beams were designed for a typical span length for the given cross-section with the harping point moved closer to midspan than is common in practice. Since shear forces tend to dominate near the ends of the girders, the researchers were able to take out the middle section of each girder, and hence, test shorter girders, without deviating from the research objectives. Fabrication drawings of the six full-size girders are given in Attachment J.

The AASHTO Type II girders were 41 feet long, but contained shear reinforcement for a 60-ft-long beam. Six of the 24 (0.5-in.-diameter) strands in these beams were harped at midspan as shown in the girder plans found in Attachment J. Additionally, two of the straight strands ran along

Table 24. Girder properties.

Property	Girder Type	
	AASHTO Type II	PCBT-45
Depth (in.)	36	45
Web Width (in.)	6	7
Width of top Flange (in.)	12	47
Width of Bottom Flange (in.)	18	32
Area ($in.^2$)	369	747
Centroid to Bottom (in.)	15.83	22.3
Moment of Inertia ($in.^4$)	50,979	207,300

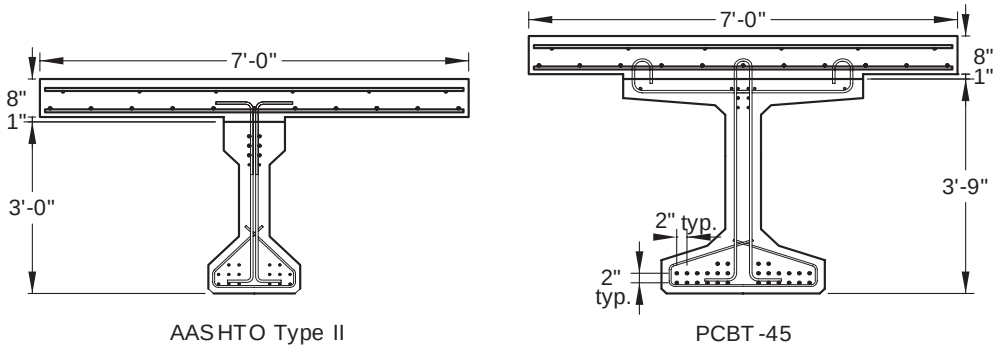

Figure 32. Cross-sections at the ends of the two girder types being tested.

the top flange in order to reduce the stresses in the top and bottom flanges at release. Likewise, the PCBT-45 beams were 59 feet long, but had shear reinforcement based on an 85-ft-long span; six of the 34 (0.5-in.-diameter) strands were harped 2.5 ft away from the beam centerline.

After steam curing at the precasting plant, the beams were transported to the laboratory. An 8-in.-deep cast-in-place deck was placed on top of each beam to simulate a deck-girder system in a bridge. Although the reinforcement was based on an 8-ft girder spacing, a 7-ft-wide deck was built due to laboratory constraints. Concrete properties for the six decks are listed in Table 25.

Instrumentation. Prior to production at the precasting yard, electrical resistance strain gages were installed on the shear reinforcement in a pattern that minimized the number of gages needed for measuring the strains at the anticipated crack locations. A typical strain gage arrangement is shown in Figure 33. Strain versus applied load plots for each gage on each girder are given in Attachment I.

Table 25. Properties of deck concrete.

Deck Designation	Fresh Concrete Properties		Hardened Concrete Properties (ksi)				
	Property	Result	Property	Days After Casting			
				1	7	28	Testing
T2.8.Typ	*Air* (%)	—	f'_c	—	—	—	5.59
	Slump (in.)	6.5	E_c	—	—	—	3403
	Unit Weight (lb/ft3)	118.4	f_{ct}	—	—	—	0.535
			f_r	—	—	—	
T2.8.Min	*Air* (%)	4.5	f'_c	1.72	3.49	4.70	5.36
	Slump (in.)	7.5	E_c	1980	2690	3080	3240
	Unit Weight (lb/ft3)	120	f_{ct}	0.280	0.440	0.495	0.530
			f_r	—	—	0.640	—
BT.8.Typ	*Air* (%)	3.5	f'_c	2.64	4.07	5.45	6.14
	Slump (in.)	6.25	E_c	3040	3175	3765	3825
	Unit Weight (lb/ft3)	127.1	f_{ct}	—	0.450	0.583	0.650
			f_r	—	—	0.780	—
BT.8N.Typ	*Air* (%)	2.63	f'_c	2.61	3.51	4.57	4.94
	Slump (in.)	7.5	E_c	2640	2635	3000	3025
	Unit Weight (lb/ft3)	122	f_{ct}	—	0.430	0.483	0.535
			f_r	—	—	0.760	—
BT.10.Typ	*Air* (%)	2.38	f'_c	1.66	3.76	—	4.53
	Slump (in.)	6.25	E_c	2300	2903	—	215
	Unit Weight (lb/ft3)	122.8	f_{ct}	—	0.490	—	0.470
			f_r	—	—	0.795	—
BT.10.Min	*Air* (%)	3.25	f'_c	1.40	3.55	4.93	5.52
	Slump (in.)	7	E_c	1870	2610	3143	3305
	Unit Weight (lb/ft3)	122.2	f_{ct}	—	—	0.525	0.498
			f_r	—	—	0.620	—

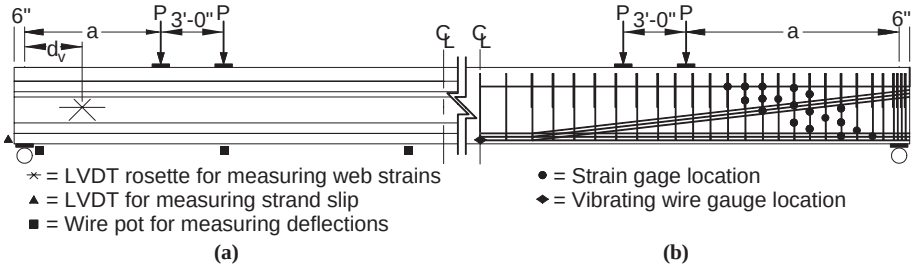

Figure 33. Instrumentation on (a) the concrete surface and (b) the reinforcement.

Also, two vibrating wire gages (VWGs) were placed at the centroid of the bottom layer of flexural reinforcement at the beam centerline. These gages were primarily used to measure prestress losses and monitor the strain in the strand during testing.

Various instruments were also deployed on the girder exteriors. In most cases, sets of three LVDTs were placed on both sides of the web in a rosette pattern to measure the principal strains in the concrete during testing. The intersection of the three LVDTs was located horizontally at the critical section as indicated by the AASHTO LRFD Specifications. Vertically, the rosettes were located $0.5d_v$ from the bottom of the girder and horizontally d_v is measured from the center of the support.

For the AASHTO Type II girders, one of the LVDT rosettes was substituted with a rosette of resistance strain gages. However, because the strain gage rosettes produced questionable post-cracking data, LVDT rosettes were used on both sides of the web for the remaining tests.

Four LVDTs were placed on strands extending from the end of the girder to determine strand slippage as load was applied. The LVDTs were placed on two exterior and two center strands on the bottom row. The LVDTs recorded measurements to the nearest 0.0002 in.

Four wire potentiometers (wire pots) were placed below the beam to measure the vertical deflection during testing. One wire pot was placed underneath one of the actuators, and a second wire pot was placed at the point of maximum deflection. The other two devices measured the vertical deflection occurring at the supports. Measurements were recorded to the nearest 0.01 in.

Each of the actuators used to apply a load to the girder had a load cell on top to determine shear force applied at the end of the girder. The load cells measured load to the nearest 500 lb.

Test Setup and Procedure. All of the girders were simply supported, with the loaded end of the girder being pin-supported to minimize actuator tilt. Figure 31 gives actuator locations for each test.

Initially consideration was given to placing the two concentrated loads 14 feet apart in order to simulate an AASHTO truck axle loading. However, analysis indicated that such a load spacing and short beam length could result in failure at the end of the girder not being tested. The 8-ft load spacing used on girder T2.8.Typ resulted in flexural failures (instead of the desired shear failure). Therefore, the two concentrated loads were placed 3 feet apart during subsequent tests.

Figure 33 shows that the first actuator was located at a distance "a" from the nearest support. Initial configurations had been selected to fill in any gaps in available data regarding this a/d_v ratio. However, preliminary analysis indicated the shear strengths of the girders in the early tests were substantially greater than predicted by the AASHTO LRFD specifications. Consequently, the a/d_v ratio for the second end of all of the PCBT girders was decreased from the planned 3.5 to about 3.0, as indicated in Table 23. The new a/d_v ratios were selected with the goal of achieving a shear failure prior to flexural failure yet keeping the a/d_v ratio large.

The load was applied to the girder using an electric hydraulic pump in stroke control in 20-kip load increments. The girder was examined at each load increment and cracks in the concrete were marked. However, no examination was made as the girder neared failure.

On two occasions, the two primary actuators were observed to be too far out of plumb. At that point, a secondary actuator at midspan was engaged to maintain the deflection in the girder to reset the two primary actuators. After the two primary actuators were realigned, load in those actuators was increased gradually to the point prior to unloading, and then the experiment progressed as planned. Loading continued at 20-kip increments until either a shear failure occurred or the girder was no longer able to withstand additional load without large increases in deflection, thus indicating that the beam was approaching a flexural failure.

Test Results. Table 26 shows a comparison of the experimental results and the values predicted by the two design methods given in AASHTO LRFD specifications (the Sectional Design Method (5.8.3 and Appendix B5 with interpolation)

Table 26. Experimental versus calculated shear strengths.

Test ID	Experimental Results		Sectional Method				Simplified Method			
	Failure Mode(s)	V_{Exp} (kips)	$V_{n.Sec}$ (kips)	$V_{n.Sec}$ No λ_v (kips)	$^{Exp}/_{Sec}$	$^{Exp}/_{Sec}$ No λ_v	$V_{n.Sim}$ (kips)	$V_{n.Sim}$ No λ_v (kips)	$^{Exp}/_{Sim}$	$^{Exp}/_{Sim}$ No λ_v
T2.8.Typ.1	Flexural / Slip	361	275	279	1.31	1.29	298	293	1.21	1.23
T2.8.Typ.2	Flexural	292	230	233	1.27	1.25	293	289	1.00	1.01
T2.8.Min.1	Web Shear / Slip	382	243	248	1.57	1.54	246	244	1.55	1.57
T2.8.Min.2	*	308	219	223	1.41	1.38	241	239	1.28	1.29
BT.8.Typ.1	Web Shear / Slip	500	329	329	1.52	1.52	313	313	1.60	1.60
BT.8.Typ.2	Flexural	407	298	303	1.37	1.34	305	307	1.34	1.33
BT.8N.Typ.1	Web Shear / Slip	431	274	—	1.58	—	246	—	1.75	—
BT.8N.Typ.2	Web Shear / Slip	382	254	—	.50	—	239	—	1.60	—
BT.10.Typ.1	Web Shear / Slip	518	293	299	1.77	1.73	296	296	1.75	1.75
BT.10.Typ.2	Web Shear / Flex. / Slip	428	286	292	1.49	1.47	293	295	1.46	1.45
BT.10.Min.1	Web Shear / Slip	475	253	260	1.88	1.83	202	207	2.35	2.30
BT.10.Min.2	Web Shear	371	240	246	1.55	1.51	199	204	1.87	1.82
Average $^{Exp}/_{Calc}$ ratio for Lightweight Concrete					1.51	1.49			1.54	1.54
Average $^{Exp}/_{Calc}$ ratio for Normal Weight Concrete					1.54	—			1.68	—

*Equipment breakdown, shear strength based on load applied at breakdown.

and the Simplified Procedure for Prestressed and Nonprestressed Sections (5.8.3.4.3)). Subsequently, these two methods will be called the sectional method and simplified methods (Sec and Sim in Table 26), respectively. The calculations using the AASHTO specifications set all load factors and strength reduction factors equal to 1.0 and were done with and without the 0.85 modifier for sand lightweight concrete (λ_v) given in 5.8.2.2 of the AASHTO LRFD specifications. The yield stress used for all mild reinforcement included in shear design calculations was 67.3 ksi (which was determined from testing samples taken from the reinforcement used in the girders). The effective strand stress (f_{pe}) was determined from the vibrating wire gages located in each girder and f'_c used in the calculations was estimated from a strength gain curve. The load needed for determining shear strength was the sum of the dead load at the middle of the shear span and the applied load. For several beam ends, the stirrup spacing varied within the shear span; this change was incorporated in V_n by using the lowest calculated V_n value within the shear span.

Table 26 also lists the type of failure that occurred in each experiment. Each beam was designed according to the requirements of the AASHTO LRFD specification such that the flexural strength exceeded the design shear strength. During the testing of T2.8.Min.2, an operational failure occurred that led to termination of the test before a flexure or shear failure occurred.

Generally, a flexural failure is characterized by yielding of the longitudinal reinforcement, followed by crushing of the deck concrete near the point of maximum moment. However, the tests were discontinued when very little additional force resulted in a relatively large increase in deflection, and crushing of the concrete at the top of the girder was imminent. A typical crack pattern for a flexural failure is shown in Figure 34. The flexural cracks extended from the bottom flange into the cast-in-place deck and the significant diagonal shear cracks within the shear span. Figure 35 indicates the level of stirrup strain in a typical test at failure. Approximately half of the gages were at or above the yield strain at failure, and there was concrete powdering or light flaking in the web, indicating that the girder was nearing its shear capacity.

Shear failures generally occur in the form of web crushing, diagonal tension, shear compression, shear-bond failure, localized crushing above the support, horizontal shear along the flange-deck interface, and strand slip. Web crushing type failures, with or without strand slip, were observed in 8 of the 12 large-scale girder tests. In these cases, the concrete on the surface of the web spalled or crushed near the support. Figure 36 shows the end of a beam that has undergone a web-shear failure with the typical diagonal tension cracking and web crushing. Another characteristic of web crushing failures was significant yielding of the stirrups within the shear span. Figures 37 and 38 show the level of strains in the stirrups for two web compression failures: a short shear span test of a lightweight girder with $f'_c = 8$ ksi and a long shear span test of a lightweight girder with $f'_c = 10$ ksi, respectively. In both cases, all stirrups yielded before or at failure. A strand slip failure was defined as when the strands protruding from the

Figure 34. Flexural failure observed in Test BT.8.Typ.2.

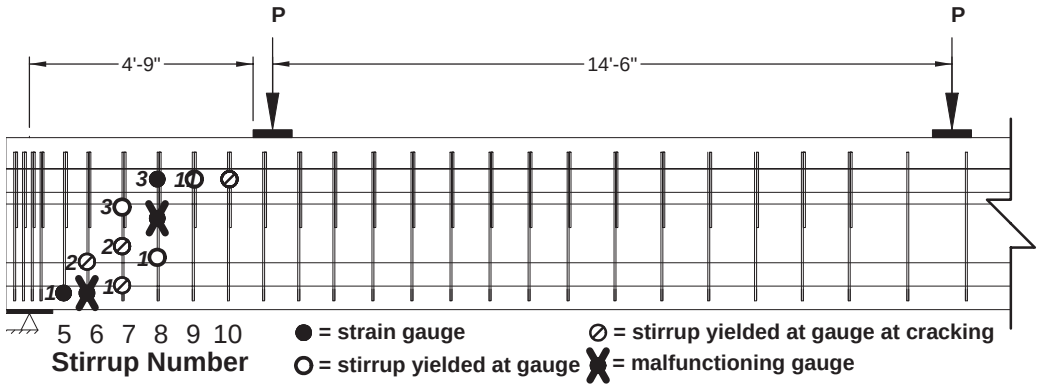

Figure 35. Strain gage locations for Test T2.8.Typ.1.

Figure 36. Web-shear failure observed in Test T2.8.Min.

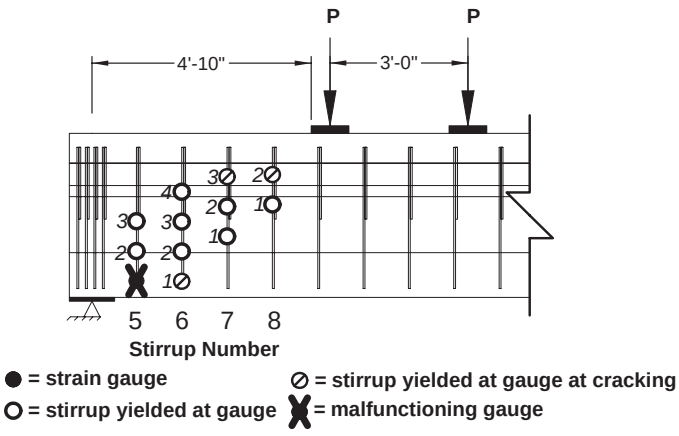

Figure 37. Strain gage locations for Test T2.8.Min.

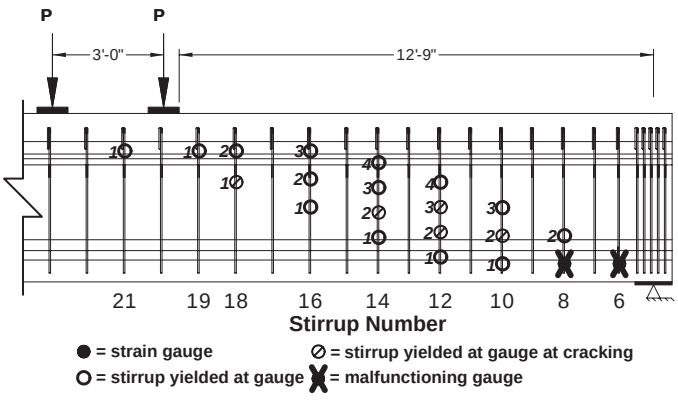

Figure 38. Strain gage locations for test BT.10.Typ.2.

Table 27. Results from previous research and current study.

Statistic	Previous Research		Current Study			
	$\frac{V_{exp}}{V_{n\,sec}}$	$\frac{V_{exp}}{V_{n\,sim}}$	$\frac{V_{exp}}{V_{n\,sec}}$	$\frac{V_{exp}}{V_{n\,sec}\ No\ \lambda_v}$	$\frac{V_{exp}}{V_{n\,sim}}$	$\frac{V_{exp}}{V_{n\,sim}\ No\ \lambda_v}$
Average	1.70	1.79	1.51	1.49	1.54	1.54
Std. Dev.	0.32	0.42	0.19	0.18	0.38	0.36
COV	0.19	0.24	0.13	0.12	0.25	0.24

beam end were pulled into the concrete more than 0.01 in. In seven of the eight tests that resulted in a web-shear failure, strand slip in excess of 0.01 in. accompanied web crushing.

Table 26 presents the calculated strengths for all of the lightweight and normal weight girders. The differences between the calculated strengths with and without $\lambda_v = 0.85$ for the general and simplified equations for shear strength are less than 3%. Also, the average ratio of experimental-to-calculated shear strength for lightweight concrete using either method was only minimally affected by the absence or presence of the λ_v factor. Therefore, including λ_v in calculating shear strength of lightweight concrete girders appears unnecessary. This is similar to the findings from the material property investigation where it was found that the tensile strength of lightweight concrete was adequately predicted by the AASHTO provisions for tensile strength of normal weight concrete.

AASHTO LRFD specifications also require the use of a lower resistance factor (ϕ) for shear design of lightweight concrete girder (0.7 as compared to 0.9 for normal weight concrete). Table 27 presents average data from previous research on prestressed beams constructed with lightweight concrete by Malone (1999), Kahn et al. (2004), and Dymond et al. (2009). This previous research reported data for concrete compressive strengths ranging from 6.5 ksi to 11.0 ksi. Cross-sectional area for the beams ranged from 468 in^2 to 1629 in^2, and shear span-to-depth ratio, a/d_v, ranged from 1.3 to 3.0. Some girders had no shear reinforcement, while others had minimal ($\rho_v \approx 0.002$) or typical ($\rho_v \approx 0.011$) shear reinforcement ratios. As listed in Table 27, the ratio of measured to calculated strengths averaged 1.52 for the present study, whereas for the previous research, this ratio is at least 1.70. Also, the coefficients of variation indicated a greater variability with the Simplified method than with the Sectional method.

In Table 28, the test results for lightweight prestressed concrete girders are compared to results for normal weight prestressed concrete girders reported by Hawkins et al. (2005). The ratio of tested to calculated strengths is higher for lightweight than for normal weight prestressed concrete girders; the coefficient of variation is also slightly higher for the lightweight girders. The bottom two rows show percentages of cases in which the measured strength would be less than 0.9 or 0.85 (the ϕ factor) times the nominal strength for a normal distribution of data. For ϕ equal to 0.9, the Sectional method for shear strength calculation of lightweight concrete prestressed girders gives a smaller percentage of cases with measured strengths less than design strengths than for normal weight prestressed concrete girders. However, the reverse is true for the Simplified method. The ratio of measured to calculated strength for lightweight concrete girders without using λ_v is 3.5 as compared to a ratio of 1.4 for normal weight girders. The bottom row in the table evaluates the test results using a ϕ of 0.85. For ϕ of 0.85, all lightweight concrete results are less than their normal weight concrete companions calculated with a ϕ of 0.9. For instance, the largest percentage for lightweight prestressed concrete girders is 2.6% which is less than the largest percentage for normal weight prestressed concrete girders (3.2%). Using ϕ as 0.85 for the shear design of prestressed girders containing sand lightweight concrete yields a maximum percentage of 2.6. This is less than the largest percentage for normal weight prestressed concrete girders using a ϕ of 0.9 (3.2%). The largest percentage for lightweight girders is for strengths calculated with the Sectional design method, whereas the largest percentage for normal weight girders is calculated using the simplified method. This comparison was made since both methods are allowed in the AASHTO LRFD specifications.

Table 28. Comparison of lightweight and normal weight concrete results.

Statistic	Lightweight Beams				Normal Weight Beams	
	$\frac{V_{exp}}{V_{n\,sec}}$	$\frac{V_{exp}}{V_{n\,sec}\ No\ \lambda_v}$	$\frac{V_{exp}}{V_{n\,sim}}$	$\frac{V_{exp}}{V_{n\,sim}\ No\ \lambda_v}$	$\frac{V_{exp}}{V_{n\,sec}}$	$\frac{V_{exp}}{V_{n\,sim}\ No\ \lambda_v}$
Average	1.61	1.56	1.67	1.58	1.23	1.54
Std. Dev.	0.28	0.27	0.42	0.38	0.18	0.29
COV	0.17	0.17	0.25	0.24	0.15	0.19
% < 0.9V_n	0.52	0.71	3.1	3.5	3.2	1.4
% < 0.85V_n	0.31	0.44	2.4	2.6		

Summary

Observations regarding shear design of lightweight prestressed concrete girders follow:

- Applying a modification factor (λ_v) to $\sqrt{f'_c}$ term in shear strength calculations is not needed for sand lightweight concrete prestressed concrete girders. This is supported by results from the material property portion of this project as well as the test results from the full-size girder tests.
- AASHTO does not give different strength reduction factors for the types of shear in concrete bridge applications (i.e., interface shear, beam shear, and two-way shear); therefore, a common strength reduction factor for shear in members containing lightweight concrete is recommended. The AASHTO LRFD specifications require that a ϕ of 0.7 be used for calculation of the shear strength of lightweight concrete girders, as opposed to 0.9 for normal weight concrete girders. Based on analysis of the full-scale girder test results, a value of 0.85 is more appropriate for lightweight prestressed concrete girders. This is consistent with, but more conservative than, the findings of the interface shear portion of this study.

3.5 Time-Dependent Behavior of Lab-Cast and Full-Scale Beams

The objective of this part of the research was to compare measured camber and strain data over time to calculated camber and prestress loss estimations to determine if the methods presented in the AASHTO LRFD specifications are applicable to lightweight concrete. Tests were conducted on 6 full-scale prestressed girders and 12 lab-cast beams.

Creep and Shrinkage

The following methods for predicting creep and shrinkage of concrete are identified in Section 5.4.2.3 in the AASHTO LRFD specifications:

- CEB MC90
- ACI 209 model
- AASHTO LRFD model

All models consider relative humidity, volume-to-surface area, and time of loading. The AASHTO LRFD model has a factor for concrete strength, and the ACI model has factors for specifics of the mix design. None of the models includes a factor for lightweight concrete.

The refined method of prestress loss calculation presented in AASHTO LRFD (Section 5.9.5.4) requires the calculation of creep coefficients and shrinkage strains. For the full-scale beams, the refined calculation was performed using each of the three creep and shrinkage models listed above. For the lab-cast beams, only the AASHTO LRFD method with AASHTO creep and shrinkage functions was compared to the measurements.

Prestress Losses in Lab-Cast Beams

Anchorage losses were compensated for by placing shims between the seating chuck and the stressing abutment during fabrication. Concrete was placed less than 24 hours after strand stressing for all placements and strand forces were continuously monitored from the beginning of stressing to release of prestressing force. Due to the heat of hydration and restraint of shrinkage and thermal effects prior to release, forces in the strands measured in the load cells at the nonstressing end of the prestressing beds varied during the curing process. Therefore, the initial and effective prestress forces were approximated based on overall loss data as measured by the vibrating wire gages and crack initiation tests, which were used to determine the effective prestress force at the time of development length testing.

Vibrating Wire Gages. Internal vibrating wire gages (VWGs) were used to measure the change in concrete strain at the level of the strands from the time of casting to the time of beam testing. All test beams were instrumented with a VWG except beams 1.LW1.5A and 1.LW1.5B. VWGs were placed 6 feet from the beam live ends, except beam 1.NW1.5A where the gage was placed 6 feet from the beam dead end. Gages were secured between the center strand and one of the outer strands using plastic zip ties. After casting, each VWG was connected to a datalogger, which recorded the measured strain at the level of the strands and temperature at specified time intervals. A sample plot of total change in strain versus time after casting is shown in Figure 39. Prestress transfer occurred at about 15 hours after concrete casting. Plots of prestress versus time for each lab-cast beam are given in Attachment L.

Figure 40 shows a typical plot of prestress loss after transfer and the corresponding AASHTO estimate. In all cases, the AASHTO refined method of prestress loss overestimated the prestress loss for the lightweight concrete beams.

Table 29 lists the experimentally determined elastic shortening prestress loss together with the loss calculated using the measured modulus of elasticity and the modulus of elasticity calculated using the measured compressive strength at time of release. As can be seen, the measured losses are close to those calculated using either the measured or the calculated modulus.

Table 30 presents the effective prestress force determined from the VWG data and as calculated using the AASHTO refined method. As can be seen, the measured effective prestress is 5 to 15% greater than that predicted by the AASHTO LRFD method.

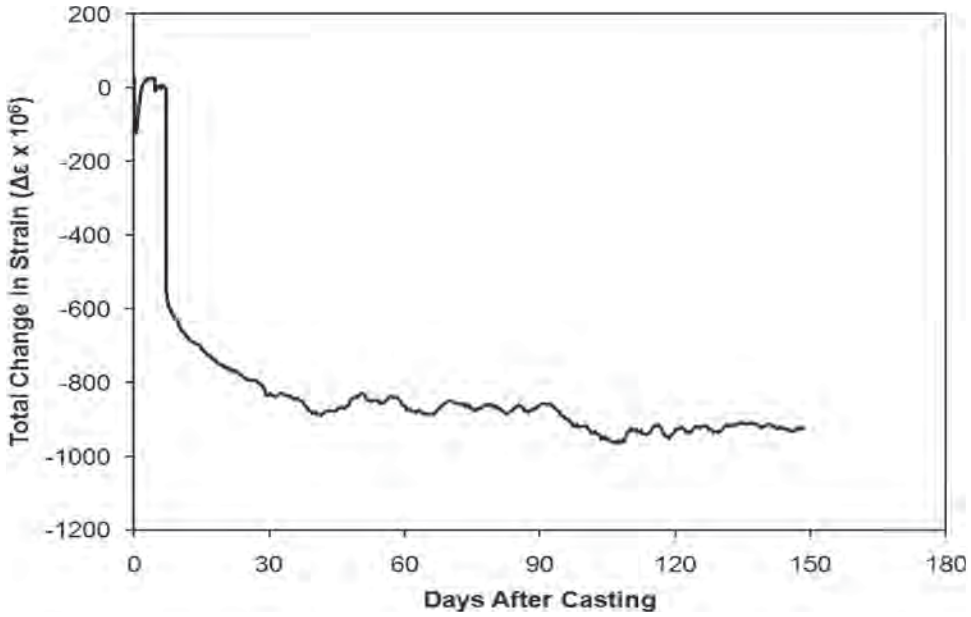

Figure 39. Change in strain versus time for 2.LW3.5A.

Crack Initiation Tests. Crack initiation tests were conducted to determine the load at which the first flexural crack occurred in order to back-calculate the effective prestress force. In these tests, load was applied to the beam in 2-kip increments. The concrete surface strains were measured directly under the load and close to the bottom beam surface using surface-mounted gage points and a DEMEC digital strain gage. Expected flexural cracking loads were calculated assuming a modulus of rupture of $0.20\sqrt{f'_c}$.

Once the applied load was within 10 kips of the expected flexural cracking load, the beams were visually examined for cracking at each load increment. The surface strain measurements helped pinpoint the initiation and location of the flexural cracks. The load versus strain plot shown in Figure 41 indicates that the measured strains increased linearly with respect to load until cracking occurred. Then the load versus strain plot became non-linear. The cracking load was taken as the lower of either the load at which a crack was visually observed or the load at which the load versus strain plot became non-linear. The beam was subsequently loaded until a crack could be visually detected across the bottom of the beam.

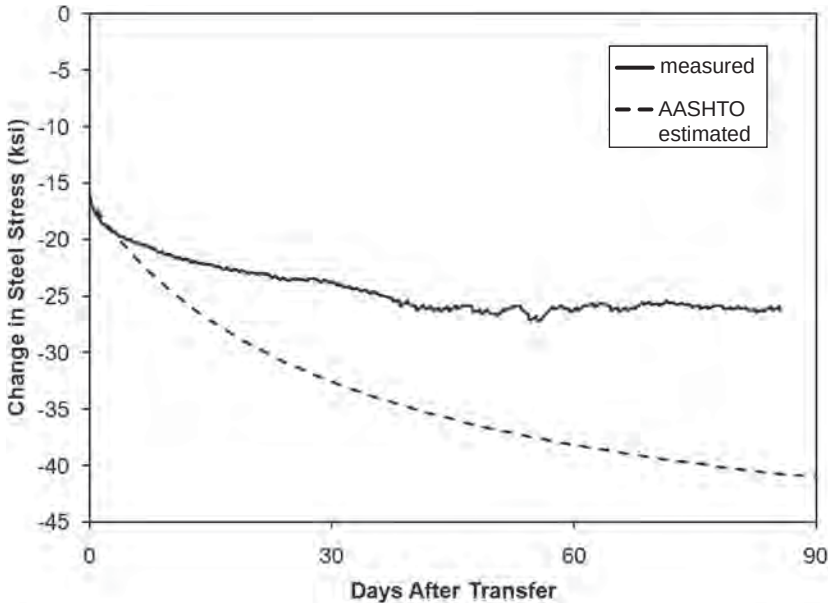

Figure 40. Prestress loss for beam 3.LW2.5A.

Table 29. Prestress loss due to elastic shortening.

Beam	Prestress Loss (ksi)		
	Calculated with Meas. E_{ci}	Calculated with Calc. E_{ci}	Measured
1.NW1.5A	10.4	10.9	11.5
1.NW1.5B	10.4	10.9	12.1
1.LW1.5A	13.5	13.4	NA
1.LW1.5B	13.5	13.4	NA
2.LW3.5A	16.6	16.7	14.2
2.LW3.5B	16.6	16.7	14.2
3.LW2.5A	16.3	15.1	15.4
3.LW2.5B	16.3	15.1	15.4
3.NW1.6A	11.0	10.8	11.2
3.NW1.6B	11.0	10.8	11.6
2.LW3.6A	17.0	17.1	15.2
2.LW3.6B	17.0	17.1	14.8

With the initial cracking load known, the effective prestress was calculated using the 28-day modulus of rupture. Table 31 lists the measured and effective prestress at the time of testing. The results show good agreement with AASHTO calculations of prestress loss.

Summary. Based on the VWG data, it appears the AASHTO LRFD specifications overestimate prestress loss in lightweight concrete beams after transfer, specifically at early ages. On the other hand, it seems possible, based on the crack initiation results, that the long-term estimate of effective prestress loss is more reliable. This could be due to losses occurring prior to transfer. Further analysis is necessary to determine the root cause.

Prestress Losses in Full-Scale Beams

For the full-scale beams, two methods were used to estimate prestress losses. The first method was the AASHTO refined method (Section 5.9.5.4) and the second accounted for change in modulus of elasticity over time. For each method, the previously mentioned creep and shrinkage models were used. Vibrating wire gage strain at the centroid of the prestressing strand at midspan of each girder was multiplied by the strand modulus of elasticity to determine a change in stress. The zero reading was taken immediately prior to release of prestress. Plots of prestress versus time for each girder are given in Attachment L.

Elastic Shortening Losses. Elastic shortening losses were calculated by applying the full jacking force to the transformed section, and the resulting stress in the concrete at the level of the strand due to prestress plus self-weight was determined. The stress in the concrete was multiplied by the strand to concrete modular ratio to arrive at the stress in the steel, which is the elastic shortening loss.

Long-Term Losses. Two methods were used to estimate long-term loss of prestress: (1) AASHTO refined method (Section 5.9.5.4) and (2) an age-adjusted effective modulus (AAEM) method. Both methods use an age-adjusted effective modulus approach to deal with the effects of the slowly changing force in the prestress. In the AASHTO approach, the effects of creep, shrinkage, and relaxation are estimated separately. In the AAEM method, they are all considered in a single formulation. Internal equilibrium, compatibility, and constitutive equations were written and solved simultaneously to determine prestress loss. This method allowed for the determination of the effect of deck

Table 30. Measured and estimated prestress losses.

Beam	Initial Stress (ksi)	Time After Transfer (days)	Prestress (ksi)		Measured/ Calculated
			Measured f_{pe}	Calculated f_{pe}	
1.NW1.5A	200	207	175	167	1.05
1.NW1.5B	200	207	174	167	1.05
1.LW1.5A	199	NA	NA	NA	NA
1.LW1.5B	199	NA	NA	NA	NA
2.LW3.5A	199	139	172	152	1.13
2.LW3.5B	199	139	172	152	1.13
3.LW2.5A	203	83	177	163	1.09
3.LW2.5A	203	83	177	163	1.09
3.NW1.6A	198	83	177	168	1.05
3.NW1.6B	198	83	176	168	1.05
2.LW3.6A	200	139	174	153	1.14
2.LW3.6B	200	139	176	153	1.14

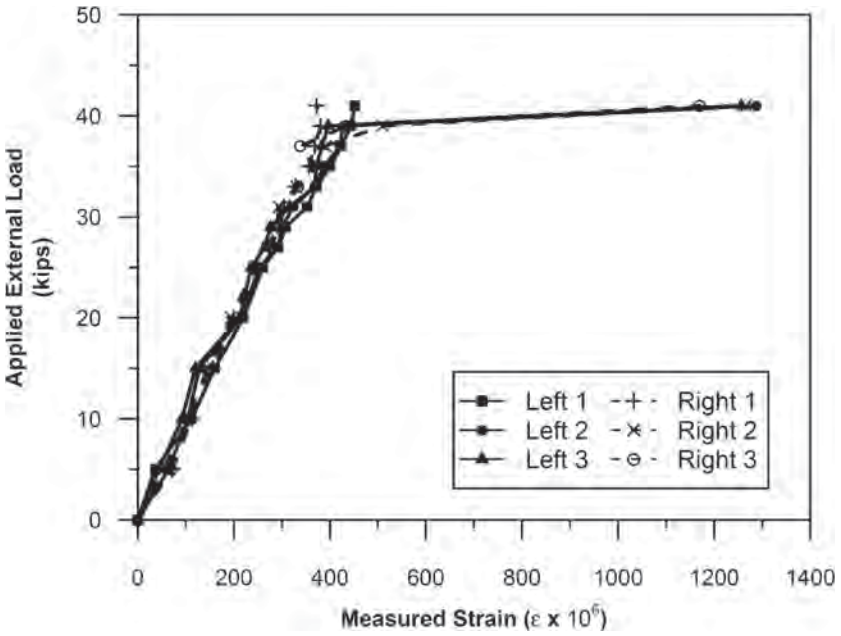

Figure 41. Sample load versus strain (beam end 1.NW1.5B.A).

Table 31. Measured and calculated effective prestress.

Beam	End	Applied Load (kips)	Measured f_{pe} (ksi)	Average Measured f_{pe} (ksi)	Calculated f_{pe} (ksi)	Measured/Calculated
1.NW1.5A	Dead	32	152	157	166	0.95
	Live	33	159			
1.NW1.5B	Dead	39	158			
	Live	39	158			
1.LW1.5B	Dead	29	149	159	161	0.99
	Live	29	149			
1.LW1.5A	Dead	39	177			
	Live	48	163			
2.lW3.5B	Dead	34	148	149	149	1.00
	Live	36	158			
2.LW3.5A	Dead	38	145			
	Live	31	146			
3.LW1.5A	Dead	40	178	165	158	1.04
	Live	38	165			
3.LW1.5B	Dead	57	155			
	Live	42	162			
3.NW1.6A	Dead	65	185	177	164	1.08
	Live	80	180			
3.NW1.6B	Dead	80	180			
	Live	93	165			
2.LW3.6B	Dead	55	149	153	149	1.03
	Live	72	158			
2.LW3.6A	Dead	66	156			
	Live	60	149			

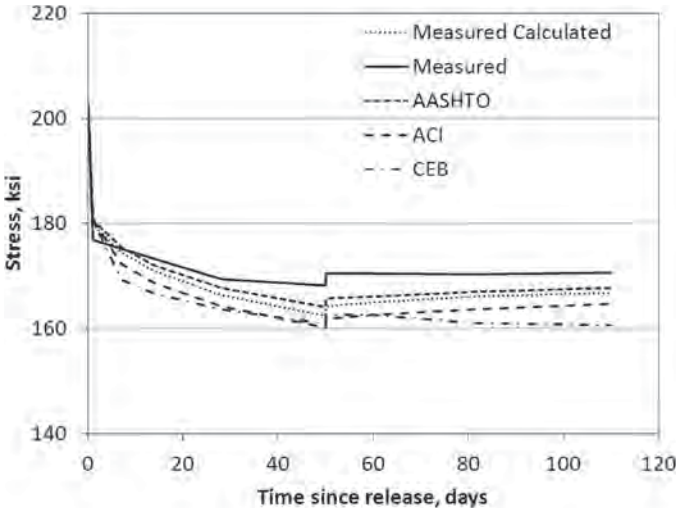

Figure 42. Measured and calculated strand stress for T2.8.Typ (AAEM method).

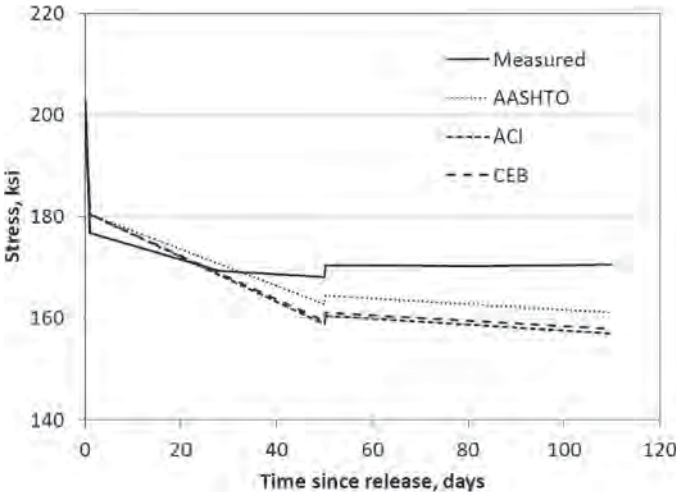

Figure 43. Strand stress for T2.8.Typ (AASHTO refined method).

reinforcement and deck shrinkage on overall time-dependent changes in prestress. Instantaneous changes, such as elastic shortening losses and increases in strain at the time of deck placement, were calculated using the transformed cross-sectional properties of the girder.

Measured Losses. The prestress loss in each girder was measured using a VWG placed at the centroid of the prestressing strands at the midspan of the beam. The initial elastic shortening losses were determined from the differences in strain before and after release. For these calculations, an initial prestressing stress of $0.75f_{pu}$ was used, which is the maximum allowed by the AASHTO LRFD specifications.

Results. Figure 42 presents the measured and calculated change in prestress force over time. The calculated prestress was estimated using the AAEM method. Figure 43 presents the change in prestress force over time as predicted by the AASHTO refined method; the changes at release and at the time of deck placement are identical for all methods. In both cases, the time of deck placement was about 50 days after release when there is a sharp increase in strand stress. These figures show that use of the ACI and CEB MC90 models overestimate prestress loss. Most of the difference occurs in the calculation of time-dependent loss between release and deck placement.

Table 32 presents the elastic changes in prestress at release and at the time of deck placement. Strains were calculated using the transformed section properties using both the measured modulus of elasticity and the modulus of elasticity calculated with the measured compressive strength at the time of load application. As can be seen in Table 32, the measured elastic shortening losses are higher than calculated for all beams. Also, the measured modulus provides a better estimate of elastic shortening loss than the calculated modulus. The change in tendon stress at deck placement was very small. Measured strains were similar to the calculated values.

Prestress Losses Using the AASHTO Refined Method

Table 33 presents the time-dependent changes in prestress from immediately after release to the time of deck placement

Table 32. Early change in prestress.

Beam	At Elastic Shortening (ksi)			At Deck Placement (ksi)		
	Calculated with Meas. E_c	Calculated with Calc. E_c	Measured	Calculated with Meas. E_c	Calculated with Calc. E_c	Measured
T2.8.Min	-22.8	-22.1	-25.8	1.8	1.7	1.8
T2.8.Typ	-22.8	-22.1	-25.9	1.8	1.7	1.8
BT.8.Typ	-19.5	-17.4	-20.5	1.7	1.5	1.7
BT.8N.Typ	-15.8	-13.1	-19.6	1.6	1.3	1.6
BT.10.Typ	-17.6	-17.3	-20.5	1.6	1.5	1.6
BT.10.Min	-17.6	-17.3	-18.3	1.6	1.4	1.6

Table 33. Time-dependent change in prestress from release to deck placement.

Beam	Change in Prestress (ksi)							
	AASHTO Refined			AAEM				Measured
	AASHTO	ACI 209	CEB MC-90	AASHTO	ACI 209	CEB MC-90	AASHTO w/meas E_c	
T2.8.Min	-17.0 (0.64)*	-22.7 (0.48)	-21.6 (0.50)	-17.0 (0.64)	-22.7 (0.48)	-21.6 (0.50)	-19.4 (0.56)	-10.9
T2.8.Typ	-17.8 (0.48)	-21.7 (0.40)	-21.1 (0.41)	-16.5 (0.52)	-20.3 (0.42)	-19.7 (0.44)	-17.4 (0.49)	-8.6
BT.8.Typ	-18.3 (0.31)	-22.8 (0.25)	-23.0 (0.25)	-19.4 (0.29)	-24.5 (0.23)	-22.3 (0.25)	-21.3 (0.26)	-5.6
BT.8N.Typ	-14.9 (0.70)	-17.9 (0.58)	-16.4 (0.64)	-12.4 (0.84)	-15.2 (0.69)	-13.4 (0.78)	-16.0 (0.65)	-10.5
BT.10.Typ	-23.5 (0.23)	-29.8 (0.18)	-29.4 (0.18)	-20.4 (0.26)	-26.4 (0.20)	-25.3 (0.21)	-21.4 (0.25)	-5.4
BT.10.Min	-22.2 (0.13)	-27.5 (0.10)	-24.9 (0.11)	-19.2 (0.15)	-24.2 (0.12)	-21.2 (0.13)	-20.1 (0.14)	-2.8

*Number in parentheses in each cell is the ratio of measured loss to calculated loss.

using each calculation method. Table 34 presents the time-dependent changes in prestress from just after deck placement to destructive testing. Table 35 presents the total change in prestress from just prior to release to test.

Figure 44 presents the bias, or measured value, divided by calculated value for the prestress change from release to testing. The data show the following:

- For the lightweight concrete girders, all methods predict higher losses than those measured.
- The magnitude of the error (prediction minus measured) was greater for the interval from just after release to deck placement, than that from deck placement to testing.
- Predicted losses for the Type II beams were slightly better than for the PCBT beams.
- The AAEM method predictions are closer to the measured values than those predicted by the AASHTO refined method for the same creep and shrinkage model.
- The AASHTO creep and shrinkage model provides slightly better predictions than the other two models.

Camber of Lab-Cast Beams

Initial Camber at Prestress Release. Initial camber values were measured using the taut-wire method. Deflections were also calculated using basic beam mechanics together with the fresh concrete unit weights and initial measured cylinder compressive strengths. The gross section moment of inertia was used in calculating displacements. The initial prestress was assumed constant along the length of the beam and was calculated at midspan as the initial jacking force minus the calculated elastic shortening losses. Beam self-weight was calculated by accounting for all steel reinforcement in the beam and using the fresh concrete unit weights. Attachment M contains camber versus time plots for each lab-cast beam. Table 36 shows a comparison of the measured and calculated cambers.

Table 34. Change in prestress from deck placement to testing.

Beam	Change in Prestress (ksi)							
	AASHTO Refined			AAEM				Measured
	AASHTO	ACI 209	CEB MC-90	AASHTO	ACI 209	CEB MC-90	AASHTO w/meas E_c	
T2.8.Min	-3.5 (-0.10)*	-2.2 (-6.5)	-2.1 (-6.3)	-1.8 (-5.5)	-0.6 (-2.5)	-1.6 (-5.0)	-1.4 (-4.5)	0.4
T2.8.Typ	-3.3 (-0.03)	-3.5 (-36)	-3.1 (-32)	-1.0 (-11)	-0.4 (-5.0)	-1.9 (-20)	-1.3 (-14)	0.1
BT.8.Typ	-0.2 (1.63)	0.2 (-1.7)	0.7 (-3.3)	-0.7 (2.3)	-0.7 (2.3)	-0.7 (2.3)	-1.0 (0.3)	-0.3
BT.8N.Typ	-2.2 (0.18)	-2.9 (7.3)	-2.2 (5.5)	-0.5 (5.5)	0.4 (-2.0)	-0.8 (2.0)	-0.4 (1.0)	-0.4
BT.10.Typ	-0.2(-3.71)	0.4 (0.6)	0.1 (0.1)	-0.6 (-1.9)	-0.8 -2.1)	-0.6 (1.9)	-0.9 (-2.3)	0.7
BT.10.Min	-0.2 (2.67)	0.4 (-2.0)	-0.6 (1.5)	-0.8 (2.0)	-0.9 (2.3)	-0.7 (1.8)	-0.8 (2.0)	-0.4

*Number in parentheses in each cell is the ratio of measured loss to calculated loss.

Table 35. Total change in prestress from prior to release to testing.

Beam	Prestress Loss (ksi)							
	AASHTO Refined			AAEM				Measured
	AASHTO	ACI 209	CEB MC-90	AASHTO	ACI 209	CEB MC-90	AASHTO w/meas E_c	
T2.8.Min	-42.3 (0.82)*	-45.4 (0.76)	-45.6 (0.76)	-39.2 (0.88)	-43.7 (0.79)	-43.7 (0.79)	-41.9 (0.83)	-34.6
T2.8.Typ	-41.5 (0.77)	-45.6 (0.70)	-44.6 (0.72)	-38.0 (0.84)	-41.2 (0.78)	-42.1 (0.76)	-39.7 (0.81)	-32.1
BT.8.Typ	-38.5 (0.63)	-43.6 (0.56)	-42.3 (0.57)	-36.1 (0.67)	-41.2 (0.59)	-38.9 (0.63)	-40.2 (0.61)	-24.3
BT.8N.Typ	-28.9 (1.01)	-32.6 (0.89)	-30.4 (0.96)	-24.7 (1.18)	-26.5 (1.10)	-25.9 (1.12)	-30.6 (0.95)	-29.1
BT.10.Typ	-39.5 (0.59)	-45.3 (0.52)	-45.2 (0.52)	-36.9 (0.63)	-43.0 (0.54)	-41.7 (0.56)	-38.3 (0.61)	-23.4
BT.10.Min	-38.3 (0.52)	-43.0 (0.46)	-41.3 (0.48)	-35.9 (0.55)	-41.0 (0.49)	-37.8 (0.53)	-37.0 (0.54)	-19.9

*Number in parentheses in each cell is the ratio of measured loss to calculated loss.

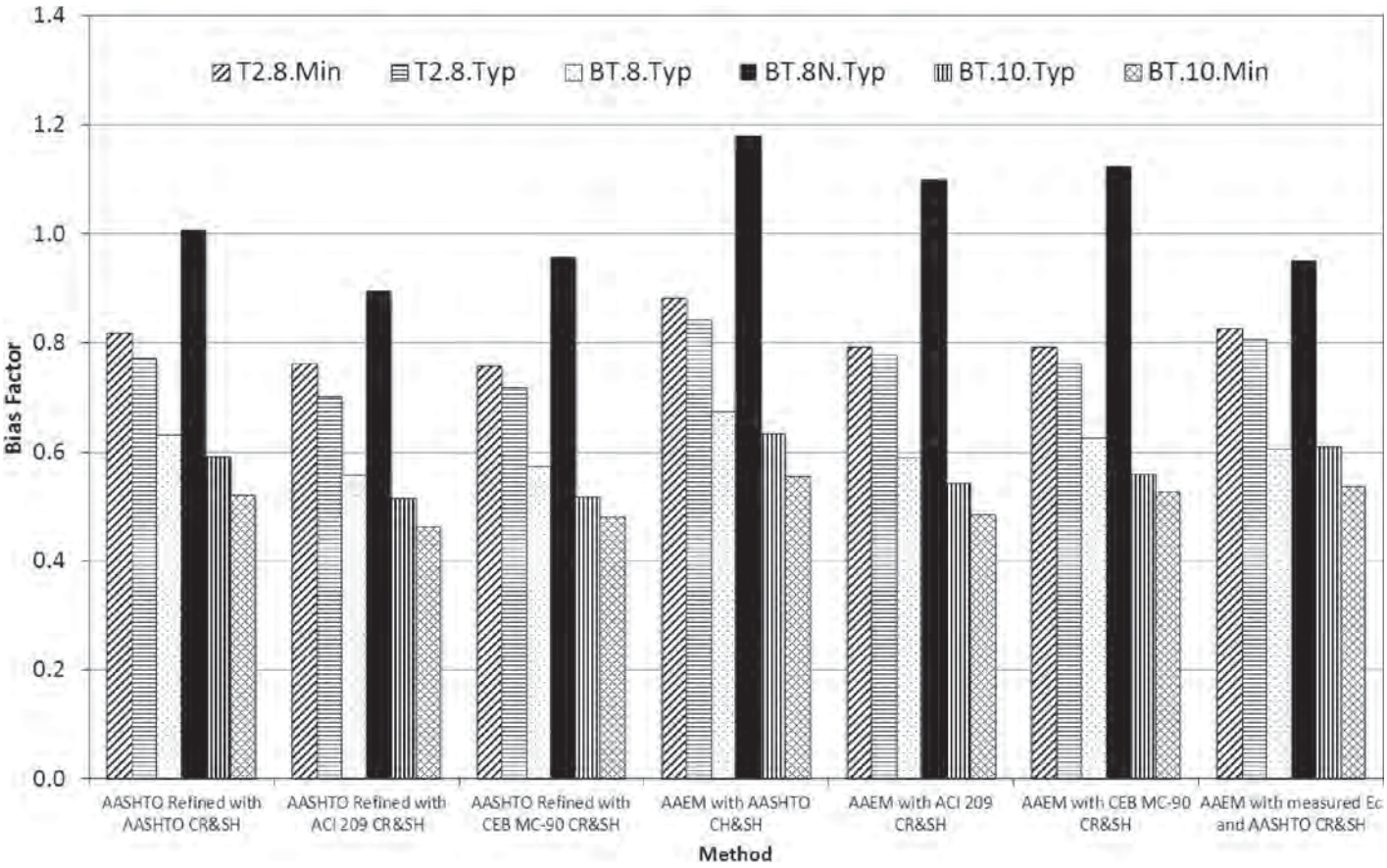

Figure 44. Measured loss/calculated loss from just prior to release to testing.

Table 36. Initial measured versus calculated cambers.

Beam ID	Camber (in.)		Measured/ Calculated	Average Measured/Calculated
	Calculated	Measured		
1.NW1.5A	0.310	0.359	1.16	1.11
1.NW1.5B	0.310	0.336	1.08	
3.NW1.6A	0.215	0.234	1.09	
3.NW1.6B	0.215	0.237	1.10	
1.LW1.5A	0.387	0.359	0.93	0.90
1.LW1.5B	0.387	0.359	0.93	
2.LW3.5A	0.481	0.414	0.86	
2.LW3.5B	0.481	0.395	0.82	
3.LW2.5A	0.433	0.422	0.97	
3.LW2.5B	0.433	0.422	0.97	
2.LW3.6A	0.345	0.297	0.86	
2.LW3.6B	0.345	0.297	0.86	

As expected, the initial measured normal weight beam cambers were less than or equal to the measured lightweight cambers due to the lower stiffness of the lightweight concrete and the higher self-weight. Also, there was a large difference between the measured and predicted values, in particular, between the lightweight concrete from pour 2 and the normal weight concrete from pour 1 (note that the first number in the beam identification indicates the concrete pour number). In all cases, the initial measured camber was higher than that predicted for normal weight beam specimens and lower than that predicted for lightweight beam specimens.

Time-Dependent Camber

Figures 45 and 46 present the average measured cambers for beam pairs versus time. There is an apparent difference in the camber of the beams with 0.5 in. and 0.6 in. strands. For the 0.5 in. strands, the total cambers for the normal weight and lightweight beams are approximately the same, despite the higher initial cambers of the lightweight beams. However, for the 0.6 in. strands, the normal weight beam pair showed a significantly smaller camber than the lightweight beam pair.

Figure 47 shows a typical plot of the measured average cambers for a beam pair and the predicted camber using both the PCI Multiplier Method and the PCI Improved Multiplier Method (*PCI Bridge Design Manual* (1997)). These predictions were calculated using tested cylinder properties. The AASHTO LRFD refined prestress loss method was used to calculate the improved PCI multipliers. Table 37 presents a summary of the measured and calculated camber. For the 0.5 in. strand normal weight beams, the PCI predictions were comparable to the measurements. However, the PCI method

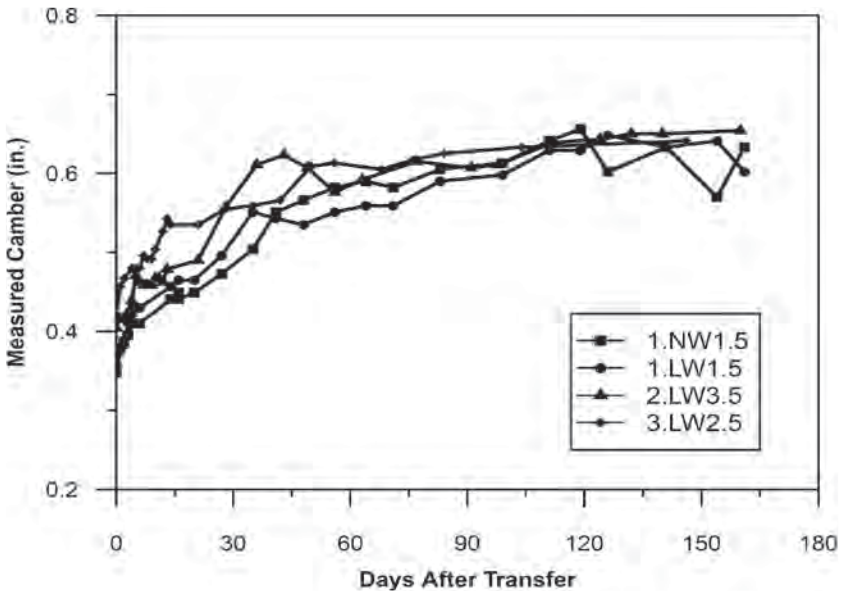

Figure 45. Time-dependent camber for beams with 0.5 in. strand.

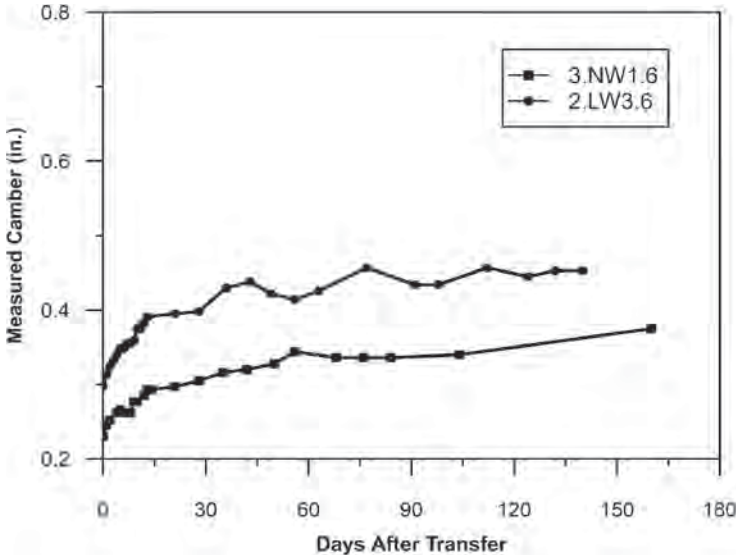

Figure 46. Time-dependent camber for beams with 0.6 in. strand.

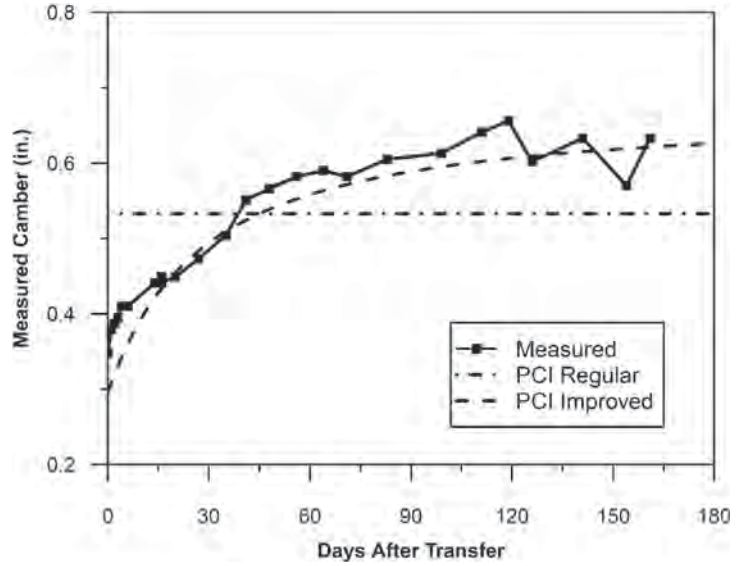

Figure 47. Camber for beam pair 1.NW1.5.

Table 37. Calculated and measured camber.

Beam	Camber (in.)						
	At release		Final				
	Calculated	Measured	Days After Transfer	PCI Multiplier, Erection	PCI Multiplier, Final	PCI Improved Multiplier	Measured
1.NW1.5A	0.310	0.359	141	0.533	0.645	0.615	0.633
1.NW1.5B	0.310	0.336	161	0.533	0.645	0.621	0.633
1.LW1.5A	0.387	0.359	119	0.697	0.845	0.747	0.609
1.LW1.5B	0.387	0.359	161	0.697	0.845	0.763	0.602
2.LW3.5A	0.481	0.414	160	0.858	1.040	1.050	0.664
2.LW3.5B	0.481	0.395	160	0.858	1.040	1.050	0.645
3.LW2.5A	0.433	0.422	146	0.840	1.018	0.968	0.641
3.LW2.5B	0.433	0.422	104	0.840	1.018	0.941	0.641
3.NW1.6A	0.215	0.234	104	0.394	0.478	0.423	0.336
3.NW1.6B	0.215	0.237	160	0.394	0.478	0.438	0.375
2.LW3.6A	0.345	0.297	140	0.616	0.748	0.714	0.453
2.LW3.6B	0.345	0.297	140	0.616	0.748	0.714	0.453

greatly over predicted cambers for all lightweight concrete beams. This may be due to sensitivity to the elastic modulus values used. As the elastic modulus for a particular beam pair decreases, the predicted deflections increase. Therefore, the low moduli of the lightweight beams resulted in high predictions. The PCI predictions were also high for both the normal weight and lightweight concrete beam pairs with 0.6 in. strand.

Full-Scale Beam Camber

For the full-scale beams, two methods were used to calculate initial cambers and three methods were used to calculate camber changes with time. Camber was calculated using the PCI Basic Multiplier method (*PCI Bridge Design Manual* (1997)), PCI Bridge Design Manual Improved Multiplier Method (*PCI Bridge Design Manual* (1997)), and the previously described AAEM method. Four camber calculations were made using the AAEM method. In one calculation, the measured values of f'_c, f'_{ci}, E'_{ci}, and E_c were used together with the AASHTO creep and shrinkage equations. The other three calculations used the measured values of f'_c and f'_{ci}, and the modulus, creep and shrinkage values calculated using AASHTO, ACI 209, and CEB MC90. The PCI Bridge Design Manual Improved Multiplier method was also used with each of the three creep and shrinkage models. Attachment M contains camber versus time plots for each girder.

Initial Camber. Two methods were used to find initial camber. For the multiplier methods, the traditional approach to account for elastic shortening losses was used. This involved determining the elastic shortening loss at midspan and assuming that loss is constant along the length of the beam (as specified in AASHTO Section 5.9.5.5). The upward camber due to prestress was then calculated based on the jacking force minus the elastic shortening loss. Gross cross-sectional properties were used with the initial prestress force.

For the second method, the transformed moment of inertia was calculated at several points along the beam. Because of the harped strands, the moment of inertia varied somewhat along the span. The points that were considered were the transfer point, quarter point, and midspan. With the transformed area, the jacking force, the self-weight moment, and the modulus of elasticity at release, the instantaneous curvature was calculated at each point. With these curvatures, the moment-area method was used to calculate the deflection at midspan. By analyzing each section separately, the elastic shortening loss at each location is different. This method also establishes the initial conditions needed to calculate camber changes using the AAEM method.

Changes in Camber with the AAEM Method. The AAEM method uses creep and shrinkage values calculated by using *AASHTO LRFD Bridge Design Specifications,* ACI 209, or CEB MC90 creep and shrinkage equations. The change in curvature at each location is then calculated using the moment-area method.

Changes in Camber with the PCI Basic Multiplier Method. The PCI Basic Multiplier method provides guidance to calculate the camber after release, before deck placement, after deck placement, and at the end of service life. For calculation of the camber before deck placement, PCI recommends multipliers found in Table 4.8.4.1 in the *PCI Design Handbook* (6th ed.). For estimating the camber after deck placement, the deflection due to the deck weight was calculated. The 28-day modulus was used for this calculation together with the transformed moment of inertia. The deflection due to deck weight was subtracted from the camber before deck placement to determine the camber after deck placement. The camber at end of service is a value that assumes the girder is about 10,000 days old. However, because the girders were considerably younger, a percentage of the end of service camber was used to estimate the camber at the time of testing.

Changes in Camber with the PCI Improved Multiplier Method. The *PCI Bridge Design Manual* (BDM) Improved Multiplier Method was used to provide three additional estimates of camber. The AASHTO Refined method was used to estimate the prestress loss, which was required to complete the analysis. The three camber estimates used the creep coefficients found in AASHTO, ACI, and CEB MC90, and the prestress loss was determined with the corresponding creep and shrinkage model. The initial camber was found with the same method as the initial camber for the PCI Basic Multiplier method. To estimate long-term deflections to initial cambers from prestress and self-weight and the camber due to time-dependent prestress loss must also be estimated.

Once the individual components of displacement were calculated, the formulas, found in Table 8.7.2-1 of the PCI BDM, were used. The final camber is typically estimated using the creep coefficient at end of service or 10,000 days. For this research, the final time was that at testing to destruction; the creep coefficient associated with that day was used. The PCI BDM notes that this method is not completely applicable to cambers in members with composite decks. It does not include effects such as the differential shrinkage of the deck and girder concrete. The PCI BDM recommends more rigorous methods of analysis for such cases.

Measured Camber. To measure the actual camber of the girders being tested, a taut-wire system was used. To determine the camber, the reader matched the wire against its reflection in the mirror and then read the value on a high-precision scale to the nearest 1/64th of an inch.

Results. Figure 48 presents the measured camber versus time and the calculated cambers using the AAEM method for a Type II girder with typical shear reinforcement. Figure 49

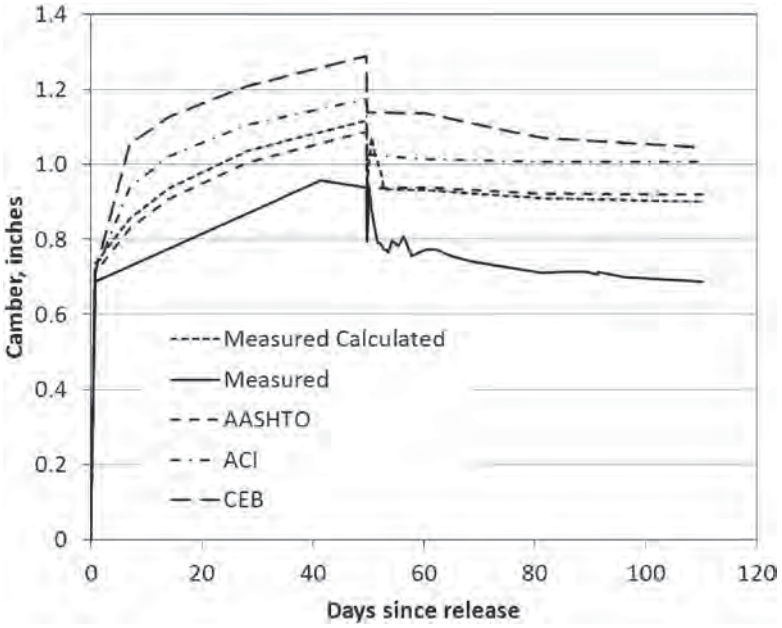

Figure 48. Measured and calculated cambers with AAEM.

presents the measured camber and the PCI multiplier methods for the same beam. The "Measured Calculated" values in Figure 48 include an allowance to account for the effects of thermal gradients that develop during deck hydration.

Table 38 presents the measured initial camber and the predictions using three methods. In the first method, the curvature was determined at several locations along the beam, and the moment-area method was used to calculate camber. The table shows estimates using (1) the measured modulus of elasticity, (2) the modulus calculated with the measured compressive strength, and (3) the traditional method of applying equivalent forces to the cross-section. The results for all methods were very similar.

Table 39 presents the measured and predicted cambers just prior to placing the deck concrete. Camber predictions using the PCI Improved Multiplier method and the AAEM method with the AASHTO creep and shrinkage model were closest to the measured values.

Table 40 presents the measured and calculated downward deflection due to the placement of the deck concrete using

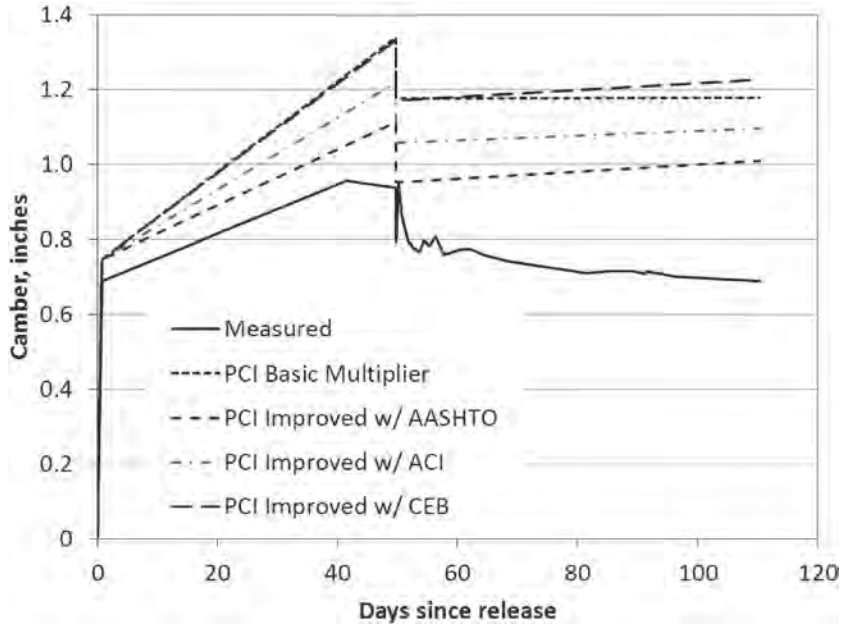

Figure 49. Measured and calculated cambers using PCI multipliers.

Table 38. Measured and calculated initial cambers.

Beam	Camber (in.)			
	Using Moment-Area w/ Measured E_c	Using Moment-Area w/ Calculated E_c	Using Traditional Method	Measured Camber
T2.8.Min	0.74	0.71	0.75	0.72
T2.8.Typ	0.74	0.71	0.75	0.69
BT.8.Typ	1.05	0.90	0.92	0.97
BT.8N.Typ	0.84	0.66	0.67	0.99
BT.10.Typ	0.96	0.90	0.92	-
BT.10.Min	0.96	0.90	0.92	-

Table 39. Camber at deck placement.

Beam	Camber (in.)								
	PCI Mult	PCI Improved Multipliers			AAEM				Measured
		AASHTO	ACI 209	CEB MC-90	AASHTO	ACI 209	CEB MC-90	AASHTO w/meas E_c	
T2.8.Min	1.34	1.11	1.27	1.39	1.08	1.21	1.34	1.16	0.95
T2.8.Typ	1.34	1.11	1.22	1.33	1.09	1.17	1.29	1.12	0.94
BT.8.Typ	1.65	1.49	1.62	1.81	1.55	1.67	1.88	1.80	1.50
BT.8N.Typ	1.20	1.00	1.10	1.21	1.04	1.12	1.25	1.29	1.44
BT.10.Typ	1.65	1.52	1.67	1.94	1.58	1.71	2.00	1.68	1.65
BT.10.Min	1.65	1.48	1.61	1.78	1.54	1.66	1.84	1.64	1.57

Table 40. Measured and calculated downward deflection from deck concrete.

Beam	Camber (in.)			
	Moment-Area w/ Measured E_c	Moment-Area w/ Measured E_c	Traditional Method	Measured Camber
T2.8.Min	-0.16	-0.15	-0.16	-0.14
T2.8.Typ	-0.16	-0.15	-0.16	-0.14
BT.8.Typ	-0.16	-0.15	-0.17	-0.20
BT.8N.Typ	-0.15	-0.14	-0.13	-0.11
BT.10.Typ	-0.16	-0.16	-0.17	-0.17
BT.10.Min	-0.15	-0.16	-0.15	-0.15

three calculation methods. The data presented in the table indicate that the methods predict camber change similar to the measured values.

Table 41 shows the measured and calculated cambers from immediately after the deck was cast to testing of the girders. The methods based on the PCI multipliers all predicted a net upward camber during this time period while the methods based on the AAEM method predicted a downward camber. A net downward deflection was measured during the time interval and was closely matched by three of the four methods using the AAEM method.

Table 42 presents the measured and calculated total camber at the time each girder was tested to destruction. The multiplier methods overestimated the camber growth after casting the girder for the majority of beams, while the AAEM method with the AASHTO creep and shrinkage model predicted cambers close to measured values for the majority of the beams. The AAEM method accounted for the downward displacement caused by differential shrinkage of the deck close to measured values for the majority of beams, but not the multiplier methods.

Figure 50 presents the bias (measured value divided by calculated value) of the camber calculation methods. The closest

Table 41. Change in camber from casting of deck concrete to testing.

Beam	Camber Change (in.)								
	PCI Mult.	PCI Improved Multipliers			AAEM				Measured
		AASHTO	ACI 209	CEB MC-90	AASHTO	ACI 209	CEB MC-90	AASHTO w/meas E_c	
T2.8.Min	0.07	0.18	0.12	0.14	-0.14	-0.14	-0.15	-0.26	-0.13
T2.8.Typ	0.07	0.16	0.15	0.17	-0.14	-0.14	-0.09	-0.23	-0.12
BT.8.Typ	0.06	0.07	0.07	0.08	-0.16	-0.10	-0.16	-0.27	-0.08
BT.8N.Typ	0.06	0.11	0.11	0.12	-0.14	-0.14	-014	-0.20	-0.09
BT.10.Typ	0.06	0.06	0.05	0.06	-0.12	-0.11	-0.12	-0.18	-0.07
BT.10.Min	0.05	0.07	0.06	0.08	-0.17	-0.18	-0.17	-0.24	-0.01

Table 42. Camber at testing.

Beam	Camber (in.)								
	PCI Mult.	PCI Improved Multipliers			AAEM				Measured
		AASHTO	ACI 209	CEB MC-90	AASHTO	ACI 209	CEB MC-90	AASHTO w/meas E_c	
T2.8.Min	1.18	1.13	1.23	1.37	0.78	0.91	1.03	0.74	0.68
T2.8.Typ	1.18	1.11	1.21	1.34	0.79	0.87	1.04	0.73	0.69
BT.8.Typ	1.48	1.40	1.53	1.73	1.23	1.35	1.56	1.37	1.22
BT.8N.Typ	1.05	0.96	1.06	1.18	0.75	0.83	0.96	0.94	1.24
BT.10.Typ	1.47	1.42	1.56	1.84	1.30	1.44	1.72	1.34	1.41
BT.10.Min	1.48	1.40	1.52	1.71	1.22	1.33	1.52	1.25	1.41

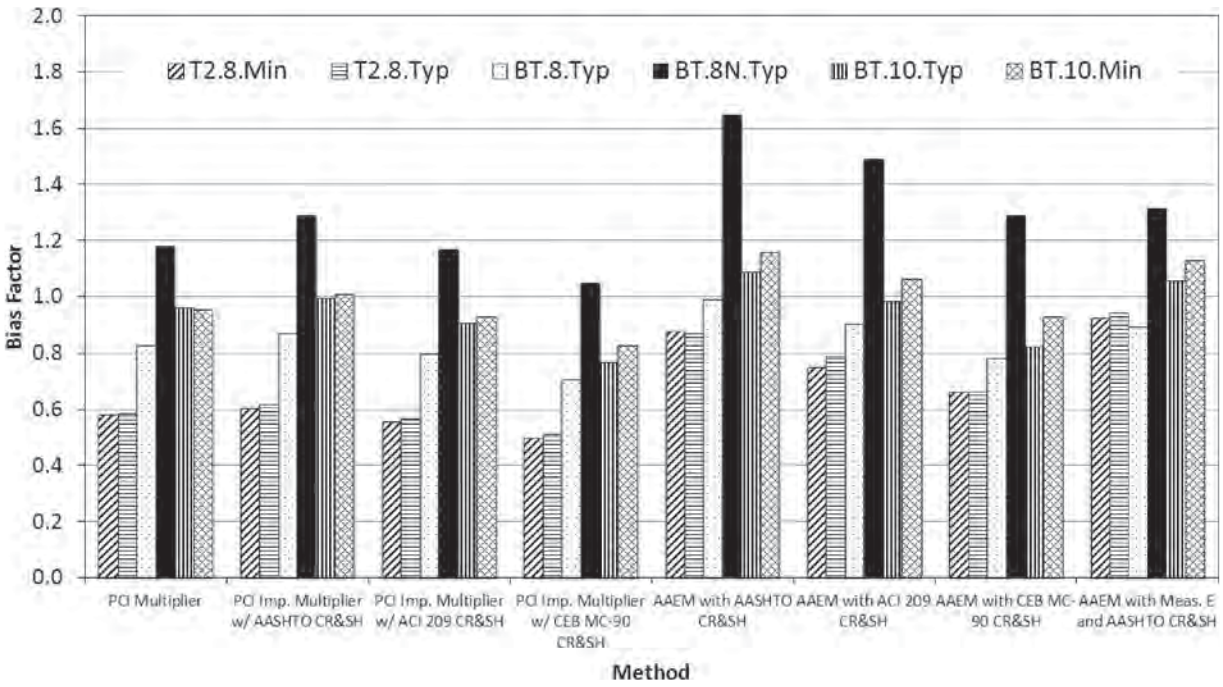

Figure 50. Bias of camber calculation methods.

predictions were those made using the AAEM method with the measured modulus of elasticity. The AAEM method with the calculated modulus and AASHTO creep and shrinkage models also predicted cambers relatively close to measured.

Summary

The following observations can be made from the camber studies:

- For the lab-cast beams with no cast-in-place deck, the PCI Improved Multiplier method predicted the camber of the normal weight beams relatively well, but over-predicted the cambers of the lightweight girders.
- For the full-scale beams, the PCI Improved Multiplier method used with the AASHTO model for creep and shrinkage predicted cambers of the lightweight girders at the time the deck was placed close to those measured. The measured camber of the normal weight girder was significantly higher than predicted with this method.
- For the full-scale beams and for calculations of camber after the composite deck was placed, the AAEM method with the AASHTO creep and shrinkage functions resulted in the closest predictions of camber to those measured.
- High camber predictions for the full-scale beams were due to an overestimation of the camber growth from time of prestress transfer to deck placement.

3.6 Design Examples

One simple composite bridge beam example was selected to investigate differences in resulting designs between lightweight and normal weight concrete. The effects on design of the elimination of the modification factor to the $\sqrt{f'_c}$ term in shear design and a change in the strength reduction factor for shear design were also investigated.

The configuration presented as Example 9.4 in the *PCI Bridge Design Manual* (1997) was chosen. The following are the key parameters of the bridge:

Overall deck width:	51.0 ft
Design span length:	120.0 ft
Number of beams:	6
Beam spacing:	9.0 ft
Deck slab thickness:	8.0 in.
Relative humidity:	70%
Deck concrete f'_c:	4000 psi
Girder concrete f'_c:	6500 psi
Girder type:	AASHTO-PCI BT-72

A typical interior girder was designed. The design was performed for the three different scenarios presented in Table 43. Sample design calculations for the three scenarios are provided in Attachments N, O, and P.

The results of the flexural designs are presented in Table 44. The designs with lightweight concrete need fewer total strands and fewer harped strands. Also, the prestress losses in the lightweight girders are somewhat higher, due to the lower modulus of elasticity.

The shear design was performed using the sectional design model presented in AASHTO Section 5.8.3. The results of the shear design are presented in Table 45.

Run B represents the current approach to shear design for lightweight concrete girders that uses both a lower strength reduction factor and a reduction to the $\sqrt{f'_c}$ term. For this run, the amount of shear reinforcement is almost twice that required for the normal weight girder. However, for Run C, with no reductions to the $\sqrt{f'_c}$ term and a strength reduc-

Table 43. Scenarios for design example.

Run	Slab and Girder Concrete	Strength Reduction Factor for Shear	Modification Factor for $\sqrt{f'_c}$ Term for Shear Design
A	Normal Weight	0.90	1.00
B	Sand Lightweight	0.70	0.85
C	Sand Lightweight	0.85	1.00

Table 44. Results of flexural designs.

Run	Concrete	ϕ (shear)	λ_v	E_c, (ksi)	Total Strands	Harped Strands	Losses at Transfer (ksi)	Total Prestress Loss	ϕM_n (k-ft)
A	NWC	0.9	1.0	4890	44	8	17.4	40.4	10,640
B	LWC	0.7	0.85	3720	40	6	21.5	46.4	9840
C	LWC	0.85	1.0	3720	40	6	21.5	46.4	9840

Table 45. Results of shear designs at critical section.

Run	Concrete	ϕ (shear)	λ_v	V_c (kips)	Stirrup Bar Size	Spacing (in.)	Add'l Flexural Reinforcement at face of Bearing (in^2)
A	NWC	0.9	1.0	200.4	#4	21	2.2
B	LWC	0.7	0.85	179.2	#4	12	3.8
C	LWC	0.85	1.0	210.8	#4	24	3.4

tion factor of 0.85, the lightweight beam requires less reinforcement, due to the lower dead load shear. Run C requires somewhat more longitudinal reinforcement at the face of the bearing because of the fewer strands.

This design example illustrates typical differences between designs with normal weight concrete and lightweight concrete. With the current specifications, for a given span length and girder spacing, the lightweight beam will require less prestressing but more shear reinforcement than a normal weight beam with the same cross section. However, with the elimination of the modification to $\sqrt{f'_c}$ and changing the strength reduction factor for shear of lightweight concrete to 0.85, lightweight girders would require less shear reinforcement than a similar normal weight beam.

CHAPTER 4

Interpretation, Appraisal, and Application

This chapter provides an interpretation of the findings of this research as they apply to highway engineering practice. Recommendations for changes and revisions to the *AASHTO LRFD Bridge Design Specifications* are presented in Attachment A. Many of the investigated design provisions were found to adequately address the behavior of prestressed concrete members containing lightweight concrete; however, there are three sections to which changes are proposed: 5.4.2.6-Modulus of Rupture, 5.5.4.2-Resistance Factors, and 5.8.2.2-Modifications for Lightweight Concrete. One revision to Section 8.5.1-Storage of Aggregates of the *AASHTO Bridge Construction Specifications* (2010) is recommended and is presented in Attachment B. Design examples for a typical lightweight concrete bridge superstructure are provided in Attachments M, N, and O, which are not included herein but can be obtained by searching the TRB website for *NCHRP Report 733.*

CHAPTER 5

Conclusions and Suggested Research

This chapter presents the major conclusions of the research effort and provides suggestions for future research. However, it should be recognized that these findings are based on the results of limited tests conducted using limited material sources. Other research may be necessary to validate these findings.

5.1 Material Properties

Ninety-five laboratory test batches and 15 production batches of lightweight concrete were tested for a wide range of material properties. Based on these tests, the following conclusions are made:

- Two lightweight aggregates used in concrete mixtures for large-scale test specimens yielded test results consistent with what is needed for structural concretes.
- Lightweight concrete with a compressive strength of 7000 psi and a unit weight less than 125 lb/ft3 can be produced with a 0.30 w/cm and 800 lb of cementitious material with expanded shales and slates. The slate (SL1) consistently produced the highest strength concretes.
- The AASHTO LRFD equation for modulus of elasticity with $K_1 = 1.0$ is appropriate for lightweight aggregates. Predictions of modulus can be improved by calibrating the K_1 value for each aggregate type.
- The average splitting tensile strength of the lightweight concrete mixtures was $0.25\sqrt{f'_c}$ which exceeded $\sqrt{f'_c}/4.7$.
- On average, the modulus of rupture of the lightweight concrete was $0.31\sqrt{f'_c}$, with a lower bound of $0.26\sqrt{f'_c}$.
- Low-permeability lightweight concrete was produced through the use of supplementary cementitious materials. Lowest permeability values were achieved with silica fume as the cement replacement product.
- The AASHTO model for shrinkage generally predicted the shrinkage of lightweight concrete better than ACI 209 or CEB MC90.
- The AASHTO model for creep generally predicted the creep coefficients of the lightweight girder mixtures better than ACI 209 or CEB MC90. The creep coefficients of the deck concrete mixtures were considerably higher than predicted by the AASHTO model and were better predicted by the ACI 209 model.

5.2 Interface Shear Strength

Nine sets of three specimens each were tested to evaluate interface shear strength. Concrete strengths for the specimens ranged from 5.73 ksi to 6.25 ksi for the deck concretes and from 7.78 ksi to 11.1 ksi for the girder concretes. Push-off tests were used, with three different reinforcement ratios for the interface shear reinforcement, and three different combinations of concrete type (normal weight deck on normal weight girder, lightweight deck on lightweight girder, and lightweight deck on normal weight girder). Analysis of the test results indicated the following:

- The bias of the measured shear strengths to the nominal shear strength computed with the AASHTO equation for a concrete deck placed on the top flange of a girder that was intentionally roughened was 1.16 for N-N, 1.29 for L-N, and 1.26 for L-L.
- The AASHTO equation is less conservative with increasing reinforcement ratios, which indicates the friction coefficient may be too high.
- Based on a reliability analysis, normal weight and lightweight concrete should have the same strength reduction factor for interface shear.

5.3 Shear Tests

Two shear tests were performed on each of six full-scale prestressed beams. Five beams were fabricated with lightweight concrete and one with normal weight. Compressive strengths of the concrete used in the full-size girders ranged

from 8.5 ksi to 10.3 ksi. Based on the results of these 12 tests, the following observations and recommendations are made:

- The factor, λ_v, has an insignificant effect on the calculated shear strength of prestressed girders, when using the AASHTO sectional or simplified shear design approach.
- The bias of measured shear strength to calculated shear strength for normal weight and lightweight prestressed girders is approximately the same.
- Modification of the $\sqrt{f'_c}$ term in shear calculations for lightweight concrete is not necessary.
- The ϕ factor for shear design of sand lightweight concrete of 0.85 is appropriate.

5.4 Transfer and Development Length Testing

Twelve lab-cast beams were constructed and tested to evaluate transfer and development length in lightweight concrete prestressed girders. Concrete compressive strengths of these beams ranged from 7.39 ksi to 8.54 ksi at 28 days of concrete age. Analysis of test results showed that the AASHTO equations and the Ramirez and Russell (2008) equations for transfer length both provide a reasonable upper bound to the measured transfer and development lengths in the lightweight and normal weight girders studied in this project and others found in the literature.

5.5 Time-Dependent Behavior

Prestress Losses

The twelve lab-cast beams and six full-scale beams were instrumented with vibrating wire gages to track changes in strain at the level of the strands. The concrete compressive strengths found in these beams and girders ranged from 7.39 ksi to 10.3 ksi. Based on comparisons of measured and calculated prestress losses, the following conclusions are made:

- The current AASHTO refined method for calculating prestress losses is appropriate for lightweight girders with lightweight decks.
- The majority of the difference between calculated and measured prestress loss occurs during the time between release and deck placement. The AASHTO method consistently predicts higher losses than were measured during this period.
- Of the three creep and shrinkage models allowed by AASHTO (AASHTO, ACI 209, and CEB MC90), the AASHTO model results in estimates of prestress loss closest to those measured and is appropriate for use with lightweight prestressed concrete girders.

Camber

The twelve lab-cast beams and six full-scale beams were instrumented with a taut-wire measuring system to track changes in camber. The concrete compressive strengths found in these beams and girders range from 7.39 ksi to 10.3 ksi. Based on comparisons of measured and calculated cambers, the following conclusions are made:

- Of the methods evaluated in the project, the *PCI Bridge Design Manual* improved multiplier method, using the AASHTO creep and shrinkage models, provides an appropriate estimate of camber at the time of erection.
- For estimates of camber after casting of the deck, the AAEM method provides good prediction of end-of-service cambers in composite girders.

5.6 Design Examples and Parametric Studies

Based on comparative designs of bridge superstructures with normal weight and lightweight concrete in the prestressed girders and deck, the following observations and recommendations are made:

- For identical configurations, the lightweight girder and deck example required 10% fewer strands than the normal weight example.
- The current strength reduction factor for a shear of 0.70 for lightweight girder results in almost twice the amount of shear reinforcement required for the normal weight example.
- A change in the strength reduction factor to 0.85 will result in required amounts of shear reinforcement similar to that required for normal weight beams.

5.7 Recommendations for Future Research

The following recommendations are made for future research related to the use of lightweight concrete in bridge girders and decks:

- Six aggregate sources from around the United States were used in this study. However, there are numerous other lightweight aggregate sources in the United States. Therefore, state and local transportation authorities need to perform material property testing for locally available lightweight aggregate to verify that other available lightweight aggregates yield concrete mixtures with structural material properties similar to those found in this research. The most important structural properties to be verified are modulus of elasticity and tensile strength. Addition-

ally, testing of Resistance to Abrasion (ASTM C944) and Resistance to Scaling (ASTM C672) of concrete mixtures containing lightweight aggregates should be performed in order to ensure proper resistance to these effects.

- The reliability study for interface shear strength was performed on a very limited data set. Further tests of interface shear strength of lightweight concrete will help to better quantify the reliability index.
- The evaluation of shear strength and strength reduction factors of lightweight girders was based on a total of less than 25 tests. Further tests of full-size prestressed girders will help to verify or modify the recommended ϕ value.

References

AASHTO (2010). *AASHTO LRFD Bridge Construction Specifications,* 3rd Edition.

AASHTO (2010). *AASHTO LRFD Bridge Design Specifications,* 5th Edition.

AASHTO T-161 (2008). Standard Method of Test for Resistance of Concrete to Rapid Freezing and Thawing, 10 pp.

ACI 209 (1997). Prediction of Creep, Shrinkage, and Temperature Effects in Concrete Structures.

ASTM C39 (2005). Standard Test Method for Compressive Strength of Cylindrical Concrete Specimens.

ASTM C78 (2007). Standard Test Method for Flexural Strength of Concrete (Using Simple Beam with Third-Point Loading).

ASTM C127 (2007). Standard Test Method for Density, Relative Density (Specific Gravity), and Absorption of Coarse Aggregate.

ASTM C150 (2009). Standard Specification for Portland Cement.

ASTM C157 (2008). Standard Test Method for Length Change of Hardened Hydraulic-Cement Mortar and Concrete.

ASTM C469 (2002e1). Standard Test Method for Static Modulus of Elasticity and Poisson's Ratio of Concrete in Compression.

ASTM C496 (2004). Standard Test Method for Splitting Tensile Strength of Cylindrical Concrete Specimens.

ASTM C512/C512M (2010). Standard Test Method for Creep of Concrete in Compression.

ASTM C567 (2005). Standard Test Method for Determining Density of Structural Lightweight Concrete.

ASTM C618 (2008). Standard Specification for Coal Fly Ash and Raw or Calcined Natural Pozzolan for Use in Concrete.

ASTM C666 (2008). Standard Test Method for Resistance of Concrete to Rapid Freezing and Thawing.

ASTM C989 (2010). Standard Specification for Slag Cement for Use in Concrete and Mortars.

ASTM C1202 (2010). Standard Test Method for Electrical Indication of Concrete's Ability to Resist Chloride Ion Penetration.

ASTM C1240 (2010). Standard Specification for Silica Fume Used in Cementitious Mixtures.

ASTM C1556 (2004). Standard Test Method for Determining the Apparent Chloride Coefficient of Cementitious Mixtures by Bulk Diffusion.

ASTM C1585 (2004). Standard Test Method for Measurement of Rate of Absorption of Water by Hydraulic-Cement Concretes.

CEB-FIP Model Code (1990), Design Code 1990, Comité Euro-International du Béton.

Dymond, B.Z., Roberts-Wollmann, C.L., & Cousins, T.E. (2009). *Shear Strength of a PCBT-53 Girder Fabricated with Lightweight Self-Consolidating Concrete. Report No. FHWA/VTRC 09-CR11.* Virginia Transportation Research Council.

Hawkins, N.M., et al. (2005). *NCHRP Report 549: Simplified Shear Design of Structural Concrete Members.* Transportation Research Board. National Academy of Sciences, Washington, DC.

Kahn, L.F., et al. (2004). "Lightweight Concrete for High Strength/High Performance Precast Prestressed Bridge Girders," Research Report No. 04-1, Georgia Institute of Technology, Jan. 2004.

Kolozs, R.T. (2000). *Transfer and Development Lengths of Fully Bonded ½ Inch Prestressing Strand in Standard AASHTO Type I Pretensioned High Performance Lightweight Concrete (HPLC) Beams.* Master's Thesis, University of Texas at Austin, Austin, TX.

Logan, D.R. (1997). "Acceptance Criteria for the Bond Quality of Strand for Pretensioned Prestressed Concrete Applications." *PCI Journal, 42*(2), 52–90.

Malone, B.J. (1999). *Shear Strength of Reinforced and Prestressed Concrete Beams With Lightweight Aggregate Concrete.* PhD Dissertation, Purdue University.

Meyer, K.F. (2002). *Transfer and Development Length of 0.6-inch Diameter Prestressing Strand in High Strength Lightweight Concrete.* Doctoral Dissertation, Georgia Institute of Technology, Atlanta, GA.

Nassar, A.J. (2002). *Investigation of Transfer Length, Development Length, Flexural Strength and Prestress Loss Trend in Full Bonded High Performance Lightweight Prestressed T-Beams.* Master's Thesis. Virginia Polytechnic Institute and State University, Blacksburg, VA.

Nowak (1999). *NCHRP Report 368: Calibration of LRFD Bridge Design Code.* Transportation Research Board. National Research Council, Washington, DC.

Nowak and Rakoczy (2010). *Strength Parameters for Compressive* Strength of Lightweight Concrete. 2010 Concrete Bridge Conference. National Concrete Bridge Council.

Nowak and Szerszen (2003). Calibration of Design Code for Buildings (ACI 318): Part 1-Statistical Models for Resistance. ACI Structural Journal. May-June 2003. 377–382.

PCI (1997). *PCI Bridge Design Manual*. Chicago, IL: Precast/Prestressed Concrete Institute.

Ramirez, J.A., and Russell, B.W. (2008). *NCHRP Report 603: Transfer, Development, and Splice Length for Strand/Reinforcement in High-Strength Concrete.* Transportation Research Board, National Research Council, Washington, DC.

Russell, B.W., and Burns, N.H. (1993). Design Guidelines for Transfer, Development and Debonding of Large Diameter Seven Wire Strands in Pretensioned Concrete Girders (Report No. 1210-5F): The University of Texas at Austin.

Zena, D. (1996). Transfer and Development Lengths of Strands in Lightweight Prestressed Concrete Members. Master's Thesis, University of Maryland, College Park, MD.

Attachment A

Proposed Changes to AASHTO LRFD Bridge Design Specifications

5.4.3.2 – Creep

The creep coefficient may be taken as:

$$\Psi(t,t_i) = 1.9k_s k_{hc} k_f k_{td} t_i^{-0.118} \qquad (5.4.2.3.2\text{-}1)$$

In which:

$$k_s = 1.45 - 0.13(V/S) \geq 1.0 \qquad (5.4.2.3.2\text{-}2)$$

$$k_{hc} = 1.56 - 0.008H \qquad (5.4.2.3.2\text{-}3)$$

$$k_f = \frac{5}{1 - f_c} \qquad (5.4.2.3.2\text{-}4)$$

$$k_f = \frac{t}{s1 - 1f_{ci} + t} \qquad (5.4.2.3.2\text{-}5)$$

Where:

H = relative humidity (%). In the absence of better information, H may be taken from Figure 5.4.2.3.3-1

k_s = factor for the effect of the volume-to-surface ratio of the component

k_f = factor for the effect of concrete strength

k_{hc} = humidity factor for creep

k_{td} = time development factor

C5.4.2.3.2

The methods of determining creep and shrinkage, as specified herein and in Article 5.4.2.3.3, are based on Huo et al. (2001), Al-Omaishi (2001), Tadros (2003), and Collins and Mitchell (1991). These methods are based on the recommendation of ACI Committee 209 as modified by additional recently published data. Other applicable references include Rusch et al. (1983), Bazant and Wittman (1982), and Ghali and Favre (1986). Based on the work of Cousins, Roberts-Wollmann and Brown (2013), the AASHTO method for determining creep and shrinkage of sand lightweight concrete yields reasonable results.

5.4.2.4 – Modulus of Elasticity

In the absence of measured data, the modulus of elasticity, E_c, for concretes with unit weights between 0.090 and 0.155 k_{cf} and specified compressive strengths up to 15.0 ksi may be taken as:

$$E_c = 33{,}000 K_1 w_c^{1.5} \sqrt{f'_c} \qquad (5.4.2.4\text{-}1)$$

where:

K_1 = correction factor for source of aggregate to be taken as 1.0 unless determined by physical test, and as approved by the authority of jurisdiction

w_c = unit weight of concrete (k_{cf}); refer to Table 3.5.1-1 or Article C5.4.2.4

f'_c = specified compressive strength of concrete (ksi)

C5.4.2.4

See commentary for specified strength in Article 5.4.2.1.

For normal weight concrete with w_c = 0.145 k_{cf} E_c may be taken as:

$$E_c = 1{,}820 \sqrt{f'_c} \qquad (C5.4.2.4\text{-}1)$$

Test data show that the modulus of elasticity of concrete is influenced by the stiffness of the aggregate. The factor K_1 is included to allow the calculated modulus to be adjusted for different types of aggregate and local materials. Unless a value has been determined by physical tests, K_1 should be taken as 1.0. Use of a measured k_1 factor permits a more accurate prediction of modulus of elasticity and other values that utilize it.

Based on the work of Cousins, Roberts-Wollmann, and Brown (2013), the AASHTO method for determining modulus of elasticity of sand lightweight concrete yields reasonable results. As with normal weight concrete, the factor K_1 is included to allow the calculated modulus to be adjusted for different types of aggregate and local materials.

5.4.2.6—Modulus of Rupture

Unless determined by physical tests, the modulus of rupture, f_r ksi, for specified concrete strengths up to 15.0 ksi, may be taken as:

- For normal weight and sand lightweight concrete:
  - When used to calculate the cracking moment of a member in Articles 5.7.3.4, 5.7.3.6.2, and 6.10.4.2.1 .....$0.24\sqrt{f'_c}$
  - When used to calculate the cracking moment of a member in Article 5.7.3.3.2 ..... $0.37\sqrt{f'_c}$
  - When used to calculate the cracking moment of a member in Article 5.8.3.4.3 ..... $0.20\sqrt{f'_c}$
- For lightweight concrete:
  - ~~For sand lightweight concrete ..... $0.20\sqrt{f'_e}$~~
  - For all-lightweight concrete ..... $0.17\sqrt{f'_c}$

When physical tests are used to determine modulus of rupture, the tests shall be performed in accordance with AASHTO T 97 and shall be performed on concrete using the same proportions and materials as specified for the structure.

5.4.2.7—Tensile Strength

Direct tensile strength may be determined by either using ASTM C900, or the split tensile strength method in accordance with AASHTO T 198 (ASTM C496).

C5.4.2.6

Data show that most modulus of rupture values for normal weight concrete are between $0.24\sqrt{f'_c}$ and $0.37\sqrt{f'_c}$ (ACI 1992; Walker and Bloem 1960; Khan, Cook, and Mitchell 1996) and for sand lightweight concrete are between $0.26\sqrt{f'_c}$ and $0.31\sqrt{f'_c}$ (Cousins, Roberts-Wollmann, and Brown 2013). It is appropriate to use the lower bound value when considering service load cracking. The purpose of the minimum reinforcement in Article 5.7.3.3.2 is to assure that the nominal moment capacity of the member is at least 20 percent greater than the cracking moment. Since the actual modulus of rupture could be as much as 50 percent greater than $0.24\sqrt{f'_c}$, the 20 percent margin of safety could be lost. Using an upper bound is more appropriate in this situation.

The properties of higher strength concretes are particularly sensitive to the constitutive materials. If test results are to be used in design, it is imperative that tests be made using concrete with not only the same mix proportions, but also the same materials as the concrete used in the structure.

The given values may be unconservative for tensile cracking caused by restrained shrinkage, anchor zone splitting, and other such tensile forces caused by effects other than flexure. The direct tensile strength stress should be used for these cases.

C5.4.2.7

For normal-weight concrete with specified compressive strengths up to 10 ksi, the direct tensile strength may be estimated as $f_r = 0.23\sqrt{f'_c}$.

5.5.4.2—Resistance Factors

5.5.4.2.1—Conventional Construction

Resistance factor ϕ shall be taken as:

- For tension-controlled reinforced concrete sections as defined in Article 5.7.2.1 .....0.90
- For tension-controlled prestressed concrete sections as defined in Article 5.7.2.1 .....1.00
- For shear and torsion:
  Normal weight concrete 0.90
  Sand lightweight concrete…....0.85
  All lightweight concrete 0.70
- For compression-controlled sections with spirals or ties, as defined in Article 5.7.2.1, except as specified in Articles 5.10.11.3 and 5.10.11.4.1b for Seismic Zones 2, 3, and 4 at the extreme event limit state 0.75
- For bearing on concrete 0.70
- For compression in strut-and-tie models 0.70

C5.5.4.2.1

In applying the resistance factors for tension-controlled and compression-controlled sections, the axial tensions and compressions to be considered are those caused by external forces. Effects of prestressing forces are not included.

In editions of and interims to the LRFD Specifications prior to 2005, the provisions specified the magnitude of the resistance factor for cases of axial load or flexure, or both, in terms of the type of loading. For these cases, the ϕ-factor is now determined by the strain conditions at a cross-section, at nominal strength. The background and basis for these provisions are given in Mast (1992) and ACI 318-02.

A lower ϕ-factor is used for compression-controlled sections than is used for tension-controlled sections because compression-controlled sections have less ductility, are more sensitive to variations in concrete strength, and generally occur in members that support larger loaded areas than members with tension-controlled sections.

For sections subjected to axial load with flexure, factored resistances are determined by multiplying both P_n and M_n by the appropriate single value of ϕ. Compression-controlled and tension-controlled sections are defined in Article 5.7.2.1 as those that have net tensile strain in the extreme tension steel at nominal strength less than or equal to or greater than 0.005, respectively. For sections with net tensile strain ε_t in the extreme tension steel at nominal strength between the above limits, the value of ϕ may be determined by linear interpolation, as shown in Figure C5.5.4.2.1-1. The concept of net tensile strain ε_t is discussed in Article C5.7.2.1. Classifying sections as tension-controlled, transition or compression-controlled, and linearly varying the resistance factor in the transition zone between reasonable values for the two extremes, provides a rational approach for determining ϕ and limiting the capacity of over-reinforced sections.

concrete. Research by Cousins, Roberts-Wollmann and Brown (2013) shows that a ϕ of 0.85 for sand lightweight concrete yields a safety index similar to that achieved when using a ϕ of 0.9 for normal weight concrete.

Previous editions of AASHTO LRFD have given a ϕ of 0.7 for shear and torsion of lightweight

5.8.2.2—Modifications for Lightweight Concrete

Where lightweight aggregate concretes are used the following modifications shall apply in determining resistance to torsion and shear.

- Where the average splitting tensile strength of lightweight concrete, f_{ct}, is specified, the term $\sqrt{f'_c}$ in the expressions given in Articles 5.8.2 and 5.8.3 shall be replaced by:

  $4.7 f_{ct} \leq \sqrt{f'_c}$

- Where f_{ct} is not specified, the term $0.75\sqrt{f'_c}$ for all lightweight concrete~~, and $0.85\sqrt{f'_c}$ for sand lightweight concrete~~ shall be substituted for $\sqrt{f'_c}$ in the expressions given in Articles 5.8.2 and 5.8.3. No modification factor is required for sand lightweight concrete.

C5.8.2.2

The tensile strength and shear capacity of all lightweight concrete is typically somewhat less than that of normal weight concrete having the same compressive strength. Tests have shown that the previous reduction factor for tensile strength of sand lightweight concrete (0.85) is not needed (Cousins, Roberts-Wollmann, and Brown (2013)).

5.8.4 – Interface Shear Transfer – Shear Friction

5.8.4.1 – General

The interface shear strength Eqs. 5.8.4.1-3, 5.8.4.1-4, and 5.8.4.1-5 are based on experimental data for normal weight, nonmonolithic concrete strengths ranging from 2.5 ksi to 16.5 ksi; normal weight, monolithic concrete strengths from 3.5 ksi to 18.0 ksi; sand lightweight concrete strengths from 2.0 ksi to ~~6.0~~ 8.0 ksi; and all-lightweight concrete strengths from 4.0 ksi to 5.2 ksi.

5.8.4.3 – Cohesion and Friction Factors

The following values shall be taken for cohesion, c, and friction factor, μ:

- For a cast-in-place concrete slab on clean concrete girder surfaces, free of laitance with surface roughened to an amplitude of 0.25 in:

  c = 0.28 ksi
  μ = 1.0
  K_1 = 0.3
  K_2 = 1.8 ksi for normal weight concrete
  = 1.3 ksi for lightweight concrete

- For normal weight concrete placed monolithically:

  c = 0.40 ksi
  μ = 1.4
  K_1 = 0.25
  K_2 = 1.5 ksi

- For lightweight concrete placed monolithically, or nonmonolithically, against a clean concrete surface, free of laitance with surface intentionally roughened to an amplitude of 0.25 in.:

  c = 0.24 ksi
  μ = 1.0
  K_1 = 0.25
  K_2 = 1.0 ksi

C5.8.4.3

The values presented provide a lower bound of the substantial body of experimental data available in the literature (Loov and Patnaik, 1994; Patnaik, 1999; Mattock, 2001; Slapkus and Kahn, 2004: Cousins, Roberts-Wollmann, and Brown (2013)). Furthermore, the inherent redundancy of girder/slab bridges distinguishes this system from other structural interfaces.

The values presented apply strictly to monolithic concrete. These values are not applicable for situations where a crack may be anticipated to occur at a Service Limit State.

The factors presented provide a lower bound of the experimental data available in the literature (Hofbeck, Ibrahim, and Mattock, 1969; Mattock, Li, and Wang, 1976; Mitchell and Kahn, 2001).

Available experimental data demonstrates that only one modification factor is necessary, when coupled with the resistance factors of Article 5.5.4.2, to accommodate both all-lightweight and sand lightweight concrete. Note that this deviates from earlier specifications that distinguished between all-lightweight and sand lightweight concrete.

Due to the absence of existing data, the prescribed cohesion and friction factors for nonmonolithic lightweight concrete are accepted as conservative for application to monolithic lightweight concrete.

Tighter constraints have been adopted for roughened interfaces, other than cast-in-place slabs on roughened girders, even though available test data does not indicate more severe restrictions are necessary. This is to account for variability in the geometry, loading, and lack of redundancy at other interfaces.

5.9.5.4 – Refined Estimates of Time-Dependent Losses

5.9.5.4.1 – General

For nonsegmental Prestressed members, more accurate values of creep-, shrinkage-, and relaxation-related losses than those specified in Article 5.9.5.3 may be determined in accordance with the provisions of this Article. For precast pretensioned girders without a composite topping and for precast or cast-in-place nonsegmental post-tensioned girders, the provisions of Articles 5.9.5.4.4 and 5.9.5.4.5, respectively, shall be considered before applying the provisions of this Article.

C5.9.5.4.1

See Castrodale and White (2004) for information on computing the interaction of creep effects for prestressing applied at different times.

Estimates of losses due to each time-dependent source, such as creep, shrinkage, or relaxation, can lead to a better estimate of total losses compared with the values obtained using Article 5.9.5.3. The individual losses are based on research published in Tadros (2003), which aimed at extending applicability of the provisions of these Specifications to high-strength concrete. Research by Cousins, Roberts-Wollmann, and Brown (2013) indicated that these provisions yield reasonable results when used to calculate prestress loss in members made with sand lightweight concrete. Also, best results are achieved with sand lightweight concrete when using the AASHTO creep and shrinkages models with the Refined Method.

5.11.4 – Development of Prestressing Strand

5.11.4.1 – General

In determining the resistance of pretensioned concrete components in their end zones, the gradual buildup of the strand force in the transfer and development lengths shall be taken into account.

The stress in the prestressing steel may be assumed to vary linearly from 0.0 at the point where bonding commences to the effective stress after losses, f_{pe}, at the end of the transfer length.

Between the end of the transfer length and the development length, the strand stress may be assumed to increase linearly, reaching the stress at nominal residence, f_{ps}, at the development length.

For the purpose of this Article, the transfer length may be taken as 60 strand diameters and the development length shall be taken as specified in Article 5.11.4.2.

The effects of debonding shall be considered as specified in Article 5.11.4.3.

C5.11.4.1

Between the end of the transfer length and development length, the strand stress grows from the effective stress in the prestressing steel after losses to the stress in the strand at nominal resistance of the member. Research by Cousins, Roberts-Wollmann, and Brown (2013) indicated that these provisions yield reasonable results when used to calculate transfer and development length in members made with sand lightweight concrete.

Attachment B

Proposed Changes to AASHTO LRFD Bridge Construction Specifications

8.5.1—Storage of Aggregates

The handling and storage of concrete aggregates shall be such as to prevent segregation or contamination with foreign materials. The methods used shall provide for adequate drainage so that the moisture content of the aggregates is uniform at the time of batching. Lightweight coarse aggregate should be subjected to a minimum 24-hour soak and allowed to drain for an additional 24 hours to place the aggregate in a saturated surface-dry condition. Different sizes of aggregate shall be stored in separate stock piles sufficiently removed from each other to prevent the material at the edges of the piles for becoming intermixed.

When specified in Table 8.2.2-1 or in the contract documents, the coarse aggregate shall be separated into two or more sizes in order to secure greater uniformity of the concrete mixture.

Abbreviations and acronyms used without definitions in TRB publications:

AAAE	American Association of Airport Executives
AASHO	American Association of State Highway Officials
AASHTO	American Association of State Highway and Transportation Officials
ACI–NA	Airports Council International–North America
ACRP	Airport Cooperative Research Program
ADA	Americans with Disabilities Act
APTA	American Public Transportation Association
ASCE	American Society of Civil Engineers
ASME	American Society of Mechanical Engineers
ASTM	American Society for Testing and Materials
ATA	American Trucking Associations
CTAA	Community Transportation Association of America
CTBSSP	Commercial Truck and Bus Safety Synthesis Program
DHS	Department of Homeland Security
DOE	Department of Energy
EPA	Environmental Protection Agency
FAA	Federal Aviation Administration
FHWA	Federal Highway Administration
FMCSA	Federal Motor Carrier Safety Administration
FRA	Federal Railroad Administration
FTA	Federal Transit Administration
HMCRP	Hazardous Materials Cooperative Research Program
IEEE	Institute of Electrical and Electronics Engineers
ISTEA	Intermodal Surface Transportation Efficiency Act of 1991
ITE	Institute of Transportation Engineers
NASA	National Aeronautics and Space Administration
NASAO	National Association of State Aviation Officials
NCFRP	National Cooperative Freight Research Program
NCHRP	National Cooperative Highway Research Program
NHTSA	National Highway Traffic Safety Administration
NTSB	National Transportation Safety Board
PHMSA	Pipeline and Hazardous Materials Safety Administration
RITA	Research and Innovative Technology Administration
SAE	Society of Automotive Engineers
SAFETEA-LU	Safe, Accountable, Flexible, Efficient Transportation Equity Act: A Legacy for Users (2005)
TCRP	Transit Cooperative Research Program
TEA-21	Transportation Equity Act for the 21st Century (1998)
TRB	Transportation Research Board
TSA	Transportation Security Administration
U.S.DOT	United States Department of Transportation